

Sensor and Simulation Notes
Note 184

30 August 1973

Early Time Performance at Large Distances of Periodic Planar
Arrays of Planar Bicones with Sources Triggered
in a Plane-Wave Sequence

Carl E. Baum
Air Force Weapons Laboratory

CLEARED
FOR PUBLIC RELEASE

PL/PA 5/19/95

Abstract

This note considers some of the characteristics of the early-time far fields from infinite planar arrays of interconnected biconical sources and relates the results to the late-time (or low-frequency) results for the far fields from such arrays. First a general result for arrays of cells, each cell consisting of two conducting cones with common apex, is developed. This leads to formulas for an effective early-time rise and early-time polarization for the far fields. The general results are then applied to the special case in which each unit cell consists of a symmetrical planar bicone. For this case the formulas for early-time rise, polarization angle, and impedance are developed and plotted as functions of the bicone angle and angles to the distant observer.

PL 96-1227

Acknowledgement

I would like to thank Sgt. Robert N. Marks of AFWL and Mr. Joe P. Martinez of Dikewood for the numerical computations and graphs.

Contents

<u>Section</u>		<u>Page</u>
I	Introduction	4
II	Periodic Planar Arrays of Sources which Each Launch a Spherical TEM Wave at Local Early Time	6
III	Early-Time Performance at Large Distances	10
IV	Comparison to Late-Time Performance at Large Distances	14
V	Spherical TEM Waves Related to Planar TEM Waves	21
VI	Planar Bicones	29
VII	Early Time Impedance for Planar Bicones and Comparison to Late-Time Impedance	32
VIII	Early Time Fields at Large Distances from an Array of Planar Bicones	40
IX	Summary	53
X	References	54

Tables

<u>Table</u>		<u>Page</u>
1a	Geometrical Impedance Factor for Symmetrical Planar Bicones and Symmetrical Coplanar Strips for $0 \leq \psi < \pi/4$	34
1b	Geometrical Impedance Factor for Symmetrical Planar Bicones and Symmetrical Coplanar Strips for $\pi/4 \leq \psi < \pi/2$	35
2	ct_1/b and Asymptotic Forms for $\theta_1 = 0$	45

Figures

<u>Figure</u>		<u>Page</u>
1	Rectangular Cells in an Infinite Planar Array	55
2	Spherical Coordinates for the Early-Time Field Distribution Near a Source Point	56
3	Stereographic Projection for Relating Spherical and Planar TEM Waves	57
4	Two Spherical Coordinate Systems with Common Origin	58
5	Unit Cell of Planar Bicone Array Centered on Coordinate Origin	59
6	Transformation from Planar Bicone to Equivalent Two Strips	60
7	Complex Potential Function for Two Symmetrical Coplanar Strips for the Case of $f_g = 0.5$	61
8	Complex Potential Function for Two Symmetrical Coplanar Strips: Expanded view of first quadrant for the case of $f_g = 0.5$	62
9	Geometrical Impedance Factor for Symmetrical Planar Bicones	63
10	ct_1/b and Asymptotic Forms for $\theta_1 = 0$	64
11	ct_1/b for $\phi_1 = 0, \pm\pi$ with θ_1 as a Parameter	65
12	ct_1/b for $\phi_1 = \pm\pi/2$ with θ_1 as a Parameter	66
13	ct_1/b for $\theta_1 = \pi/2$ with ϕ_1 as a Parameter	67
14	ct_1/b and ρ for $(2/\pi)\phi_1 = .1$ with θ_1 as a Parameter	68
15	ct_1/b and ρ for $(2/\pi)\phi_1 = .2$ with θ_1 as a Parameter	69
16	ct_1/b and ρ for $(2/\pi)\phi_1 = .3$ with θ_1 as a Parameter	70
17	ct_1/b and ρ for $(2/\pi)\phi_1 = .4$ with θ_1 as a Parameter	71
18	ct_1/b and ρ for $(2/\pi)\phi_1 = .5$ with θ_1 as a Parameter	72
19	ct_1/b and ρ for $(2/\pi)\phi_1 = .6$ with θ_1 as a Parameter	73
20	ct_1/b and ρ for $(2/\pi)\phi_1 = .7$ with θ_1 as a Parameter	74
21	ct_1/b and ρ for $(2/\pi)\phi_1 = .8$ with θ_1 as a Parameter	75
22	ct_1/b and ρ for $(2/\pi)\phi_1 = .9$ with θ_1 as a Parameter	76
23	ct_1/b and ρ for $(2/\pi)\phi_1 = .95$ with θ_1 as a Parameter	77

I. Introduction

It is sometimes convenient or even necessary to configure pulsers for use with EMP simulators as arrays. The pulser array is configured to synthesize some desired field distribution appropriate to a particular type of wave to be launched. There are various types of waves which one can launch depending on the type of antenna structures (including earth presence, etc.) connected to or in proximity of the pulser array. Previous notes have discussed such pulser array and antenna combinations for some cases such as spherical waves from radiating antennas^{3,4} and inhomogeneous TEM plane or spherical waves on cylindrical or conical transmission lines.^{5,6,7,8}

Pulsers arrays for EMP simulators are not the same as used in radar applications, for example. One distinctive feature of pulser arrays for EMP simulators is that the desired pulse typically has important low frequencies with wavelengths large compared to the individual pulser (or module) size. This has the practical effect of making it important to connect the individual modules to adjacent modules in a manner which passes current through the array (with no shorting paths) at low frequencies. This typically implies conductors connecting at least the series modules in an array. Conductors connecting the parallel modules together are optional, depending on other considerations. Such pulser arrays then cannot be considered as planar arrays of point electric dipoles, for example. At low frequencies such pulser arrays can be approximated as sources which specify the tangential electric field in an average sense so as to approximately match the desired electric field distribution.

The conductors connecting adjacent modules are an important part of the array for understanding its performance at higher frequencies as well. They need to be considered as part of boundary value problems in calculating the high-frequency or early-time performance of such a pulser array. One might divide the times (and frequencies) of interest according to the characteristic dimensions of the array and of the individual modules. One characteristic time is associated with the total size of the array. A second characteristic time is associated with the module size which determines (with any spaces between) the periodicity of the array. Effects associated with the total array size are not considered in this note.

Considering a planar array, if we assume that the module spacing is small compared to the total array size then we can consider some of the effects associated with the module size by letting the array be infinitely large. In this note we consider infinitely large planar arrays triggered in a sequence so as to launch a plane wave (at least for frequencies with wavelengths large compared to the module size). There are many module or unit cell designs for such arrays that one might

consider, each having one or more boundary value problems appropriate to it that one can consider. Hopefully many such calculations will appear in future notes.

This note considers one aspect of the performance of various module designs in infinite planar arrays. If the individual module is constructed such that at early times the fields produced by the module are a spherical TEM wave, such as on biconical structures, then the individual module performance at early times can be combined with the array triggering sequence (assumed planar) to give the early retarded time far fields for the array. In this note the individual modules have spherical TEM waves at early times which behave as step function waves. However, one can generalize the results to other forms of early time performance using convolution techniques.

After considering the general far field results for modules with early time spherical TEM waves, we consider the specific case of planar bicones for the module design near the module center where the wave is first launched. For the case of planar bicones the numerical values of the resulting early retarded time far field rise of the wave are graphically displayed. Thus one can see the effects of the angle of the planar bicones and the direction of launch for the far field plane wave on the early retarded time far field performance. The early time impedance each module sees is also tabulated.

II. Periodic Planar Arrays of Sources which Each Launch a Spherical TEM Wave at Local Early Time

Let us first consider a general characteristic of planar arrays of spherical TEM elements. As illustrated in figure 1 for the case of a rectangular array consider an infinite array of source points which are assumed to lie in a plane, taken as $z = 0$. Each source point lies in an area A , the area of the unit cell in the periodic structure. For the rectangular array with spacing $2a$ in the x direction and $2b$ in the y direction A is just $4ab$. For a more general periodic planar array A is the average area per source point. For our present purposes each source point is assumed to launch a wave identical to that launched at every other source point except for a translation in the $z = 0$ plane and in general a shift in time. The present calculations can be easily generalized to other cases involving more than one type of source point, each type with different TEM characteristics such as launching differently polarized fields with different amplitudes at early times. Such generalization can be accomplished by adding the results at early times for more than one array of sources where the source elements for each array are interspersed among those for the other arrays in a periodic manner such that at local early times the various array elements do not interact with each other (at least in a "clear time" sense related to the far field results).

There are various types of periodicity in a plane that one might consider, such as those based on various polygons and/or combinations of polygons. What is required for the present development to apply is that the array of sources be periodic in position such that translations of the array in two dimensions (in at least two independent directions) precisely reproduce the original array (at least near the sources). Associated with such a shift perpendicular to the z axis there is also required a constant time shift for the turn-on time of the sources; this is basically the requirement for the plane-wave turn-on sequence for the array. The source points need not be all in the same plane but can be in different planes all parallel to the z axis, provided that the turn-on time of the sources in the various source planes is arranged to have signals arrive in the far field at the same time (retarded), and that the conductors (dielectrics, etc.) associated with the source points in one plane do not interfere with the wave propagating from other planes of source points to the far field at early retarded times. This is basically a requirement for line-of-sight clearance between each source and the far field direction in which the wave is being launched. This line-of-sight clearance can be blocked, for example, by the positioning of conical-transmission-line conductors attached to sources in the one or more source planes. If such conductors do not themselves lie in the source plane, then for certain launch angles (referred to the far field plane wave) the conductors may

interfere with the early-time wave to the far field. The results of this note do not consider cases which have such interference.

Consider now a spherical TEM wave launched from one source point. For convenience take this source point as $\vec{r} = \vec{0}$ and utilize the spherical coordinates as illustrated in figure 2. Consider a step function wave (at early times) of the form

$$\vec{E}(\vec{r}, t) = -\frac{V_0}{r} \nabla_s f(\theta, \phi) u\left(t - \frac{r}{c}\right) \quad (2.1)$$

leaving the source at $\vec{r} = \vec{0}$ at a time $t = 0$. This is a spherical TEM wave which is valid for times at each position of space before discontinuities in the conical conductors and/or similar waves from other launch points can alter the form of the wave at a particular \vec{r} . The electric field launched from $\vec{r} = \vec{0}$ has only θ and ϕ components given by the gradient ∇_s on the unit sphere operating on the potential function $f(\theta, \phi)$. Note that for a conical transmission line the corresponding potential is

$$V(\vec{r}, t) = V_0 f(\theta, \phi) u\left(t - \frac{r}{c}\right) \quad (2.2)$$

The voltage impressed on the conical transmission line for the typical case of two separate conductors is $V_0 u(t)$ between the conductors provided $f(\theta, \phi)$ is normalized such that its line integral between the two conductors (on the unit sphere) is just one.

On the unit sphere the surface gradient is

$$\nabla_s = \vec{e}_\theta \frac{\partial}{\partial \theta} + \vec{e}_\phi \frac{1}{\sin(\theta)} \frac{\partial}{\partial \phi} \quad (2.3)$$

The early time electric field from the source point at $\vec{r} = \vec{0}$ can then be written as

$$\vec{E}(\vec{r}, t) = -\frac{V_0}{r} \vec{F}(\theta, \phi) u\left(t - \frac{r}{c}\right) \quad (2.4)$$

where

$$\vec{F}(\theta, \phi) \equiv \nabla_s f(\theta, \phi)$$

$$= \vec{e}_\theta \frac{\partial}{\partial \theta} f(\theta, \phi) + \vec{e}_\phi \frac{1}{\sin(\theta)} \frac{\partial}{\partial \phi} f(\theta, \phi) \quad (2.5)$$

Consider some desired direction of propagation \vec{e}_1 for the wave leaving the source plane toward large positive z . (A wave also propagates toward negative z but this does not concern the present calculations.) Define retarded time as

$$t^* \equiv t - \frac{\vec{e}_1 \cdot \vec{r}}{c} \quad (2.6)$$

Define a turn-on time for the source points on the $z = 0$ plane as

$$t' \equiv \left. \frac{\vec{e}_1 \cdot \vec{r}}{c} \right|_{z=0} = \frac{1}{c} [x e_{1x} + y e_{1y}] \quad (2.7)$$

corresponding to retarded time equal to zero on the source plane. Equation 2.7 defines what it means to trigger the sources in a plane-wave sequence.

The voltages at the individual sources are specified to have step-function waveforms of the form

$$V = V_0 u\left(t - \frac{\vec{e}_1 \cdot \vec{r}_s}{c}\right) \quad (2.8)$$

where \vec{r}_s is the position of any source point being considered. Note that for source points \vec{r}_s not necessarily in a plane one can still define a turn-on time for each source point for a wave propagating in direction \vec{e}_1 as

$$t' \equiv \frac{\vec{e}_1 \cdot \vec{r}_s}{c} \quad (2.9)$$

There are various ways that one might set up a periodic array of such identical spherical TEM sources. As an example a rectangular array in the $z = 0$ plane could have source points $\vec{r}_{n,m}$ specified by

$$\vec{r}_s = \vec{r}_{n,m} = \vec{e}_x x_n + \vec{e}_y y_m$$

$$x_n = 2an \quad (2.10)$$

$$y_m = 2bm$$

with n and m taking all positive, negative, and zero integer values. For this case the sources would be turned on, for step function excitation, as

$$V = V_{n,m} = V_o u\left(t - \frac{e_1 x_n}{c} - \frac{e_1 y_m}{c}\right) \quad (2.11)$$

The electric field distribution function $\vec{F}(\theta, \phi)$ is made to be the same for all the sources, indicated by index pair n, m , as for the $0, 0$ source. For this purpose one can consider the angles θ, ϕ as being redefined for each source about a center at that source point. Note that only translation of the source field distribution is assumed here, with no rotation in going from one source to another. Viewed another way if we shift \vec{r} to $\vec{r} + \vec{r}_{n,m}$ the source field distributions must still be the same with only a constant shift for all the turn-on times.

If more than one type of source each with perhaps its own amplitude and distribution function $f(\theta, \phi)$ (and corresponding $\vec{F}(\theta, \phi)$) is used then the corresponding far field early time results can be added for the various source types. For the time window for which the early time results apply to be common to all the source types used in the one array the turn-on time formula (equation 2.8) can be applied to all the source types. However, some small time shifts between the source types can also be used, if desired, giving a more complex result.

III. Early-Time Performance at Large Distances

Consider an observer at large distance r in a direction \vec{e}_1 from the origin. This direction vector \vec{e}_1 is characterized by two angles $\theta = \theta_1$ and $\phi = \phi_1$ with respect to a spherical coordinate system centered on the origin. The cartesian components are

$$\begin{aligned} e_{1_x} &= \vec{e}_x \cdot \vec{e}_1 = \sin(\theta_1) \cos(\phi_1) \\ e_{1_y} &= \vec{e}_y \cdot \vec{e}_1 = \sin(\theta_1) \sin(\phi_1) \\ e_{1_z} &= \vec{e}_z \cdot \vec{e}_1 = \cos(\theta_1) \end{aligned} \quad (3.1)$$

While the observer is at a distance of $r \cos(\theta_1)$ from the $z = 0$ plane the closest position on this plane $(x,y) = (r \cos(\phi_1), r \sin(\phi_1))$, or the closest source to this position does not send the first signal to the observer unless the closest source is at $\vec{r} = \vec{0}$.

The first signal to arrive at the observer arrives from $\vec{r} = \vec{0}$ because of the plane-wave sequence for triggering the sources. Given an observer far from the $z = 0$ plane, the first signal to arrive at the observer can be used to define the origin $\vec{r} = \vec{0}$ for our calculations. However, given \vec{e}_1 for the triggering sequence and a distant observer position then $\vec{r} = \vec{0}$ will not fall precisely on a source position in which case the first signal will arrive from one of the source points nearest to $\vec{r} = \vec{0}$.

The observer at large r receives a signal at or near a direction \vec{e}_1 at early retarded time since the only source positions which can send a signal to the observer for early retarded times are near $\vec{r} = \vec{0}$. Consider retarded times for which t^* is less than an appropriate clear time t_{cf} (appropriate to the far field) for which the form of the wave from equation 2.4 is a valid representation of the signal reaching the far field from a single source. Including the turn-on time of the different sources each source radiates a field of the form

$$\vec{E}_s(\vec{r}, t) = -\frac{V_0}{|\vec{r} - \vec{r}_s|} \vec{F}_s(\theta_s, \phi_s) u\left(t - \frac{\vec{e}_1 \cdot \vec{r}_s}{c} - \frac{|\vec{r} - \vec{r}_s|}{c}\right) \quad ((3.2)$$

where the subscript s refers to the quantity appropriate to the individual source at \vec{r}_s .

A signal from \vec{r}_s arrives at $\vec{r} = \vec{e}_1 r$ at retarded time

$$\begin{aligned}
ct^* &= ct - r = \vec{e}_1 \cdot \vec{r}_s + |\vec{r}\vec{e}_1 - \vec{r}_s| - r \\
&= [r^2 - 2r\vec{e}_1 \cdot \vec{r}_s + r_s^2]^{1/2} - r + \vec{e}_1 \cdot \vec{r}_s \\
&= r \left\{ \frac{1}{2} \left[-\frac{2}{r} \vec{e}_1 \cdot \vec{r}_s + \frac{r_s^2}{r^2} \right] - \frac{1}{8} \left[-\frac{2}{r} \vec{e}_1 \cdot \vec{r}_s + \frac{r_s^2}{r^2} \right]^2 + O(r^{-3}) \right\} + \vec{e}_1 \cdot \vec{r}_s \\
&= \frac{1}{2r} [r_s^2 - (\vec{e}_1 \cdot \vec{r}_s)^2] + O(r^{-2}) \tag{3.3}
\end{aligned}$$

For a given t^* this equation gives the boundary for sources seen by the observer. Define orthogonal cartesian coordinates p and q on the source surface centered on $\vec{r} = \vec{0}$ but rotated so that

$$\begin{aligned}
e_{1q} &= 0 \\
e_{1p} &= \sin(\theta_1) \\
p^2 + q^2 &= r_s^2
\end{aligned} \tag{3.4}$$

Then the boundary equation becomes

$$\begin{aligned}
ct^* &= \frac{1}{2r} [p^2 + q^2 - \sin^2(\theta_1)p^2] + O(r^{-2}) \\
&= \frac{1}{2r} [\cos^2(\theta_1)p^2 + q^2] + O(r^{-2}) \tag{3.5}
\end{aligned}$$

This is an ellipse with

$$\text{semimajor axis length} = \frac{1}{\cos(\theta_1)} [2rct^*]^{1/2} + O(r^{-1})$$

$$\text{semiminor axis length} = [2rct^*]^{1/2} + O(r^{-1}) \quad (3.6)$$

$$\text{area} = \pi [\text{semimajor}] [\text{semiminor}]$$

$$= \frac{\pi}{\cos(\theta_1)} 2rct^* + O(1)$$

In order to keep this area bounded let us require that

$$0 \leq \theta_1 < \pi/2 \quad (3.7)$$

with θ_1 bounded away from $\pi/2$.

The distance from a position on the source plane to the observer at large r is

$$\begin{aligned} |\vec{r} - \vec{r}_s| &= [r^2 - 2r\vec{e}_1 \cdot \vec{r}_s + r_s^2]^{1/2} \\ &= r - \vec{e}_1 \cdot \vec{r}_s + O(r^{-1}) \end{aligned} \quad (3.8)$$

$$|\vec{r} - \vec{r}_s|^{-1} = \frac{1}{r} + O(r^{-2})$$

The angles from a source at \vec{r}_s to the observer are θ_s, ϕ_s in equation 3.2. We can write

$$\theta_s = \theta_1 + \Delta\theta \quad (3.9)$$

$$\phi_s = \phi_1 + \Delta\phi$$

where now

$$\Delta\theta = O(r^{-1}) \quad (3.10)$$

$$\Delta\phi = O(r^{-1})$$

Provided that $\vec{F}(\theta_s, \phi_s)$ has continuous derivatives near θ_1, ϕ_1 (which is the case unless θ_1, ϕ_1 are at or intersect one of the boundaries of the wave launcher) then one can write

$$\vec{F}(\theta_s, \phi_s) = \vec{F}(\theta_1, \phi_1) + O(r^{-1}) \quad (3.11)$$

The number of sources in the area seen by the observer (equations 3.6) is just that area divided by A ($= 4ab$ for the previously discussed case of rectangular cells) to within a number proportional to the perimeter of the source area seen, or proportional to the square root of that area, or \sqrt{r} . This error estimate is rather large for the case of an elliptical area including sources based on rectangular cells. Then summing up the electric field contributions from the sources "seen" by the observer at retarded time t^* we have

$$\vec{E} = -\frac{V_o}{A} \left\{ \frac{\pi}{\cos(\theta_1)} 2rct^* + O(r^{1/2}) \right\} \left\{ \frac{1}{r} + O(r^{-2}) \right\} \left\{ \vec{F}(\theta_1, \phi_1) + O(r^{-1}) \right\} u(t^*) \quad (3.12)$$

From this the far field form is obtained as

$$\vec{E}_f = -\frac{2\pi V_o}{A \cos(\theta_1)} \vec{F}(\theta_1, \phi_1) ct^* u(t^*) \quad \text{for } t^* < t_{cf} \quad (3.13)$$

This is the fundamental result for periodic planar arrays with plane-wave turn-on sequence and early time spherical TEM waves for the sources. For step excitation the far field has a ramp rise. Convolution techniques readily generalize this result to other forms of early time waveforms for the sources. Note that the validity of this result is limited in general to retarded times t^* less than the clear time t_{cf} as pertinent to a far field observer. This clear time gives the first retarded time that a wave other than the early time spherical TEM wave can reach the observer. Such other waves are associated with changes in the conical geometries leading away from the source points. Thus the clear time limitation is a function of the specific design of the conductors etc. connecting the sources and launching the wave. Note also that the far field is independent of r (for fixed t^*) because of the infinite planar source geometry.

IV. Comparison to Late-Time Performance at Large Distances

In order to better understand the quantitative effect of the early time result of the previous section let us compare it to the late time performance of the periodic array. Let the array be designed such that it has a well defined orientation \vec{e}_s for increase of scalar potential (voltage) on the source plane. This is defined by finding a direction that there is no net change in potential in going from one position in a cell to the corresponding position in an adjacent cell with no change in potential in a static sense (late time for step excitation). \vec{e}_s is then taken as perpendicular to this direction and oriented in the direction of increasing potential. Note that the late time electric field near the source plane is required to be a conservative field. Late time generally requires that time after nearby source turn on be large compared to transit times across the unit cells forming the array.

At low frequencies or late times the launched plane wave has the same electric field tangential to the source plane (or normal to \vec{e}_z) as the average tangential electric field on the source plane itself. This can be easily derived by considering wavelengths to be large compared to the cell dimensions. Within the region (small compared to a wavelength) where the electric field is conservative the line integral of the electric field across a cell dimension is independent of which plane of constant z we place this path on, just to satisfy the periodic boundary condition for such a periodic array. The higher order modes within one cell are evanescent and do not contribute to the average field. The average \vec{E} tangential to the source plane at late times for step excitation (equation 2.8) is

$$\vec{E}_{\text{tan}} = -\vec{e}_s \frac{V_0}{h} \quad (4.1)$$

where h is the distance in the \vec{e}_s direction between sources (or combinations of sources) with net late time voltage V_0 .

Define another unit vector \vec{e}_t parallel to the $z = 0$ plane and normal to \vec{e}_s . Let $\vec{e}_t, \vec{e}_s, \vec{e}_z$ form a right handed system so that we have

$$\begin{aligned} \vec{e}_s \times \vec{e}_t &= \vec{e}_z \\ \vec{e}_s \cdot \vec{e}_t &= 0 \\ \vec{e}_s \cdot \vec{e}_z &= 0 \\ \vec{e}_t \cdot \vec{e}_z &= 0 \end{aligned} \quad (4.2)$$

For our later calculations for rectangular arrays we will take

$$\begin{aligned}\vec{e}_s &= \vec{e}_x \\ \vec{e}_t &= \vec{e}_y\end{aligned}\tag{4.3}$$

as a convenient choice.

The far field plane wave at late retarded time has the form

$$\vec{E} = \vec{E}_O, \quad \vec{e}_l \cdot \vec{E}_O = 0\tag{4.4}$$

This can be considered as an ideal form for the far field wave. It does not apply for early retarded times and how soon the late retarded time form applies is a measure of the early time or high frequency quality of the array.^{6,7,8}

Relating the late retarded time far field to the array parameters we have for the tangential components (with respect to the $z = 0$ plane)

$$\begin{aligned}\vec{e}_s \cdot \vec{E}_O &= \vec{e}_s \cdot \vec{E}_{\text{tan}} = -\frac{V_O}{h} \equiv E_s \\ \vec{e}_t \cdot \vec{E}_O &= 0\end{aligned}\tag{4.5}$$

Let

$$\vec{E}_O = E_O \vec{e}_O\tag{4.6}$$

with E_O taken to have the same sign as E_s . Now we have

$$\begin{aligned}\vec{e}_l &= e_{l_x} \vec{e}_x + e_{l_y} \vec{e}_y + e_{l_z} \vec{e}_z \\ &= e_{l_s} \vec{e}_s + e_{l_t} \vec{e}_t + e_{l_z} \vec{e}_z\end{aligned}\tag{4.7}$$

Then we can obtain the equations

$$\vec{e}_1 \cdot \vec{E}_O = e_{1s} E_s + e_{1z} \vec{e}_z \cdot \vec{E}_O = 0$$

$$\vec{e}_z \cdot \vec{E}_O \equiv E_{Oz} = -\frac{e_{1s}}{e_{1z}} E_s = -\frac{\vec{e}_1 \cdot \vec{e}_s}{\vec{e}_1 \cdot \vec{e}_z} E_s$$

(4.8)

$$E_O = \left[E_{Oz}^2 + E_{Os}^2 \right]^{1/2} = E_s \left[1 + \left[\frac{\vec{e}_1 \cdot \vec{e}_s}{\vec{e}_1 \cdot \vec{e}_z} \right]^2 \right]^{1/2}$$

$$E_{Os} = E_s$$

Letting $\vec{e}_{x\rightarrow}$ be taken as \vec{e}_s with no loss of generality, and similarly with \vec{e}_t taken as \vec{e}_y , we have

$$\vec{e}_1 \cdot \vec{e}_z = \cos(\theta_1)$$

$$\vec{e}_1 \cdot \vec{e}_s = \vec{e}_1 \cdot \vec{e}_x = \sin(\theta_1) \cos(\phi_1)$$

(4.9)

$$\vec{e}_1 \cdot \vec{e}_t = \vec{e}_1 \cdot \vec{e}_y = \sin(\theta_1) \sin(\phi_1)$$

giving

$$E_O = E_s [1 + \tan^2(\theta_1) \cos^2(\phi_1)]^{1/2}$$

(4.10)

$$= \frac{E_s}{\cos(\theta_1)} [1 - \sin^2(\theta_1) \sin^2(\phi_1)]^{1/2}$$

This also gives the angles for \vec{e}_O as

$$e_{Os} = \vec{e}_O \cdot \vec{e}_s = \vec{e}_O \cdot \vec{e}_x = \frac{E_s}{E_O} = -\frac{V_O}{hE_O}$$

$$= \cos(\theta_1) [1 - \sin^2(\theta_1) \sin^2(\phi_1)]^{-1/2}$$

$$e_{o_t} = \vec{e}_o \cdot \vec{e}_t = \vec{e}_o \cdot \vec{e}_y = 0 \quad (4.11)$$

$$e_{o_z} = \vec{e}_o \cdot \vec{e}_z = - \frac{\vec{e}_1 \cdot \vec{e}_s}{\vec{e}_1 \cdot \vec{e}_z} \left[1 + \left[\frac{\vec{e}_1 \cdot \vec{e}_s}{\vec{e}_1 \cdot \vec{e}_z} \right]^2 \right]^{-1/2}$$

$$= -\sin(\theta_1) \cos(\phi_1) [1 - \sin^2(\theta_1) \sin^2(\phi_1)]^{-1/2}$$

The far field may now be normalized to its late time value (for step excitation) as

$$\frac{\vec{E}_f}{E_o} = \frac{\vec{E}_f}{E_s} \cos(\theta_1) [1 - \sin^2(\theta_1) \sin^2(\phi_1)]^{-1/2}$$

$$= -\frac{h}{V_o} \vec{E}_f \cos(\theta_1) [1 - \sin^2(\theta_1) \sin^2(\phi_1)]^{-1/2}$$

$$= 2\pi \vec{F}(\theta_1, \phi_1) [1 - \sin^2(\theta_1) \sin^2(\phi_1)]^{-1/2} \frac{h}{A} ct^* u(t^*)$$

for $t^* < t_{c_f}$ (4.12)

The normalized component in the \vec{e}_o direction (the direction of the late time electric field) is

$$\frac{E_{f_o}}{E_o} = \frac{\vec{e}_o \cdot \vec{E}_f}{E_o} = 2\pi \vec{e}_o \cdot \vec{F}(\theta_1, \phi_1) [1 - \sin^2(\theta_1) \sin^2(\phi_1)]^{-1/2} \frac{h}{A} ct^* u(t^*)$$

for $t^* < t_{c_f}$ (4.13)

Setting this ramp function equal to 1 (while perhaps extrapolating the result for $t^* > t_{c_f}$) defines an effective time constant for the early-time rise of the far-field wave as

$$t_1 = \frac{A}{2\pi ch} [\vec{e}_o \cdot \vec{F}(\theta_1, \phi_1)]^{-1} [1 - \sin^2(\theta_1) \sin^2(\phi_1)]^{1/2} \quad (4.14)$$

Then with A and h specified (say $A = 4ab$ and $h = 2a$ for rectangular cells) t_1 can be calculated in a form scaled to a convenient dimension of the cell geometry chosen.

This last result brings up an interesting point. The early-time \vec{E}_f is not necessarily parallel to the late time \vec{E}_0 , in which case the far-field polarization must rotate as a function of retarded time. One measure of the matching of the early-time and late-time far-field directions is given by the fraction of the early-time field perpendicular to \vec{e}_0 (as compared to the parallel part). Thus define a ratio

$$\rho \equiv \frac{\vec{e}'_0 \cdot \vec{F}(\theta_1, \phi_1)}{\vec{e}_0 \cdot \vec{F}(\theta_1, \phi_1)} \quad (4.15)$$

where \vec{e}'_0 is a unit vector orthogonal to both \vec{e}_0 and \vec{e}_1 in a right handed system $\vec{e}_0, \vec{e}'_0, \vec{e}_1$ such that

$$\begin{aligned} \vec{e}'_0 &= \vec{e}_1 \times \vec{e}_0 \\ \vec{e}_0 \cdot \vec{e}'_0 &= 0 \\ \vec{e}_0 \cdot \vec{e}_1 &= 0 \\ \vec{e}'_0 \cdot \vec{e}_1 &= 0 \end{aligned} \quad (4.16)$$

Note that ρ can be considered as the tangent of the polarization angle for early time with respect to the late-time electric field direction.

Now \vec{e}_0 and \vec{e}'_0 can be written in terms of the unit vectors for the far field \vec{e}_1 (or \vec{e}_{r1}), $\vec{e}_{\theta 1}$, $\vec{e}_{\phi 1}$ directions with respect to the array coordinates and triggering sequence. First we have

$$\vec{e}_0 = e_{\theta 1} \vec{e}_{\theta 1} + e_{\phi 1} \vec{e}_{\phi 1} \quad (4.17)$$

Using the identity dyadic

$$\begin{aligned}
\vec{1} &= \vec{e}_s \vec{e}_s + \vec{e}_t \vec{e}_t + \vec{e}_z \vec{e}_z \\
&= \vec{e}_x \vec{e}_x + \vec{e}_y \vec{e}_y + \vec{e}_z \vec{e}_z
\end{aligned} \tag{4.18}$$

and relations to complement equations 3.1

$$\begin{aligned}
e_{\theta_1 x} &= \vec{e}_{\theta_1} \cdot \vec{e}_x = \cos(\theta_1) \cos(\phi_1) \\
e_{\theta_1 y} &= \vec{e}_{\theta_1} \cdot \vec{e}_y = \cos(\theta_1) \sin(\phi_1) \\
e_{\theta_1 z} &= \vec{e}_{\theta_1} \cdot \vec{e}_z = -\sin(\theta_1) \\
e_{\phi_1 x} &= \vec{e}_{\phi_1} \cdot \vec{e}_x = -\sin(\phi_1) \\
e_{\phi_1 y} &= \vec{e}_{\phi_1} \cdot \vec{e}_y = \cos(\phi_1) \\
e_{\phi_1 z} &= \vec{e}_{\phi_1} \cdot \vec{e}_z = 0
\end{aligned} \tag{4.19}$$

then we have

$$\begin{aligned}
e_{o\theta_1} &= \vec{e}_o \cdot \vec{e}_{\theta_1} = \vec{e}_o \cdot \vec{1} \cdot \vec{e}_{\theta_1} \\
&= \cos^2(\theta_1) \cos(\phi_1) [1 - \sin^2(\theta_1) \sin^2(\phi_1)]^{-1/2} \\
&\quad + \sin^2(\theta_1) \cos(\phi_1) [1 - \sin^2(\theta_1) \sin^2(\phi_1)]^{-1/2} \\
&= \cos(\phi_1) [1 - \sin^2(\theta_1) \sin^2(\phi_1)]^{-1/2}
\end{aligned}$$

$$\begin{aligned}
e_{o\phi_1} &= \vec{e}_o \cdot \vec{e}_{\phi_1} = \vec{e}_o \cdot \vec{I} \cdot \vec{e}_{\phi_1} & (4.20) \\
&= -\cos(\theta_1) \sin(\phi_1) [1 - \sin^2(\theta_1) \sin^2(\phi_1)]^{-1/2}
\end{aligned}$$

which gives

$$\vec{e}_o = [1 - \sin^2(\theta_1) \sin^2(\phi_1)]^{-1/2} \{ \cos(\phi_1) \vec{e}_{\theta_1} - \cos(\theta_1) \sin(\phi_1) \vec{e}_{\phi_1} \} \quad (4.21)$$

Then from equations 4.16 we also have

$$\begin{aligned}
\vec{e}'_o &= \vec{e}_1 \times \vec{e}_o \\
&= [1 - \sin^2(\theta_1) \sin^2(\phi_1)]^{-1/2} \{ \cos(\theta_1) \sin(\phi_1) \vec{e}_{\theta_1} + \cos(\phi_1) \vec{e}_{\phi_1} \} \quad (4.22)
\end{aligned}$$

Combining the results for \vec{e}_o and \vec{e}'_o with equations 4.14 and 4.15 we have

$$\begin{aligned}
t_1 &= \frac{A}{2\pi ch} \{ [\cos(\phi_1) \vec{e}_{\theta_1} - \cos(\theta_1) \sin(\phi_1) \vec{e}_{\phi_1}] \cdot \vec{F}(\theta_1, \phi_1) \}^{-1} \\
&\quad \cdot [1 - \sin^2(\theta_1) \sin^2(\phi_1)] \quad (4.23)
\end{aligned}$$

$$\rho = \frac{[\cos(\theta_1) \sin(\phi_1) \vec{e}_{\theta_1} + \cos(\phi_1) \vec{e}_{\phi_1}] \cdot \vec{F}(\theta_1, \phi_1)}{[\cos(\phi_1) \vec{e}_{\theta_1} - \cos(\theta_1) \sin(\phi_1) \vec{e}_{\phi_1}] \cdot \vec{F}(\theta_1, \phi_1)}$$

Thus, for a given cell design for which we have A, h, and $\vec{F}(\theta_1, \phi_1)$ we can calculate both t_1 and ρ as functions of θ_1 and ϕ_1 .

V. Spherical TEM Waves Related to Planar TEM Waves

As mentioned in section I the individual module is assumed to be of a type which has an early time performance characterized by a spherical TEM mode such as exist on biconical (or multiconical, all with the same apex) perfectly conducting structures. Such cones are not necessarily circular, but can be planar or have a variety of other shapes which are independent of r in a spherical coordinate system centered on the common apex. The TEM mode (or modes) is (are) characterized by one or more scalar potential functions $f(\theta, \phi)$ and the gradient of this function on the unit sphere $\vec{\nabla} f(\theta, \phi)$ as in equation 2.5. For our present purposes we assume a general biconical configuration which has one and only one such TEM mode.

For a given biconical (or higher order) configuration the spherical TEM mode can be related to an equivalent planar TEM mode on a cylindrical transmission line by a well known transformation for the potential function.^{10,11} This is basically a coordinate transformation known as a stereographic projection. It is illustrated in figure 3 and has the transformation equations

$$\begin{aligned}x' &= 2z_0 \cos(\phi) \tan\left(\frac{\theta}{2}\right) \\y' &= -2z_0 \sin(\phi) \tan\left(\frac{\theta}{2}\right)\end{aligned}\tag{5.1}$$

where the spherical r, θ, ϕ coordinates can be assumed to be based on some arbitrary x'', y'', z'' cartesian coordinates and where z_0 is an arbitrary scaling constant and x' and y' are the new coordinates (on a plane of constant z') in the transformed equivalent cartesian coordinate system.

The potential function for the spherical TEM mode can then be related to that for the planar TEM mode by a simple coordinate transformation. In the x', y' plane one can define a complex potential function

$$w = u + iv\tag{5.2}$$

which is a function of the complex coordinate $x' + iy'$ or some constant times this. Then $f(\theta, \phi)$ can be equated to $\text{Re}[w]$ times an appropriate constant which simplifies the results.

First let us explicitly exhibit the coordinate transformations. Equations 5.1 (as illustrated in figure 3) give the stereographic transformation between the reference cartesian system x', y', z' (for which only the cross section coordinates

x' and y' are important) and the angular coordinates θ, ϕ of a general spherical coordinate system r, θ, ϕ for which $r = 0$ is chosen at the apex of the cones. However $\theta = 0$ and $\phi = 0$ can be chosen arbitrarily for convenience in the particular problem. This modifies the cross section in a transformed plane of constant z' , thereby giving various possible equivalent cylindrical transmission lines.

Let us choose two spherical coordinate systems for the biconical wave launcher with apex at $r = 0$ as shown in figure 4. The r, θ, ϕ system is appropriate for describing the coordinates of an observer with $\theta = 0$ perpendicular to the source plane $z = 0$. The r, θ, ϕ system is useful in the transformation for the equivalent transmission line for a cell for early time. In this note a particular relation between the two spherical coordinate systems is chosen to be appropriate for a planar bicone. This choice is not necessarily appropriate for other unit cell geometries.

As illustrated in figure 4 let us choose

$$\begin{aligned} x &= r \sin(\theta) \cos(\phi) = r \sin(\theta) \cos(\phi) \\ y &= r \sin(\theta) \sin(\phi) = r \cos(\theta) & (5.3) \\ z &= r \cos(\theta) \quad = -r \sin(\theta) \sin(\phi) \end{aligned}$$

The r, θ, ϕ system is chosen to have the standard relation to the cartesian x, y, z system which we use to describe the array. The r, θ, ϕ system is chosen so as to conveniently map the planar bicone unit cell onto the equivalent x', y' coordinates while maintaining the conductors in one plane for convenience. The planar bicone unit cell is considered later in this note.

Define normalized coordinates for the equivalent cylindrical transmission line as

$$\begin{aligned} X' &\equiv \frac{x'}{2z_0} = \cos(\phi) \tan\left(\frac{\theta}{2}\right) \\ Y' &\equiv \frac{y'}{2z_0} = -\sin(\phi) \tan\left(\frac{\theta}{2}\right) \end{aligned} \quad (5.4)$$

Define a complex normalized coordinate as

$$\zeta' \equiv X' + iY' = \frac{x' + iy'}{2z_0} \quad (5.5)$$

which can be written in terms of θ, ϕ as

$$\zeta' = e^{-i\phi} \tan\left(\frac{\theta}{2}\right) \quad (5.6)$$

giving for θ, ϕ real

$$|\zeta'| = \tan\left(\frac{\theta}{2}\right) \quad (5.7)$$

$$\arg(\zeta') = -\phi$$

Equations 5.3 can be used to relate θ, ϕ and θ, ϕ as

$$\cos(\theta) = \sin(\theta) \sin(\phi) \quad (5.8)$$

$$\tan(\phi) = -\cot(\theta) \sec(\phi)$$

Then using positive square roots for θ, ϕ real we have

$$\begin{aligned} \tan\left(\frac{\theta}{2}\right) &= \pm \left[\frac{1 - \cos(\theta)}{1 + \cos(\theta)} \right]^{1/2} = \pm \left[\frac{1 - \sin(\theta) \sin(\phi)}{1 + \sin(\theta) \sin(\phi)} \right]^{1/2} \\ \cos(\phi) &= \pm [1 + \tan^2(\phi)]^{-1/2} = \pm [1 + \cot^2(\theta) \sec^2(\phi)]^{-1/2} \\ &= \sin(\theta) \cos(\phi) [\cos^2(\theta) + \sin^2(\theta) \cos^2(\phi)]^{-1/2} \\ &= \sin(\theta) \cos(\phi) [1 - \sin^2(\theta) \sin^2(\phi)]^{-1/2} \\ &= \sin(\theta) \cos(\phi) [1 + \sin(\theta) \sin(\phi)]^{-1/2} [1 - \sin(\theta) \sin(\phi)]^{-1/2} \\ \sin(\phi) &= \pm \tan(\phi) [1 + \tan^2(\phi)]^{-1/2} = \mp \cot(\theta) \sec(\phi) [1 + \cot^2(\theta) \sec^2(\phi)]^{-1/2} \\ &= -\cos(\theta) [\cos^2(\theta) + \sin^2(\theta) \cos^2(\phi)]^{-1/2} \\ &= -\cos(\theta) [1 - \sin^2(\theta) \sin^2(\phi)]^{-1/2} \\ &= -\cos(\theta) [1 + \sin(\theta) \sin(\phi)]^{-1/2} [1 - \sin(\theta) \sin(\phi)]^{-1/2} \end{aligned} \quad (5.9)$$

In terms of θ, ϕ the normalized coordinates become

$$\begin{aligned} X' &= \frac{\sin(\theta) \cos(\phi)}{1 + \sin(\theta) \sin(\phi)} \\ Y' &= \frac{\cos(\theta)}{1 + \sin(\theta) \sin(\phi)} \\ \zeta' &= X' + iY' = \frac{\sin(\theta) \cos(\phi) + i \cos(\theta)}{1 + \sin(\theta) \sin(\phi)} \end{aligned} \quad (5.10)$$

In section I a normalized potential function $f(\theta, \phi)$ is introduced to describe the potential for the spherical TEM mode. By mapping θ, ϕ to x', y' we have a solution for $f(\theta, \phi)$ provided we have the solution for the complex potential function $w = u + iv$ in the complex plane $x' + iy'$. For convenience one can define a complex variable

$$\zeta = \frac{x' + iy'}{x_0} \quad (5.11)$$

where x_0 is some convenient constant. Relating this to ζ' we have

$$\begin{aligned} \zeta &= \alpha \zeta' = \alpha [X' + iY'] \\ \alpha &= \frac{2z_0}{x_0} \end{aligned} \quad (5.12)$$

We can later choose x_0 to be some convenient constant related to the geometry of the equivalent cylindrical transmission line. In relating $f(\theta, \phi)$ to w we simply then set f equal to some convenient constant times u .

Having the potential function for the spherical TEM wave one would also like to obtain the field distribution. For this we need

$$\begin{aligned} \vec{F}(\theta, \phi) &\equiv \nabla_s f(\theta, \phi) \\ &= \vec{e}_\theta \frac{\partial}{\partial \theta} f(\theta, \phi) + \vec{e}_\phi \frac{1}{\sin(\theta)} \frac{\partial}{\partial \phi} f(\theta, \phi) \end{aligned} \quad (5.13)$$

which was introduced in section II. As a step in obtaining this we need

$$\nabla' f = \vec{e}_{X'} \frac{\partial f}{\partial X'} + \vec{e}_{Y'} \frac{\partial f}{\partial Y'} \quad (5.14)$$

which in turn can be derived from

$$\nabla' w = \nabla' (u + iv) \equiv \vec{g}_0 + i\vec{h}_0 \quad (5.15)$$

where the gradient is taken with respect to the normalized X' , Y' coordinates for our present considerations.

The vector functions \vec{g}_0 and \vec{h}_0 describe normalized electric and magnetic fields respectively for the equivalent cylindrical transmission line and can be written as

$$\begin{aligned} \vec{g}_0 &\equiv \vec{e}_{X'} g_{0X'} + \vec{e}_{Y'} g_{0Y'} \\ \vec{h}_0 &\equiv \vec{e}_{X'} h_{0X'} + \vec{e}_{Y'} h_{0Y'} \end{aligned} \quad (5.16)$$

As discussed in a previous note we can define complex TEM mode functions for cylindrical transmission lines as⁸

$$\begin{aligned} g_0(\zeta') &= g_{0X'}(\zeta') - i g_{0Y'}(\zeta') \\ h_0(\zeta') &= h_{0X'}(\zeta') - i h_{0Y'}(\zeta') \end{aligned} \quad (5.17)$$

These have the relations

$$\begin{aligned} g_{0X'} &= h_{0Y'}, \quad g_{0Y'} = -h_{0X'} \\ g_0(\zeta') &= i h_0(\zeta') = \frac{dw(\zeta')}{d\zeta'} = \alpha \frac{dw(\zeta)}{d\zeta} \end{aligned} \quad (5.18)$$

The quantity $dw(\zeta)/d\zeta$ can be found from the equivalent cylindrical transmission line solution thereby giving $\nabla' w$ and thus $\nabla' u$ and $\nabla' f$.

Now relate $\nabla' f(\zeta')$ to $\vec{F}(\theta, \phi)$ through the chain rule as

$$\frac{\partial}{\partial \theta} f(\theta, \phi) = \frac{\partial X'}{\partial \theta} \frac{\partial f}{\partial X'} + \frac{\partial Y'}{\partial \theta} \frac{\partial f}{\partial Y'} \quad (5.19)$$

$$\frac{1}{\sin(\theta)} \frac{\partial}{\partial \phi} f(\theta, \phi) = \frac{1}{\sin(\theta)} \frac{\partial X'}{\partial \phi} \frac{\partial f}{\partial X'} + \frac{1}{\sin(\theta)} \frac{\partial Y'}{\partial \phi} \frac{\partial f}{\partial Y'}$$

Thus we can transform a gradient in cartesian X', Y' space to one in spherical θ, ϕ space via

$$\vec{\nabla} f(\theta, \phi) \equiv \nabla_{\mathbf{S}} f(\theta, \phi) = \vec{\nabla} \cdot \nabla' f(X', Y') \quad (5.20)$$

where $\vec{\nabla}$ is a transformation matrix given by

$$\vec{\nabla} = \begin{pmatrix} \frac{\partial X'}{\partial \theta} & \frac{\partial Y'}{\partial \theta} \\ \frac{1}{\sin(\theta)} \frac{\partial X'}{\partial \phi} & \frac{1}{\sin(\theta)} \frac{\partial Y'}{\partial \phi} \end{pmatrix} \quad (5.21)$$

where the order of the components for $\nabla_{\mathbf{S}} f$ and $\nabla' f$ must be taken as θ, ϕ and X', Y' respectively.

From equations 5.10 the matrix elements for $\vec{\nabla}$ can be readily found. The result is

$$\vec{\nabla} = [1 + \sin(\theta) \sin(\phi)]^{-2} \begin{pmatrix} \cos(\theta) \cos(\phi) & -\sin(\theta) - \sin(\phi) \\ -\sin(\theta) - \sin(\phi) & -\cos(\theta) \cos(\phi) \end{pmatrix} \quad (5.22)$$

Note that

$$\frac{\partial X'}{\partial \theta} = - \frac{1}{\sin(\theta)} \frac{\partial Y'}{\partial \phi} \quad (5.23)$$

$$\frac{\partial Y'}{\partial \theta} = \frac{1}{\sin(\theta)} \frac{\partial X'}{\partial \phi}$$

If one has f as a function of ζ (the coordinates for the equivalent cylindrical transmission line) and the factor α to relate ζ to ζ' (the normalized coordinates used in the transformation) then equations 5.20 and 5.22 give the field distribution for the spherical TEM mode.

From equations 4.23 we have the far field effective early-time rise as

$$\begin{aligned}
\frac{2\pi ch}{A} t_1 &= [1 - \sin^2(\theta_1) \sin^2(\phi_1)] \\
&\cdot \{[\cos(\phi_1)\vec{e}_{\theta_1} - \cos(\theta_1) \sin(\phi_1)\vec{e}_{\phi_1}] \cdot \vec{F}(\theta_1, \phi_1)\}^{-1} \\
&= [1 - \sin^2(\theta_1) \sin^2(\phi_1)] \\
&\cdot \{[\cos(\phi_1)\vec{e}_{\theta_1} - \cos(\theta_1) \sin(\phi_1)\vec{e}_{\phi_1}] \cdot \vec{T} \}^{-1} \quad (5.24) \\
&\cdot \{\nabla'f(X', Y')\}^{-1} \\
&= [1 - \sin(\theta_1) \sin(\phi_1)][1 + \sin(\theta_1) \sin(\phi_1)]^2 \\
&\cdot \left\{ \cos(\theta_1) \frac{\partial f}{\partial X'_1} - \sin(\theta_1) \cos(\phi_1) \frac{\partial f}{\partial Y'_1} \right\}^{-1}
\end{aligned}$$

The fraction of the early time field perpendicular to the late time field direction is the ratio

$$\begin{aligned}
\rho &= \frac{[\cos(\theta_1) \sin(\phi_1)\vec{e}_{\theta_1} + \cos(\phi_1)\vec{e}_{\phi_1}] \cdot \vec{F}(\theta_1, \phi_1)}{[\cos(\phi_1)\vec{e}_{\theta_1} - \cos(\theta_1) \sin(\phi_1)\vec{e}_{\phi_1}] \cdot \vec{F}(\theta_1, \phi_1)} \\
&= \frac{[\cos(\theta_1) \sin(\phi_1)\vec{e}_{\theta_1} + \cos(\phi_1)\vec{e}_{\phi_1}] \cdot \vec{T} \cdot \nabla'f(X', Y')}{[\cos(\phi_1)\vec{e}_{\theta_1} - \cos(\theta_1) \sin(\phi_1)\vec{e}_{\phi_1}] \cdot \vec{T} \cdot \nabla'f(X', Y')} \\
&= \frac{-\sin(\theta_1) \cos(\phi_1) \frac{\partial f}{\partial X'_1} - \cos(\theta_1) \frac{\partial f}{\partial Y'_1}}{\cos(\theta_1) \frac{\partial f}{\partial X'_1} - \sin(\theta_1) \cos(\phi_1) \frac{\partial f}{\partial Y'_1}} \quad (5.25)
\end{aligned}$$

Note that X_1', Y_1' is used to correspond to θ_1, ϕ_1 which characterizes the direction of propagation of the wave from the array. Our two early time array parameters, t_1 and ρ , are now characterized in terms of θ_1, ϕ_1 and $f(\zeta_1')$.

VI. Planar Bicones

Consider a planar bicone for each unit cell on the plane $z = 0$. In particular consider the unit cell centered on $\vec{r} = \vec{0}$ as illustrated in figure 5. The half angle of the symmetrical planar bicone is ψ . The planar bicones are oriented symmetrically with respect to the x and y axes with the late time average source field, \vec{E}_{tan} from equation 4.1, so that $\vec{e}_s = \vec{e}_x$ as in equations 4.3. The unit cell has coordinates for the four corners

$$(x, y, z) = (\pm a, \pm b, 0) \quad (6.1)$$

One can define a special value of ψ as

$$\psi_0 = \arctan\left(\frac{b}{a}\right) \quad (6.2)$$

Figure 5A shows the case for $0 < \psi < \psi_0$; note that there are assumed to be conductors connecting between cells in the y direction so as to make the late time average source field have no y component. Figure 5B shows the case for $\psi_0 < \psi < \pi/2$.

For this case of a rectangular cell we have

$$h = 2a, \quad A = 4ab, \quad \frac{A}{h} = 2b \quad (6.3)$$

$$\vec{e}_s = \vec{e}_x, \quad \vec{e}_t = \vec{e}_y$$

In considering the early-time rise characteristics it will be convenient to normalize t_1 with respect to a, b, or some combination thereof.

Using the normalized transformation from equations 5.4

$$x' = \frac{x'}{2z_0} = \cos(\phi) \tan\left(\frac{\theta}{2}\right) \quad (6.4)$$

$$y' = \frac{y'}{2z_0} = -\sin(\phi) \tan\left(\frac{\theta}{2}\right)$$

together with the coordinate definitions in equations 5.3 and figure 4 gives the transformation of the planar bicone near $\vec{r} = \vec{0}$ in figure 5 to an equivalent cylindrical transmission line.² The conductors go to two line segments in the x', y'

plane on the $y' = 0$ line. The two resulting lines (or the cross section of the two uniform perfectly conducting strips) lie in the range $x_2' \leq |x'| \leq x_3'$ or $X_2' \leq |X'| \leq X_3'$ where 2 and 3 indicate inside and outside edges respectively for the equivalent strips. This is illustrated in figure 6.

In the normalized X', Y' coordinates we have the edge equations

$$\begin{aligned} x_2' &= \frac{x_2'}{2z_0} = \tan\left(\frac{\pi - \psi}{2}\right) = \tan\left(\frac{\pi}{4} - \frac{\psi}{2}\right) \\ &= \cot\left(\frac{\pi}{4} + \frac{\psi}{2}\right) \end{aligned} \tag{6.5}$$

$$\begin{aligned} x_3' &= \frac{x_3'}{2z_0} = \tan\left(\frac{\pi + \psi}{2}\right) = \tan\left(\frac{\pi}{4} + \frac{\psi}{2}\right) \\ &= \cot\left(\frac{\pi}{4} - \frac{\psi}{2}\right) \end{aligned}$$

giving

$$x_2' x_3' = 1 \tag{6.6}$$

The conformal transformation for the complex potential function is¹¹

$$\zeta \equiv \frac{x' + iy'}{x_0} = \alpha \zeta' = \alpha [X' + iY'] = \operatorname{sn}(w|m) \tag{6.7}$$

$$w = u + iv$$

As illustrated in figures 7 and 8 the real part of the potential function has values $u = \pm K(m)$ on the two strips with v changing from $-K(m_1)$ to $+K(m_1)$ in going around one strip. The parameter in the elliptic functions is

$$m \equiv 1 - m_1 = \left(\frac{x_2'}{x_3'}\right)^2 = \left(\frac{X_2'}{X_3'}\right)^2 = \tan^4\left(\frac{\pi}{4} - \frac{\psi}{2}\right) \tag{6.8}$$

We also have

$$\begin{aligned} \tan\left(\frac{\pi}{4} - \frac{\psi}{2}\right) &= \frac{1 - \cos\left(\frac{\pi}{2} - \psi\right)}{\sin\left(\frac{\pi}{2} - \psi\right)} = \frac{1 - \sin(\psi)}{\cos(\psi)} \\ &= \frac{\sin\left(\frac{\pi}{2} - \psi\right)}{1 + \cos\left(\frac{\pi}{2} - \psi\right)} = \frac{\cos(\psi)}{1 + \sin(\psi)} \end{aligned} \quad (6.9)$$

for calculating m . The edges are at $\zeta = \pm 1$ and $\zeta = \pm m^{-1/2}$.

From the edge equations we have in the normalized coordinates

$$\alpha X'_2 = \alpha \frac{x'_2}{2z_0} = 1 \quad (6.10)$$

$$\alpha X'_3 = \alpha \frac{x'_3}{2z_0} = m^{-1/2}$$

Combining this with equation 6.6 gives

$$\alpha = m^{-1/4} = \frac{\cos(\psi)}{1 - \sin(\psi)} = \frac{1 + \sin(\psi)}{\cos(\psi)} = \cot\left(\frac{\pi}{4} - \frac{\psi}{2}\right) \quad (6.11)$$

Thus we have $X'_2 < 1$ and $X'_3 > 1$ with specific equations

$$\begin{aligned} X'_2 &= \frac{1}{\alpha} = \frac{1 - \sin(\psi)}{\cos(\psi)} = \tan\left(\frac{\pi}{4} - \frac{\psi}{2}\right) \\ X'_3 &= \alpha = \frac{\cos(\psi)}{1 - \sin(\psi)} = \cot\left(\frac{\pi}{4} - \frac{\psi}{2}\right) \end{aligned} \quad (6.12)$$

VII. Early Time Impedance for Planar Bicones and Comparison to Late-Time Impedance

The impedance for a single planar bicone driven at the apex is²

$$Z_b = Z_o f_g$$

$$Z_o = \sqrt{\frac{\mu_o}{\epsilon_o}} \tag{7.1}$$

$$f_g = \frac{K(m)}{K(m_1)}$$

where Z_o is the impedance of free space (or the medium in which the array is located) and μ_o and ϵ_o are the permeability and permittivity respectively of free space. The geometrical impedance factor can also be written as

$$f_g = -\frac{1}{\pi} \ln(q_1) = \frac{1}{\pi} \ln\left(\frac{1}{q_1}\right)$$

$$= -\frac{\pi}{\ln(q)} = \frac{\pi}{\ln\left(\frac{1}{q}\right)} \tag{7.2}$$

$$q = e^{-\pi \frac{K(m_1)}{K(m)}}$$

$$q_1 = e^{-\pi \frac{K(m)}{K(m_1)}}$$

where q is called the nome and q_1 the complementary nome.^{1,2}

For small m which implies $\psi \rightarrow \pi/2$ we have

$$\begin{aligned}
f_g &= \frac{\pi}{\ln\left(\frac{1}{q}\right)} = \frac{\pi}{\ln\left(\frac{16}{m} + O(1)\right)} = \frac{\pi}{\ln\left(\frac{16}{m}\right) + O(m)} \\
&= \pi \left\{ \ln \left[16 \tan^{-4} \left(\frac{\pi}{4} - \frac{\psi}{2} \right) \right] + o \left(\left(\frac{\pi}{2} - \psi \right)^4 \right) \right\}^{-1} \\
&= \frac{\pi}{4} \left\{ \ln \left[2 \cot \left(\frac{\pi}{4} - \frac{\psi}{2} \right) \right] \right\}^{-1} \left\{ 1 + o \left(\left(\frac{\frac{\pi}{4} - \frac{\psi}{2}}{\ln \left[\cot \left(\frac{\pi}{4} - \frac{\psi}{2} \right) \right]} \right)^4 \right) \right\} \\
&= \frac{\pi}{4} \left\{ \ln \left[\frac{4}{\frac{\pi}{2} - \psi} \right] \right\}^{-1} \left\{ 1 + o \left(\frac{\frac{\pi}{2} - \psi}{\ln \left[\frac{\pi}{2} - \psi \right]} \right) \right\} \tag{7.3}
\end{aligned}$$

as an approximation for f_g for ψ near $\pi/2$. For small m_1 (m near 1) which implies $\psi \rightarrow 0$ we have

$$f_g = \frac{1}{\pi} \ln\left(\frac{1}{q_1}\right) = \frac{1}{\pi} \ln\left(\frac{16}{m_1}\right) + O(m_1) \tag{7.4}$$

For ψ near zero we have

$$\begin{aligned}
m_1 &= 1 - \tan^4 \left(\frac{\pi}{4} - \frac{\psi}{2} \right) = 1 - \tan^4 \left(\frac{\pi}{4} \right) - 4 \tan^3 \left(\frac{\pi}{4} \right) \sec^2 \left(\frac{\pi}{4} \right) \left(\frac{-\psi}{2} \right) + O(\psi^2) \\
&= 4\psi + O(\psi^2) \tag{7.5}
\end{aligned}$$

which gives

$$\begin{aligned}
f_g &= \frac{1}{\pi} \ln \left[\frac{4}{\psi + O(\psi^2)} \right] + O(\psi) \\
&= \frac{1}{\pi} \ln \left[\frac{4}{\pi} \right] + O(\psi) \tag{7.6}
\end{aligned}$$

Figure 9 and table 1 show the functional dependence of f_g on ψ and the accuracies of the asymptotic forms for ψ near 0 and 1. For the case of small ψ (with $\psi > 0$) note that equation 7.6 gives a better approximation for f_g than does equation 7.4. For $2\psi/\pi = .1$, for example, $(1/\pi)\ln(4/\psi)$ is accurate to 1 part in 10^3 . On the other hand for ψ near $\pi/2$ the approximation in

$\frac{2}{\pi} \psi$	$\frac{x_2}{x_3}$	m	f_g	$\frac{1}{\pi} \ln\left(\frac{16}{m_1}\right)$	$\frac{1}{\pi} \ln\left(\frac{4}{\psi}\right)$
0	1	1	∞	∞	∞
.001	.99686	.99374	2.49633	2.49733	2.49633
.002	.99374	.98751	2.27570	2.27770	2.27570
.003	.99062	.98133	2.14664	2.14963	2.14664
.004	.98751	.97518	2.05506	2.05905	2.05506
.005	.98441	.96907	1.98403	1.98902	1.98403
.006	.98133	.96300	1.92600	1.93198	1.92600
.007	.97825	.95697	1.87693	1.88390	1.87693
.008	.97518	.95098	1.83442	1.84239	1.83443
.009	.97212	.94502	1.79693	1.80588	1.79694
.010	.96907	.93910	1.76339	1.77333	1.76340
.020	.93909	.88189	1.54274	1.56250	1.54276
.030	.91003	.82815	1.41364	1.44312	1.41370
.040	.88184	.77764	1.32202	1.36111	1.32213
.050	.85450	.73017	1.25094	1.29951	1.25110
.060	.82797	.68554	1.19283	1.25079	1.19306
.070	.80223	.64358	1.14368	1.21092	1.14400
.080	.77725	.60412	1.10107	1.17750	1.10149
.090	.75300	.56701	1.06347	1.14898	1.06400
.100	.72945	.53210	1.02981	1.12430	1.03046
.110	.70659	.49927	.99933	1.10271	1.00013
.120	.68438	.46837	.97148	1.08366	.97243
.130	.66280	.43931	.94584	1.06671	.94695
.140	.64184	.41196	.92207	1.05155	.92336
.150	.62147	.38623	.89991	1.03792	.90140
.160	.60168	.36202	.87916	1.02560	.88086
.170	.58244	.33923	.85965	1.01444	.86156
.180	.56373	.31779	.84122	1.00427	.84337
.190	.54555	.29762	.82376	.99500	.82616
.200	.52786	.27864	.80717	.98651	.80983
.210	.51067	.26078	.79136	.97872	.79430
.220	.49394	.24398	.77626	.97157	.77949
.230	.47768	.22818	.76181	.96498	.76534
.240	.46186	.21331	.74794	.95891	.75179
.250	.44646	.19933	.73461	.95330	.73880
.260	.43149	.18618	.72177	.94812	.72631
.270	.41692	.17382	.70939	.94332	.71430
.280	.40274	.16220	.69744	.93888	.70273
.290	.38895	.15128	.68587	.93475	.69156
.300	.37552	.14102	.67466	.93093	.68076
.310	.36246	.13138	.66380	.92738	.67033
.320	.34975	.12233	.65325	.92408	.66022
.330	.33738	.11383	.64299	.92101	.65043
.340	.32534	.10585	.63301	.91816	.64092
.350	.31363	.09836	.62328	.91550	.63170
.360	.30223	.09134	.61380	.91303	.62273
.370	.29114	.08476	.60455	.91073	.61401
.380	.28034	.07859	.59551	.90860	.60552
.390	.26984	.07281	.58667	.90661	.59725
.400	.25962	.06740	.57803	.90475	.58919
.410	.24967	.06234	.56956	.90303	.58133
.420	.24000	.05760	.56126	.90143	.57366
.430	.23059	.05317	.55313	.89993	.56617
.440	.22143	.04903	.54514	.89855	.55885
.450	.21253	.04517	.53730	.89725	.55170
.460	.20387	.04156	.52960	.89605	.54470
.470	.19545	.03820	.52202	.89494	.53786
.480	.18726	.03507	.51457	.89391	.53116
.490	.17931	.03215	.50723	.89294	.52459
.500	.17157	.02944	.50000	.89205	.51816

Table 1a. Geometrical Impedance Factor for Symmetrical Planar Bicones and Symmetrical Coplanar Strips for $0 \leq \psi \leq \pi/4$

$\frac{2}{\pi} \psi$	$\frac{X_2}{X_3}$	m	f_g	$\pi \left\{ \ln \left(\frac{16}{m} \right) \right\}^{-1}$	$\frac{\pi}{4} \left\{ \ln \left(\frac{4}{\frac{\pi}{2} - \psi} \right) \right\}^{-1}$
.500	.17157	.02944	.50000	.49882	.48247
.510	.16406	.02692	.49287	.49182	.47656
.520	.15676	.02457	.48584	.48491	.47067
.530	.14967	.02240	.47891	.47808	.46481
.540	.14278	.02039	.47205	.47133	.45896
.550	.13610	.01852	.46529	.46464	.45314
.560	.12962	.01680	.45859	.45803	.44734
.570	.12332	.01521	.45197	.45148	.44156
.580	.11722	.01374	.44542	.44499	.43580
.590	.11131	.01239	.43893	.43855	.43005
.600	.10557	.01115	.43251	.43217	.42431
.610	.10002	.01000	.42613	.42584	.41858
.620	.09464	.00896	.41981	.41956	.41287
.630	.08944	.00800	.41353	.41331	.40716
.640	.08441	.00712	.40730	.40711	.40146
.650	.07954	.00633	.40110	.40094	.39576
.660	.07484	.00560	.39494	.39480	.39006
.670	.07030	.00494	.38881	.38869	.38436
.680	.06592	.00435	.38270	.38260	.37866
.690	.06170	.00381	.37662	.37654	.37295
.700	.05764	.00332	.37055	.37048	.36723
.710	.05373	.00289	.36450	.36444	.36150
.720	.04996	.00250	.35846	.35840	.35576
.730	.04635	.00215	.35241	.35237	.34999
.740	.04289	.00184	.34637	.34633	.34420
.750	.03957	.00157	.34032	.34029	.33839
.760	.03639	.00132	.33425	.33423	.33254
.770	.03335	.00111	.32817	.32815	.32665
.780	.03046	.00093	.32206	.32204	.32072
.790	.02770	.00077	.31591	.31590	.31474
.800	2.5E-02	6.3E-04	.30972	.30971	.30871
.810	2.3E-02	5.1E-04	.30349	.30348	.30261
.820	2.0E-02	4.1E-04	.29719	.29718	.29643
.830	1.8E-02	3.3E-04	.29082	.29081	.29017
.840	1.6E-02	2.5E-04	.28436	.28436	.28381
.850	1.4E-02	2.0E-04	.27780	.27780	.27735
.860	1.2E-02	1.5E-04	.27113	.27113	.27075
.870	1.0E-02	1.1E-04	.26432	.26431	.26401
.880	8.9E-03	8.0E-05	.25734	.25734	.25709
.890	7.5E-03	5.6E-05	.25017	.25017	.24997
.900	6.2E-03	3.8E-05	.24276	.24276	.24261
.910	5.0E-03	2.5E-05	.23508	.23508	.23496
.920	4.0E-03	1.6E-05	.22705	.22705	.22696
.930	3.0E-03	9.2E-06	.21859	.21859	.21853
.940	2.2E-03	4.9E-06	.20959	.20959	.20954
.950	1.5E-03	2.4E-06	.19985	.19985	.19982
.960	9.9E-04	9.8E-07	.18910	.18910	.18909
.970	5.6E-04	3.1E-07	.17685	.17685	.17684
.980	2.5E-04	6.1E-08	.16205	.16205	.16205
.990	6.2E-05	3.8E-09	.14177	.14177	.14177
.991	5.0E-05	2.5E-09	.13913	.13913	.13913
.992	3.9E-05	1.6E-09	.13628	.13628	.13628
.993	3.0E-05	9.1E-10	.13320	.13320	.13320
.994	2.2E-05	4.9E-10	.12980	.12980	.12980
.995	1.5E-05	2.4E-10	.12601	.12601	.12601
.996	9.9E-06	9.7E-11	.12165	.12165	.12165
.997	5.6E-06	3.1E-11	.11646	.11646	.11646
.998	2.5E-06	6.1E-12	.10986	.10986	.10986
.999	6.2E-07	3.8E-13	.10017	.10015	.10015
1	0	0	0	0	0

Table 1b. Geometrical Impedance Factor for Symmetrical Planar Bicones and Symmetrical Coplanar Strips for $\pi/4 \leq \psi < \pi/2$

terms of m is more accurate than the one in terms of ψ ; for $\psi = \pi/4$ the formula in terms of m is still accurate to about 2 parts in 10^3 . Figure 9 shows the range of validity of four approximating functions for f_g for relevant regions of ψ .

Having the early-time impedance of a single planar bicone it is interesting to compare the result to the late-time impedance each source (at the apex to each planar bicone) drives. The late-time impedance involves all the mutual interactions of the planar bicones and is influenced by the turn-on-time sequence for the source points (equation 2.7).⁴

Section IV has considered the late-time fields at large distances from the array. These are the same (except for delay) for components parallel to the x, y plane as the average tangential fields on the source plane (averaged over a unit cell). On the source plane the late-time average electric field has no y component. The impedance driven by each source (including both forward and back waves on both sides of the array) is then given by

$$\begin{aligned}
 Z_\ell &= \frac{Z_0}{2} \frac{a}{b} \frac{\vec{e}_s \cdot \vec{E}_0}{\vec{e}_t \cdot (\vec{e}_1 \times \vec{E}_0)} \\
 &= \frac{Z_0}{2} \frac{a}{b} \frac{\vec{e}_s \cdot \vec{e}_0}{\vec{e}_t \cdot \vec{e}'_0} = \frac{Z_0}{2} \frac{a}{b} \frac{\vec{e}_x \cdot \vec{e}_0}{\vec{e}_y \cdot \vec{e}'_0} \\
 &= \frac{Z_0}{2} \frac{a}{b} \frac{\cos(\theta_1) [1 - \sin^2(\theta_1) \sin^2(\phi_1)]^{-1/2}}{[\cos^2(\theta_1) \sin^2(\phi_1) + \cos^2(\phi_1)] [1 - \sin^2(\theta_1) \sin^2(\phi_1)]^{-1/2}} \\
 &= \frac{Z_0}{2} \frac{a}{b} \frac{\cos(\theta_1)}{1 - \sin^2(\theta_1) \sin^2(\phi_1)} \tag{7.7}
 \end{aligned}$$

Note that this result applies to more than just planar bicone arrays provided $2a$ is taken as the periodicity in the x direction and $2b$ as the periodicity in the y direction with one source per unit cell.

Consider a few special cases. First let $\phi_1 = 0$ so that the radiated wave is propagating parallel to the x, z plane and the electric field is also parallel to this plane. Then we have

$$Z_{\ell} = \frac{Z_0}{2} \frac{a}{b} \cos(\theta_1) \quad (7.8)$$

In this case Z_{ℓ} decreases from the case of normal propagation, $(\theta_1, \phi_1) = (0, 0)$, as θ_1 is increased from zero.

Next let $\phi_1 = \pi/2$ so that the radiated wave is propagating parallel to the y, z plane and the magnetic field is also parallel to this plane. Then we have

$$Z_{\ell} = \frac{Z_0}{2} \frac{a}{b} \frac{1}{\cos(\theta_1)} \quad (7.9)$$

In this case Z_{ℓ} increases from the case of normal propagation as θ_1 is increased from zero.

For various choices of θ_1 and ϕ_1 one might choose ψ and a/b to make the early-time and late-time impedances match or have some other specified relationship to each other. Given θ_1 , ϕ_1 , ψ , and a/b equations 7.1 and 7.7 can be used to relate the early-time and late-time impedances. One might wish, for example, to make the early-time and late-time impedances equal and use this criterion to constrain the relation between b/a and ψ as a function of θ_1 and ϕ_1 .

As an interesting example suppose $\theta_1 = 0$ (propagation perpendicular to array) and let $\psi = \pi/4$. For $a/b = 1$ the ratio of early-time and late-time impedances is 1 if $f_g = 1/2$ for a single planar bicone. For $\psi = \pi/4$ it is the case that $f_g = .5$ as can be seen in the following derivation. This choice of f_g was used for the complex potential function plot in figures 7 and 8 for the equivalent two symmetrical coplanar strips.

For $\psi = \pi/4$ we have the parameter and complementary parameter for the elliptic integrals as

$$\begin{aligned} m &= \tan^4\left(\frac{\pi}{4} - \frac{\psi}{2}\right) = \tan^4\left(\frac{\pi}{8}\right) = \left[\frac{1 - \cos(\pi/4)}{1 + \cos(\pi/4)}\right]^2 \\ &= \left[\frac{\sqrt{2} - 1}{\sqrt{2} + 1}\right]^2 = [\sqrt{2} - 1]^4 = [3 - 2\sqrt{2}]^2 = 17 - 12\sqrt{2} \quad (7.10) \end{aligned}$$

$$m_1 = 1 - m = 1 - [\sqrt{2} - 1]^4 = 12\sqrt{2} - 16 = 4[3\sqrt{2} - 4]$$

Then consider the special formula for the complete elliptic integral of the first kind as¹²

$$K(m') = 2[1 + m_1'^{1/2}]^{-1} K\left(\left[\frac{1 - m_1'^{1/2}}{1 + m_1'^{1/2}}\right]^2\right) \quad (7.11)$$

$$m' + m_1' = 1$$

First choose

$$m' = m_1' = \frac{1}{2}$$

$$\left[\frac{1 - m_1'^{1/2}}{1 + m_1'^{1/2}}\right]^2 = \left[\frac{\sqrt{2} - 1}{\sqrt{2} + 1}\right]^2 = m \quad (7.12)$$

which gives

$$K(m) = \frac{\sqrt{2} + 1}{2\sqrt{2}} K(1/2) \quad (7.13)$$

Next choose

$$\left[\frac{1 - m_1'^{1/2}}{1 + m_1'^{1/2}}\right]^2 = \frac{1}{2}$$

$$m_1'^{1/2} = \frac{\sqrt{2} - 1}{\sqrt{2} + 1} = [\sqrt{2} - 1]^2 \quad (7.14)$$

$$m_1' = [\sqrt{2} - 1]^4 = m$$

$$m' = 1 - m_1' = m_1$$

which gives

$$K(m_1) = \frac{\sqrt{2} + 1}{\sqrt{2}} K(1/2) \quad (7.15)$$

The early-time geometrical impedance factor for $\psi = \pi/4$ is then

$$f_g = \frac{K(m)}{K(m_1)} = \frac{1}{2} \quad (7.16)$$

exactly.

VIII. Early Time Fields at Large Distances from an Array of Planar Bicones

The conformal transformation for the complex potential function (from equations 6.7 and 6.11) is

$$\zeta = \alpha \zeta' = \alpha [X' + iY'] = \operatorname{sn}(w|m)$$

$$w = u + iv \tag{8.1}$$

$$\alpha = \frac{\cos(\psi)}{1 - \sin(\psi)} = m^{-1/4}$$

For use in the formulas to follow we have the Jacobian elliptic functions of complex argument¹²

$$\begin{aligned} \operatorname{sn}(w|m) &= \frac{\operatorname{sn}(u|m) \operatorname{dn}(v|m_1) + i \operatorname{cn}(u|m) \operatorname{dn}(u|m) \operatorname{sn}(v|m_1) \operatorname{cn}(v|m_1)}{\operatorname{cn}^2(v|m_1) + m \operatorname{sn}^2(u|m) \operatorname{sn}^2(v|m_1)} \\ \operatorname{cn}(w|m) &= \frac{\operatorname{cn}(u|m) \operatorname{cn}(v|m_1) - i \operatorname{sn}(u|m) \operatorname{dn}(u|m) \operatorname{sn}(v|m_1) \operatorname{dn}(v|m_1)}{\operatorname{cn}^2(v|m_1) + m \operatorname{sn}^2(u|m) \operatorname{sn}^2(v|m_1)} \\ \operatorname{dn}(w|m) &= \frac{\operatorname{dn}(u|m) \operatorname{cn}(v|m_1) \operatorname{dn}(v|m_1) - i \operatorname{sn}(u|m) \operatorname{cn}(u|m) \operatorname{sn}(v|m_1)}{\operatorname{cn}^2(v|m_1) + m \operatorname{sn}^2(u|m) \operatorname{sn}^2(v|m_1)} \end{aligned} \tag{8.2}$$

where

$$m \equiv 1 - m_1 = \tan^4\left(\frac{\pi}{4} - \frac{\psi}{2}\right) = \alpha^{-4} \tag{8.3}$$

Now we require that $f(\theta, \phi)$ change by 1.0 in going from one conductor to another in the planar bicone. Let us require that f be $\pm 1/2$ on the two conductors. Thus we set

$$f = \frac{u}{2K(m)} \tag{8.4}$$

Then taking the gradient in the X', Y' coordinate system we have

$$\begin{aligned}\nabla' f &= \frac{1}{2K(m)} \nabla' u \\ &= \frac{\alpha}{2K(m)} \left\{ \vec{e}_X, \operatorname{Re} \left[\frac{dw}{d\zeta} \right] - \vec{e}_Y, \operatorname{Im} \left[\frac{dw}{d\zeta} \right] \right\}\end{aligned}\tag{8.5}$$

This gives

$$\begin{aligned}\frac{\partial f}{\partial X'} &= \frac{\alpha}{2K(m)} \operatorname{Re} \left[\frac{dw}{d\zeta} \right] \\ \frac{\partial f}{\partial Y'} &= -\frac{\alpha}{2K(m)} \operatorname{Im} \left[\frac{dw}{d\zeta} \right]\end{aligned}\tag{8.6}$$

for which we need

$$\frac{dw}{d\zeta} = \left[\frac{d\zeta}{dw} \right]^{-1} = \{ \operatorname{cn}(w|m) \operatorname{dn}(w|m) \}^{-1}\tag{8.7}$$

Using the relations among the elliptic functions as

$$\begin{aligned}\operatorname{cn}(w|m) &= [1 - \operatorname{sn}^2(w|m)]^{1/2} \\ \operatorname{dn}(w|m) &= [1 - m \operatorname{sn}^2(w|m)]^{1/2}\end{aligned}\tag{8.8}$$

the derivative of the complex potential function can be expressed in terms of ζ as

$$\frac{dw}{d\zeta} = \{ [1 - \zeta^2] [1 - m\zeta^2] \}^{-1/2}\tag{8.9}$$

where one should be careful in evaluating the square root so as to have

$$\left. \frac{dw}{d\zeta} \right|_{\zeta=0} = 1\tag{8.10}$$

For this purpose one can refer to figure 7 and define branch cuts along the $\operatorname{Re}[\zeta]$ line from $\zeta = +1$ to $\zeta = +\infty$ and from $\zeta = -1$ to $\zeta = -\infty$.

For a given θ_1, ϕ_1 we can calculate the corresponding X'_1, Y'_1 and thus the corresponding ζ'_1 from equations 5.10. As in equations 8.1 one calculates ζ since α and m are known from ψ . Equation 8.9 gives $dw/d\zeta$ without having to first calculate w . This gives $\partial f/\partial X'$ and $\partial f/\partial Y'$ in equations 8.6. The far-field effective early-time rise t_1 can then be calculated from equation 5.24 and the fraction ρ of the early-time field perpendicular to the late-time field direction can be calculated from equation 5.25. Note that the quantities $\theta, \phi, X', Y', \zeta', \zeta$ can all be given subscript 1 to make them correspond to the direction to the observer at large distances from the array. For convenience one can write

$$\begin{aligned}\zeta &= \alpha \zeta' = m^{-1/4} \zeta' \\ &= \alpha \frac{\sin(\theta) \cos(\phi) + i \cos(\theta)}{1 + \sin(\theta) \sin(\phi)}\end{aligned}\quad (8.11)$$

which brings into this section all the necessary terms to substitute into equations 5.24 and 5.25 for the field related quantities.

Consider some special cases for which the expressions for the fields simplify somewhat. First let $\theta_1 = 0$ (for which ϕ_1 can take on any value). The normalized potential function is

$$f(0, \phi_1) = 0 \quad (8.12)$$

The normalized coordinates for the equivalent cylindrical system are

$$\begin{aligned}\zeta &= X' + iY' = i \\ X' &= 0, \quad Y' = 1 \\ \zeta &= \alpha \zeta' = i\alpha\end{aligned}\quad (8.13)$$

The normalized potential is found (since α is real) from

$$\begin{aligned}\text{sn}(w|m) &= i\alpha = im^{-1/4} \\ \text{sc}(v|m) &= \alpha = m^{-1/4}, \quad u = 0\end{aligned}\quad (8.14)$$

The derivative of the normalized potential at $\zeta = i\alpha$ is real and positive and is given by

$$\begin{aligned} \left. \frac{dw}{d\zeta} \right|_{\zeta=i\alpha} &= \{[1 + \alpha^2][1 + \alpha^{-2}]\}^{-1/2} \\ &= \frac{\alpha}{1 + \alpha^2} \end{aligned} \quad (8.15)$$

Thus for our special case of $\theta_1 = 0$ we have

$$\begin{aligned} \frac{\partial f}{\partial X'} &= \frac{1}{2K(m)} [1 + \alpha^{-2}]^{-1} \\ \frac{\partial f}{\partial Y'} &= 0 \\ \frac{2\pi ch}{A} t_1 &= \pi \frac{ct_1}{b} = 2K(m) [1 + \alpha^{-2}] \\ &= 2K(m) [1 + m^{1/2}] \end{aligned} \quad (8.16)$$

$$\rho = 0$$

For small m with $\psi \rightarrow \pi/2$ we have

$$\begin{aligned} \frac{2\pi ch}{A} t_1 &= \pi [1 + O(m)] [1 + m^{1/2}] \\ &= \pi [1 + m^{1/2} + O(m)] \\ &= \pi \left[1 + \tan^2 \left(\frac{\pi}{4} - \frac{\psi}{2} \right) + o \left(\left(\frac{\pi}{2} - \psi \right)^4 \right) \right] \\ &= \pi \left[1 + \frac{1}{4} \left(\frac{\pi}{2} - \psi \right)^2 + o \left(\left(\frac{\pi}{2} - \psi \right)^4 \right) \right] \end{aligned} \quad (8.17)$$

For small m_1 with $\psi \rightarrow 0$ we have

$$\begin{aligned}
\frac{2\pi ch}{A} t_1 &= \pi \left[1 + \frac{m_1}{4} + O(m_1^2) \right] \ln \left[\frac{1}{\frac{m_1}{16} + O(m_1^2)} \right] \\
&= \pi [1 + O(m_1)] \left[\ln \left[\frac{16}{m_1} \right] + O(m_1) \right] \\
&= \pi \ln \left[\frac{16}{m_1} \right] + O(m_1 \ln(m_1)) \\
&= \pi \ln \left[\frac{4}{\psi} \right] + O(\psi \ln(\psi)) \tag{8.18}
\end{aligned}$$

The numerical results for the case of $\theta_1 = 0$ are given in figure 10 and table 2. Note that for the special case of $\psi = \pi/4$ so that $f_g = 0.5$ the characteristic time ct_1/b for the rise of far field is 1.18 which is roughly 1; this result is not surprising.⁹ Note, however, for small ψ that ct_1/b becomes somewhat larger, indicating a less efficient early time performance. For ψ near $\pi/2$ on the other hand the early-time impedance of a planar bicone (figure 9) is rather small; a pulse generator with some inductive limitation on the signal it can deliver to the bicone will then produce a comparatively slow rising pulse on the bicone. (The present graphs assume zero source impedance.) For a practical pulser then some intermediate value of ψ (between 0 and $\psi/2$) will be optimum for a particular application. This is further complicated by the fact that in a practical application times of several nanoseconds can be of importance while times of zero nanoseconds have no practical importance, except insofar as they characterize early times of interest. Furthermore an intermediate value of ψ is also needed to match early and late time impedances and thereby minimize oscillation of the array unit cells.

Now let $\phi_1 = 0$ with $0 \leq \theta_1 < \pi/2$. Then we have

$$\begin{aligned}
\zeta_1 &= \alpha \zeta_1' = \alpha [\sin(\theta_1) + i \cos(\theta_1)] = i \alpha e^{-i\theta_1} \\
\frac{dw}{d\zeta_1} &= [1 + \alpha^2 e^{-i2\theta_1}] [1 + \alpha^{-2} e^{-i2\theta_1}]^{-1/2} \\
&= e^{i\theta_1} \lambda_o^{-1/2}
\end{aligned}$$

$\frac{2}{\pi} \psi$	ct_1/b	$\ln\left(\frac{4}{\psi}\right)$	$\frac{2}{\pi} \psi$	ct_1/b	$1 + \frac{1}{4}\left(\frac{\pi}{2} - \psi\right)^2$
0	∞	∞	.50	1.18034	1.15421
.01	3.52700	5.53988	.51	1.17201	1.14811
.02	3.08624	4.84673	.52	1.16397	1.14212
.03	2.82885	4.44127	.53	1.15619	1.13626
.04	2.64666	4.15359	.54	1.14868	1.13053
.05	2.50573	3.93044	.55	1.14142	1.12491
.06	2.39097	3.74812	.56	1.13441	1.11942
.07	2.29428	3.59397	.57	1.12763	1.11406
.08	2.21087	3.46044	.58	1.12109	1.10881
.09	2.13761	3.34266	.59	1.11477	1.10369
.10	2.07239	3.23730	.60	1.10867	1.09870
.11	2.01368	3.14199	.61	1.10279	1.09382
.12	1.96036	3.05498	.62	1.09711	1.08907
.13	1.91159	2.97493	.63	1.09163	1.08445
.14	1.86668	2.90082	.64	1.08635	1.07994
.15	1.82513	2.83183	.65	1.08125	1.07556
.16	1.78650	2.76729	.66	1.07635	1.07131
.17	1.75045	2.70667	.67	1.07163	1.06717
.18	1.71669	2.64951	.68	1.06708	1.06317
.19	1.68497	2.59544	.69	1.06272	1.05928
.20	1.65510	2.54415	.70	1.05852	1.05552
.21	1.62688	2.49536	.71	1.05449	1.05188
.22	1.60019	2.44884	.72	1.05062	1.04836
.23	1.57487	2.40439	.73	1.04691	1.04497
.24	1.55083	2.36183	.74	1.04337	1.04170
.25	1.52795	2.32101	.75	1.03997	1.03855
.26	1.50615	2.28179	.76	1.03673	1.03553
.27	1.48535	2.24404	.77	1.03364	1.03263
.28	1.46548	2.20768	.78	1.03070	1.02986
.29	1.44648	2.17259	.79	1.02790	1.02720
.30	1.42829	2.13868	.80	1.02525	1.02467
.31	1.41086	2.10589	.81	1.02273	1.02227
.32	1.39414	2.07415	.82	1.02036	1.01999
.33	1.37809	2.04337	.83	1.01812	1.01783
.34	1.36267	2.01352	.84	1.01602	1.01579
.35	1.34785	1.98453	.85	1.01406	1.01388
.36	1.33360	1.95636	.86	1.01223	1.01209
.37	1.31988	1.92896	.87	1.01053	1.01042
.38	1.30667	1.90230	.88	1.00896	1.00888
.39	1.29395	1.87632	.89	1.00752	1.00746
.40	1.28169	1.85100	.90	1.00620	1.00617
.41	1.26986	1.82631	.91	1.00502	1.00500
.42	1.25846	1.80221	.92	1.00396	1.00395
.43	1.24745	1.77868	.93	1.00303	1.00302
.44	1.23683	1.75569	.94	1.00223	1.00222
.45	1.22658	1.73322	.95	1.00154	1.00154
.46	1.21668	1.71124	.96	1.00099	1.00099
.47	1.20712	1.68973	.97	1.00056	1.00056
.48	1.19788	1.66868	.98	1.00025	1.00025
.49	1.18896	1.64806	.99	1.00006	1.00006
.50	1.18034	1.62786	1.00	1.00000	1.00000

Table 2. ct_1/b and Asymptotic Forms for $\theta_1 = 0$

$$\lambda_0 = \left[\frac{e^{i\theta_1}}{\alpha} + \alpha e^{-i\theta_1} \right] \left[\frac{e^{-i\theta_1}}{\alpha} + \alpha e^{i\theta_1} \right] \quad (8.19)$$

$$= \left| \frac{e^{-i\theta_1}}{\alpha} + \alpha e^{i\theta_1} \right|^2$$

$$\text{Im}(\lambda_0) = 0$$

where we note that λ_0 is the product of two terms, each of which is the complex conjugate of the other. The terms in the expression for the early-time field fraction are

$$\begin{aligned} & -\sin(\theta_1) \frac{\partial f}{\partial X'_1} - \cos(\theta_1) \frac{\partial f}{\partial Y'_1} \\ &= \frac{\alpha}{2K(m)} \left\{ -\sin(\theta_1) \text{Re} \left[\frac{dw}{d\zeta} \right] + \cos(\theta_1) \text{Im} \left[\frac{dw}{d\zeta} \right] \right\} \\ &= \frac{\alpha}{2K(m)} \left\{ -\sin(\theta_1) \cos(\theta_1) \lambda_0^{-1/2} + \cos(\theta_1) \sin(\theta_1) \lambda_0^{-1/2} \right\} \\ &= 0 \end{aligned} \quad (8.20)$$

$$\begin{aligned} & \cos(\theta_1) \frac{\partial f}{\partial X'_1} - \sin(\theta_1) \frac{\partial f}{\partial Y'_1} \\ &= \frac{\alpha}{2K(m)} \left\{ \cos^2(\theta_1) \lambda_0^{-1/2} + \sin^2(\theta_1) \lambda_0^{-1/2} \right\} \\ &= \frac{\alpha}{2K(m)} \lambda_0^{-1/2} \end{aligned}$$

Thus we have

$$\begin{aligned} \frac{2\pi ch}{A} t_1 = \pi \frac{ct_1}{b} &= \left\{ \cos(\theta_1) \frac{\partial f}{\partial X'_1} - \sin(\theta_1) \frac{\partial f}{\partial Y'_1} \right\}^{-1} \\ &= \frac{2}{\alpha} K(m) \lambda_0^{1/2} \end{aligned} \quad (8.21)$$

$$\rho = 0$$

Similarly for $\phi_1 = \pm\pi$ with $0 \leq \theta_1 < \pi/2$ we have

$$\zeta_1 = \alpha \zeta'_1 = \alpha [-\sin(\theta_1) + i \cos(\theta_1)] = i\alpha e^{i\theta_1}$$

$$\begin{aligned} \frac{dw}{d\zeta_1} &= \left\{ [1 + \alpha^2 e^{i2\theta_1}] [1 + \alpha^{-2} e^{i2\theta_1}] \right\}^{-1/2} \\ &= e^{-i\theta_1} \lambda_0^{-1/2} \end{aligned} \quad (8.22)$$

with λ_0 the same as before. The terms in the expression for the early-time field fraction are

$$\begin{aligned} &\sin(\theta_1) \frac{\partial f}{\partial X'_1} - \cos(\theta_1) \frac{\partial f}{\partial Y'_1} \\ &= \frac{\alpha}{2K(m)} \left\{ \sin(\theta_1) \cos(\theta_1) \lambda_0^{-1/2} - \cos(\theta_1) \sin(\theta_1) \lambda_0^{-1/2} \right\} \\ &= 0 \end{aligned} \quad (8.23)$$

$$\begin{aligned} &\cos(\theta_1) \frac{\partial f}{\partial X'_1} + \sin(\theta_1) \frac{\partial f}{\partial Y'_1} \\ &= \frac{\alpha}{2K(m)} \left\{ \cos^2(\theta_1) \lambda_0^{-1/2} + \sin^2(\theta_1) \lambda_0^{-1/2} \right\} \\ &= \frac{\alpha}{2K(m)} \lambda_0^{-1/2} \end{aligned}$$

Thus we have

$$\begin{aligned} \frac{2\pi ch}{A} t_1 &= \pi \frac{ct_1}{b} = \left\{ \cos(\theta_1) \frac{\partial f}{\partial X'_1} + \sin(\theta_1) \frac{\partial f}{\partial Y'_1} \right\}^{-1} \\ &= \frac{2}{\alpha} K'(m) \lambda_0^{1/2} \end{aligned} \quad (8.24)$$

$$\rho = 0$$

The cases of $\phi_1 = 0$ and $\phi_1 = \pm\pi$ then have the same results as one would expect from symmetry.

Figure 11 shows the variation of ct_1/b as a function of ψ for various values of θ_1 with $\phi_1 = 0, \pm\pi$. Note for small ψ and for θ_1 near $\pi/2$ that ct_1/b becomes small, but for more moderate values of θ_1 and ψ then ct_1/b is near 1.

For $\phi_1 = \pi/2$ we have

$$\zeta_1 = \alpha \zeta_1' = i\alpha \frac{\cos(\theta_1)}{1 + \sin(\theta_1)} = i\alpha \tan\left(\frac{\pi}{4} - \frac{\theta_1}{2}\right)$$

$$\begin{aligned} \frac{dw}{d\zeta_1} &= \left\{ \left[1 + \alpha^2 \tan^2\left(\frac{\pi}{4} - \frac{\theta_1}{2}\right) \right] \left[1 + \alpha^{-2} \tan^2\left(\frac{\pi}{4} - \frac{\theta_1}{2}\right) \right] \right\}^{-1/2} \\ &= \cot\left(\frac{\pi}{4} - \frac{\theta_1}{2}\right) \lambda_1^{-1/2} \end{aligned} \quad (8.25)$$

$$\lambda_1 = \left[\frac{1}{\alpha} \cot\left(\frac{\pi}{4} - \frac{\theta_1}{2}\right) + \alpha \tan\left(\frac{\pi}{4} - \frac{\theta_1}{2}\right) \right] \left[\alpha \cot\left(\frac{\pi}{4} - \frac{\theta_1}{2}\right) + \frac{1}{\alpha} \tan\left(\frac{\pi}{4} - \frac{\theta_1}{2}\right) \right]$$

$$\text{Im}\left[\frac{dw}{d\zeta_1}\right] = 0$$

Thus we have

$$\begin{aligned} \frac{2\pi ch}{A} t_1 &= \pi \frac{ct_1}{b} = \cos(\theta_1) [1 + \sin(\theta_1)] \left[\frac{\partial f}{\partial X_1'} \right]^{-1} \\ &= \cos(\theta_1) \sin(\theta_1) \cot\left(\frac{\pi}{4} - \frac{\theta_1}{2}\right) \left[\frac{\partial f}{\partial X_1'} \right]^{-1} \\ &= \frac{2}{\alpha} K(m) \cos(\theta_1) \sin(\theta_1) \lambda_1^{1/2} \end{aligned} \quad (8.26)$$

$$\rho = 0$$

Similarly for $\phi_1 = -\pi/2$ with $0 \leq \theta_1 < \pi/2$ we have

$$\zeta_1 = \alpha \zeta_1' = i\alpha \frac{\cos(\theta_1)}{1 - \sin(\theta_1)} = i\alpha \cot\left(\frac{\pi}{4} - \frac{\theta_1}{2}\right)$$

$$\begin{aligned} \frac{dw}{d\zeta_1} &= \left\{ \left[1 + \alpha^2 \cot^2\left(\frac{\pi}{4} - \frac{\theta_1}{2}\right) \right] \left[1 + \alpha^{-2} \cot^2\left(\frac{\pi}{4} - \frac{\theta_1}{2}\right) \right] \right\}^{-1/2} \\ &= \tan\left(\frac{\pi}{4} - \frac{\theta_1}{2}\right) \lambda_1^{-1/2} \end{aligned} \quad (8.27)$$

$$\text{Im}\left[\frac{dw}{d\zeta_1}\right] = 0$$

with λ_1 the same as before. Thus we have

$$\begin{aligned} \frac{2\pi ch}{A} t_1 &= \pi \frac{ct_1}{b} = \cos(\theta_1) [1 - \sin(\theta_1)] \left[\frac{\partial f}{\partial X_1'}\right]^{-1} \\ &= \frac{2}{\alpha} K(m) \cos(\theta_1) \sin(\theta_1) \tan\left(\frac{\pi}{4} - \frac{\theta_1}{2}\right) \left[\frac{\partial f}{\partial X_1'}\right]^{-1} \\ &= \frac{2}{\alpha} K(m) \cos(\theta_1) \sin(\theta_1) \lambda_1^{1/2} \end{aligned} \quad (8.28)$$

$$\rho = 0$$

The cases of $\phi_1 = \pm\pi/2$ then have the same results as one would expect from symmetry. Figure 12 summarizes the results for this special ϕ_1 case. Again note for ϕ_1 near $\pi/2$ that ct_1/b is decreased.

For the special case of $\theta_1 = \pi/2$ we have

$$\zeta_1 = \alpha \zeta_1' = \alpha \frac{\cos(\phi_1)}{1 + \sin(\phi_1)} = \alpha \tan\left(\frac{\pi}{4} - \frac{\phi_1}{2}\right) \quad (8.29)$$

$$\frac{dw}{d\zeta_1} = \left\{ \left[1 - \alpha^2 \tan^2\left(\frac{\pi}{4} - \frac{\phi_1}{2}\right) \right] \left[1 - \alpha^{-2} \tan^2\left(\frac{\pi}{4} - \frac{\phi_1}{2}\right) \right] \right\}^{-1/2}$$

Now for various ranges of ϕ_1 we then have

$$\text{Im}\left[\frac{dw}{d\zeta_1}\right] = 0 \quad \text{for } \psi < |\phi_1| < \pi - \psi \quad (8.30)$$

$$\text{Re}\left[\frac{dw}{d\zeta_1}\right] = 0 \quad \text{for } |\phi_1| < \psi \text{ or } |\pi - \phi_1| < \psi$$

Referring to figures 7 and 8 this special result for $\theta_1 = \pi/2$ applies along the line $\text{Im}[\zeta] = 0$. On the conductors the electric field is in the $\text{Im}[\zeta]$ direction; off the conductors the electric field is in the $\text{Re}[\zeta]$ direction. Then t_1 and ρ become

$$\begin{aligned} \frac{2\pi ch}{A} t_1 &= \pi \frac{ct_1}{b} = |\cos(\phi_1)| [1 + \sin(\phi_1)] \left| \left[\frac{\partial f}{\partial Y_1'} \right]^{-1} \right| \\ &= \cos^2(\phi_1) \left| \cot\left(\frac{\pi}{4} - \frac{\phi_1}{2}\right) \left[\frac{\partial f}{\partial Y_1'} \right]^{-1} \right| \\ &= \frac{2}{\alpha} K(m) \lambda_2^{1/2} \quad \text{for } |\phi_1| < \psi \text{ or } |\pi - \phi_1| < \psi \end{aligned} \quad (8.31)$$

$$\lambda_2 = - \left[\frac{1}{\alpha} \cot\left(\frac{\pi}{4} - \frac{\phi_1}{2}\right) - \alpha \tan\left(\frac{\pi}{4} - \frac{\phi_1}{2}\right) \right] \left[\alpha \cot\left(\frac{\pi}{4} - \frac{\phi_1}{2}\right) - \frac{1}{\alpha} \tan\left(\frac{\pi}{4} - \frac{\phi_1}{2}\right) \right]$$

$$\frac{2\pi ch}{A} t_1 = \pi \frac{ct_1}{b} = \infty \quad \text{for } \psi < |\phi_1| < \pi - \psi$$

$$\rho = \frac{\frac{\partial f}{\partial X_1'}}{\frac{\partial f}{\partial Y_1'}} = \begin{cases} \pm\infty & \text{for } \psi < |\phi_1| < \pi - \psi \\ 0 & \text{for } |\phi_1| < \psi \text{ or } |\pi - \phi_1| < \psi \end{cases}$$

Note that for $\theta_1 = \pi/2$ the clear time t_{cf} for the validity of the spherical TEM formulas goes to zero so the above expressions are limiting cases. Also note that replacing ϕ_1 by $-\phi_1$ or $\pi - \phi_1$ or $\pi + \phi_1$ leaves λ_2 unchanged. Figure 13 plots ct_1/b as a function of ψ for various values of ϕ_1 for this special case of θ_1 .

From figures 4, 5, and 6 one can note that each unit cell of our special planar bicones has 3 symmetry planes: the xz plane ($\phi_1 = 0, \pm\pi$), the yz plane ($\phi_1 = \pm\pi/2$), and the xy plane

($\theta_1 = \pi/2$). The presence of a symmetry plane introduces certain symmetries into the electromagnetic field distribution.⁹ Note that the voltage source at $r = 0$ connecting to the planar bicones makes the scalar potential the same for $\pm y$ and $\pm z$, but opposite (given the convention on $f(\theta, \phi)$) for $\pm x$. The fields are then symmetric with respect to the xy and xz planes, but antisymmetric with respect to the yz plane (using the definitions from ref. 9).

The unit vector \vec{e}_1 (propagation direction) is symmetric with respect to all 3 symmetry planes, noting that it is the same as \vec{e}_r , considering one cell. The late time electric field direction \vec{e}_0 is parallel to the xz plane and therefore symmetric with respect to the xz plane; it is also symmetric with respect to the xy plane and antisymmetric with respect to the yz plane.

The symmetry properties of the fields can be carried over directly to the symmetries of t_1 and ρ with respect to θ_1 and ϕ_1 . For $t_1(\theta_1, \phi_1)$ we have

$$\begin{aligned}
 t_1(\theta_1, \phi_1) &= t_1(\pi - \theta_1, \phi_1) \\
 &= t_1(\theta_1, -\phi_1) \\
 &= t_1(\theta_1, \pi - \phi_1) \\
 &= t_1(\theta_1, \pi + \phi_1)
 \end{aligned} \tag{8.32}$$

which is the same as the symmetries of $\vec{e}_0 \cdot \vec{F}$. The symmetries of $\rho(\theta_1, \phi_1)$ are then the same as those of $\vec{e}'_0 \cdot \vec{F} = [\vec{e}_1 \times \vec{e}_0] \cdot \vec{F}$ giving

$$\begin{aligned}
 \rho(\theta_1, \phi_1) &= -\rho(\pi - \theta_1, \phi_1) \\
 &= -\rho(\theta_1, -\phi_1) \\
 &= -\rho(\theta_1, \pi - \phi_1) \\
 &= \rho(\theta_1, \pi + \phi_1)
 \end{aligned} \tag{8.33}$$

since $\vec{e}'_0 = \vec{e}_1 \times \vec{e}_0$ is antisymmetric with respect to the xy and xz planes but symmetric with respect to the yz plane. The symmetries of \vec{e}'_0 are the same as those of the magnetic field and are thus the opposite of those for the electric field and \vec{e}_0 .

Figures 14 through 23 plot ct_1/b and ρ as functions of ψ with θ_1 and ϕ_1 as parameters. The ranges of θ_1 and ϕ_1 in these plots are restricted to $0 \rightarrow \pi/2$. Other values can be obtained through use of the symmetry relations in equations 8.32 and 8.33. Note for ψ near $\pi/2$ that ρ is small for all θ_1 and ϕ_1 as long as θ_1 is not too near to $\pi/2$. Small values of θ_1 also keep ρ small for even small values of ψ .

IX. Summary

This note has treated a special example of a periodic planar array, specifically an array of planar bicones in rectangular unit cells. Using special techniques the early and late time characteristics of the far fields have been found and presented in numerical form in tables and graphs for the case of zero impedance sources triggered in plane wave sequence with step function voltages. These techniques can be readily applied to other unit cell geometries and other bicone shapes. Unfortunately these techniques do not give the intermediate time results in general.

The present results depend on the plane wave trigger sequence as well as biconical fields near sources. However, each of these restrictions can be considered separately and applied independently to different types of source array problems. For example, one might consider a plane wave sequence of unit cells with non TEM early-time fields. Alternatively one might consider other than planar (say spherical) trigger sequences of unit cells with early-time conical TEM waves.

In addition to these early-time and late-time solutions it would be desirable to solve some appropriate array problems for all times and frequencies. At least a few of these solutions would help to optimize array design for intermediate times and frequencies.

X. References

1. C. E. Baum, Sensor and Simulation Note 31, The Conical Transmission Line as a Wave Launcher and Terminator for a Cylindrical Transmission Line, January 1967.
2. C. E. Baum, Sensor and Simulation Note 42, A Conical-Transmission-Line Gap for a Cylindrical Loop, May 1967.
3. C. E. Baum, Sensor and Simulation Note 84, The Distributed Source for Launching Spherical Waves, May 1969.
4. C. E. Baum, Sensor and Simulation Note 100, Some Characteristics of Planar Distributed Sources for Radiating Transient Pulses, March 1970.
5. C. E. Baum, Sensor and Simulation Note 108, Distributed Sources and Terminations for Launching and Terminating Plane Waves Either With or Without a Reflected Plane Wave, May 1970.
6. C. E. Baum, Sensor and Simulation Note 143, General Principles for the Design of ATLAS I and II, Part I: ATLAS: Electromagnetic Design Considerations for Horizontal Version, January 1972.
7. C. E. Baum, Sensor and Simulation Note 146, General Principles for the Design of ATLAS I and II, Part IV: Additional Considerations for the Design of Pulser Arrays, March 1972.
8. C. E. Baum, Sensor and Simulation Note 148, General Principles for the Design of ATLAS I and II, Part V: Some Approximate Figures of Merit for Comparing the Waveforms Launched by Imperfect Pulser Arrays onto TEM Transmission Lines, May 1972.
9. C. E. Baum, Interaction Note 63, Interaction of Electromagnetic Fields with an Object which has an Electromagnetic Symmetry Plane, March 1971.
10. W. R. Smythe, Static and Dynamic Electricity, 3rd ed., section 12.06, McGraw Hill, 1968.
11. Moon and Spencer, Field Theory Handbook, section II, Springer-Verlag, 1961.
12. Abramowitz and Stegun, ed., Handbook of Mathematical Functions, chapters 16 and 17, U.S. Gov't Printing Office, 1964.

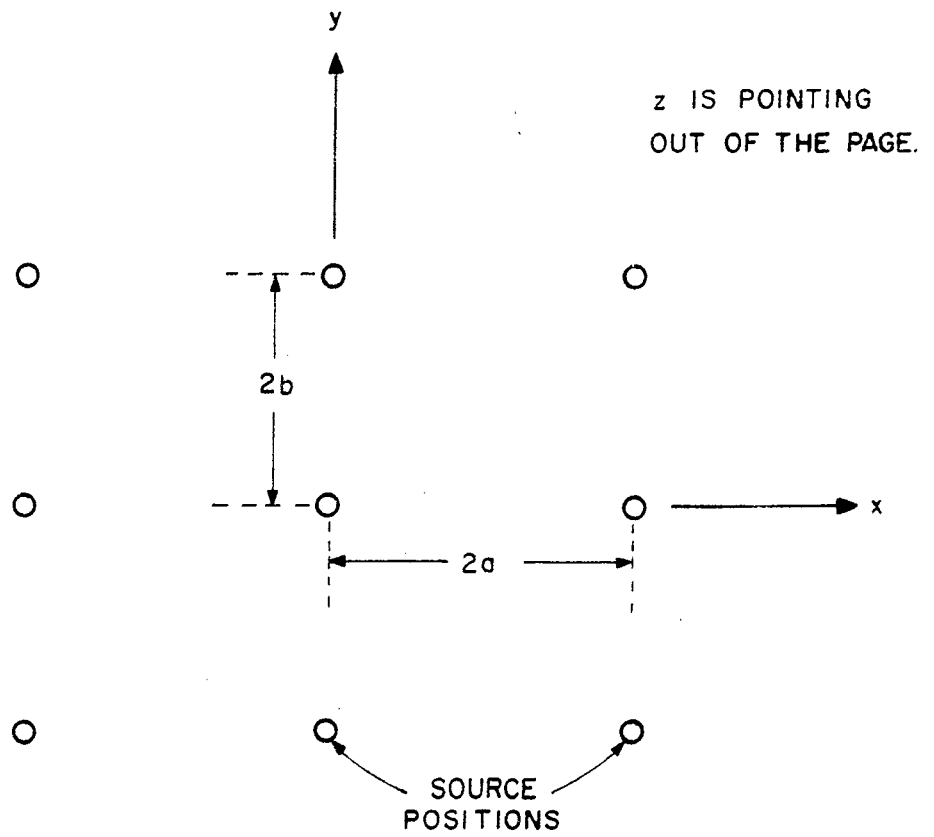


FIGURE I. RECTANGULAR CELLS IN AN INFINITE PLANAR ARRAY

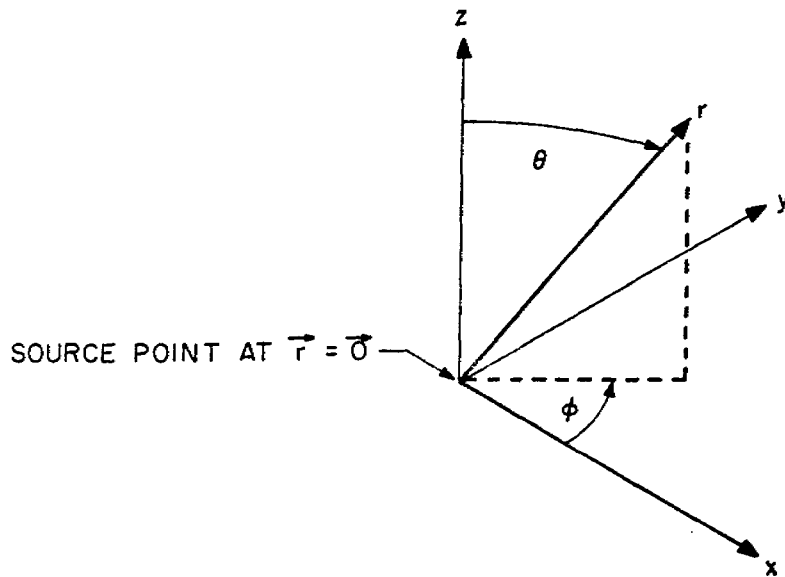


FIGURE 2. SPHERICAL COORDINATES FOR THE EARLY-TIME FIELD DISTRIBUTION NEAR A SOURCE POINT

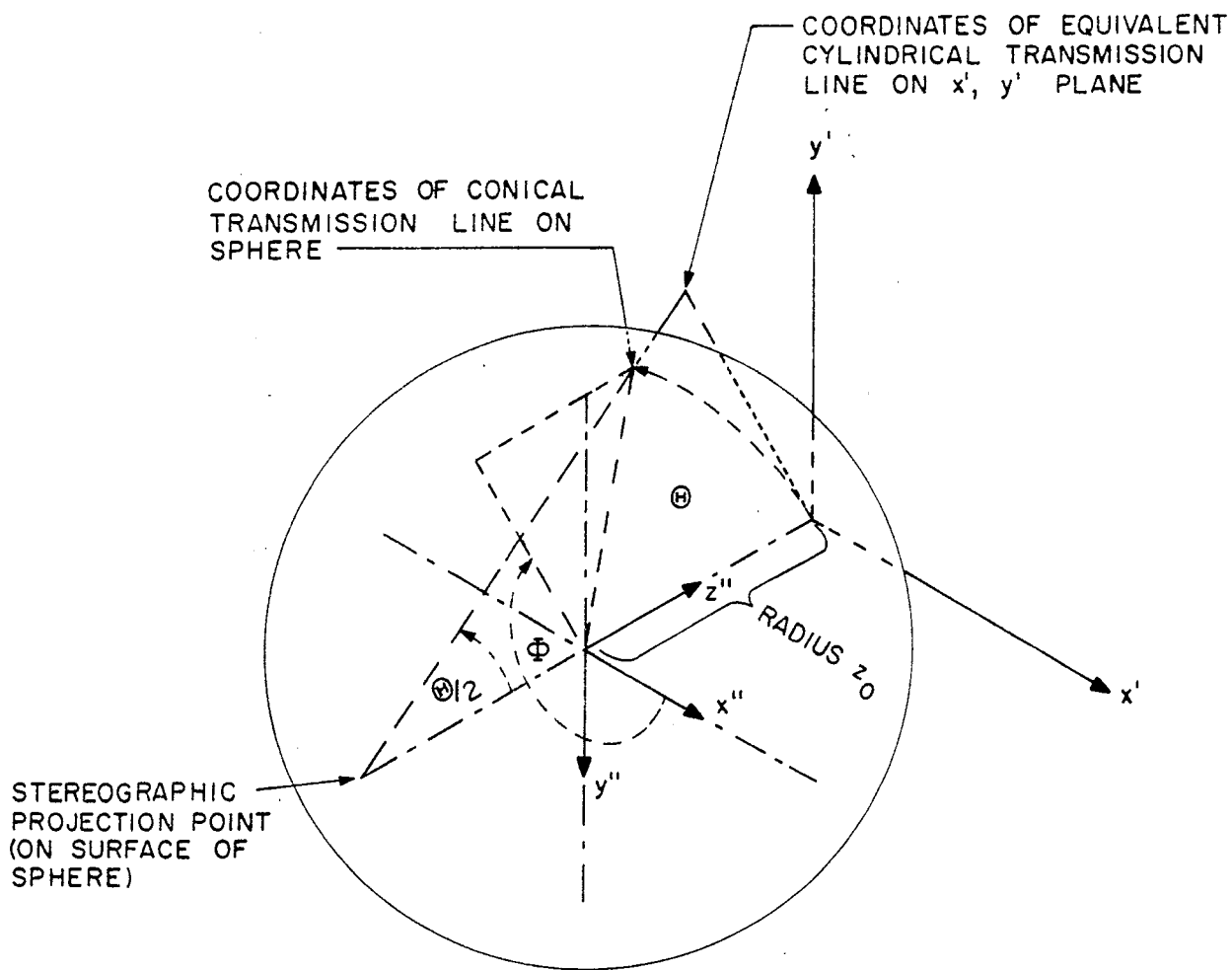


FIGURE 3. STEREOGRAPHIC PROJECTION FOR RELATING SPHERICAL AND PLANAR TEM WAVES

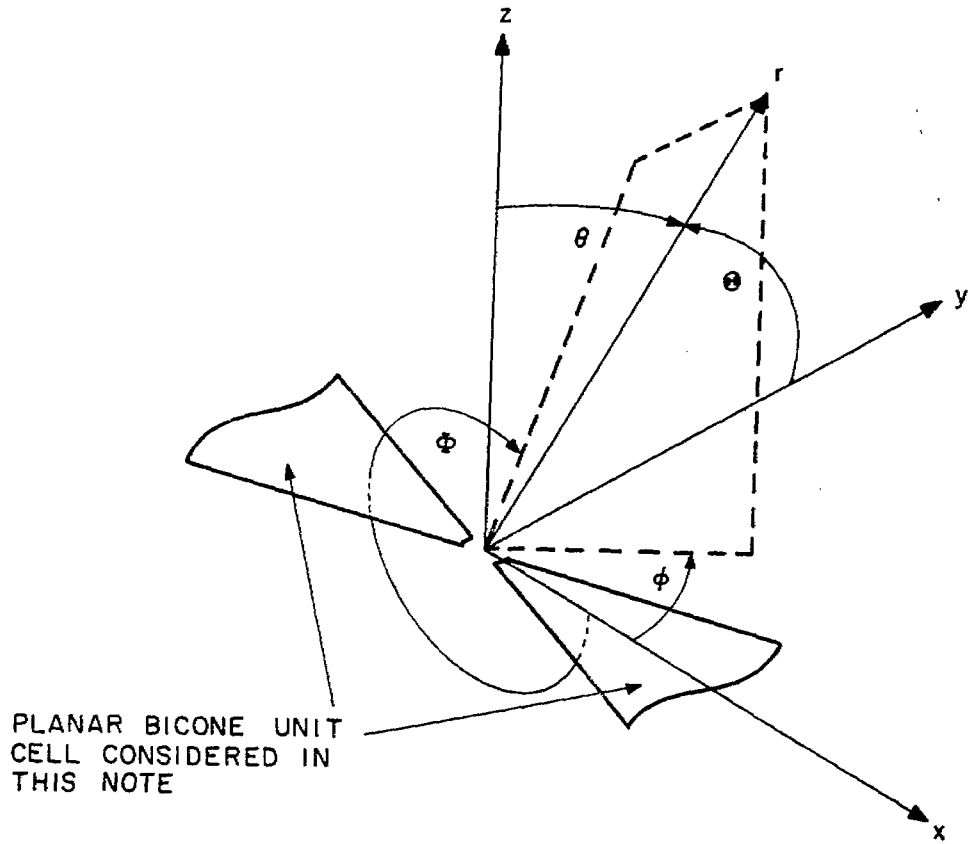
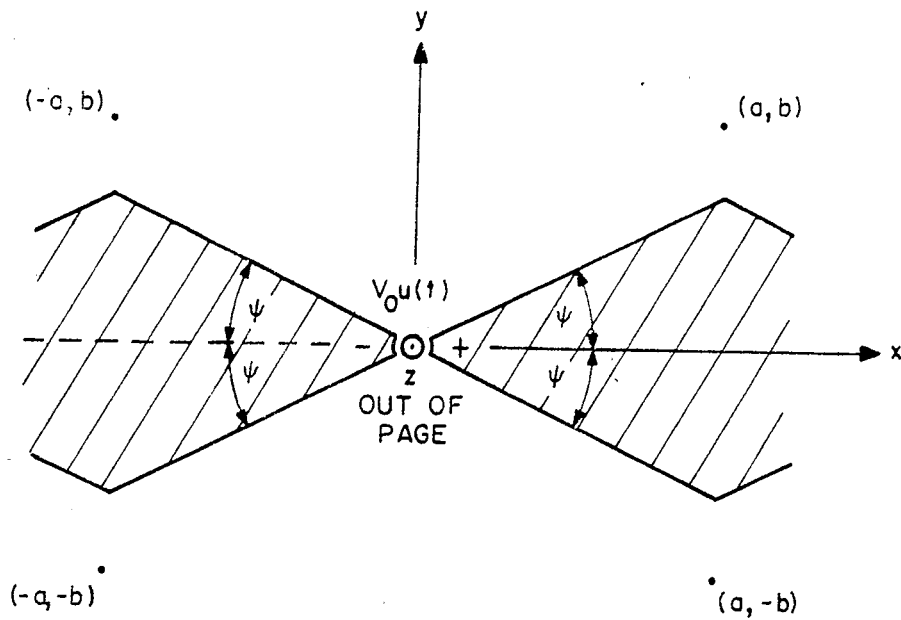
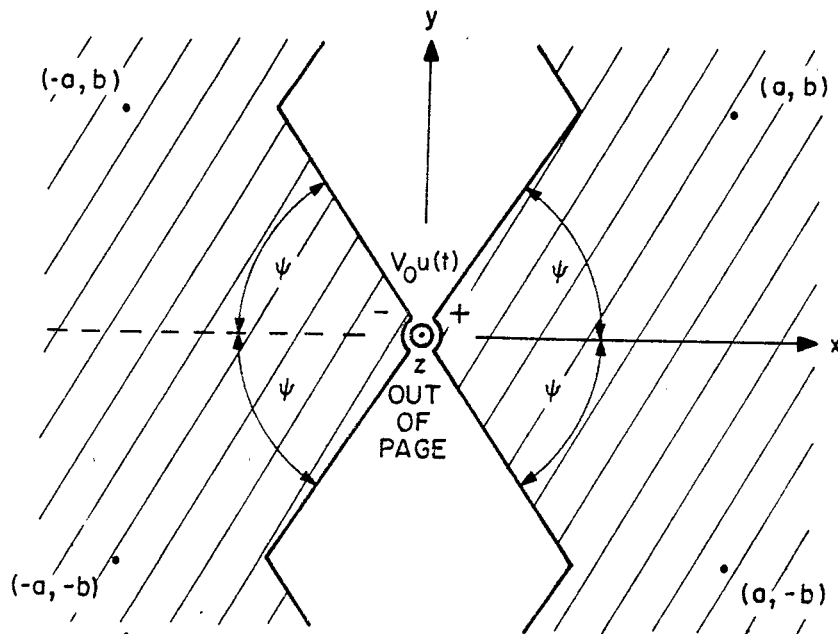


FIGURE 4. TWO SPHERICAL COORDINATE SYSTEMS WITH COMMON ORIGIN



A. $0 < \psi < \psi_0 = \text{ARCTAN}(b/a)$



B. $\text{ARCTAN}(b/a) = \psi_0 < \psi < \pi/2$

FIGURE 5. UNIT CELL OF PLANAR BICONE ARRAY
CENTERED ON COORDINATE ORIGIN

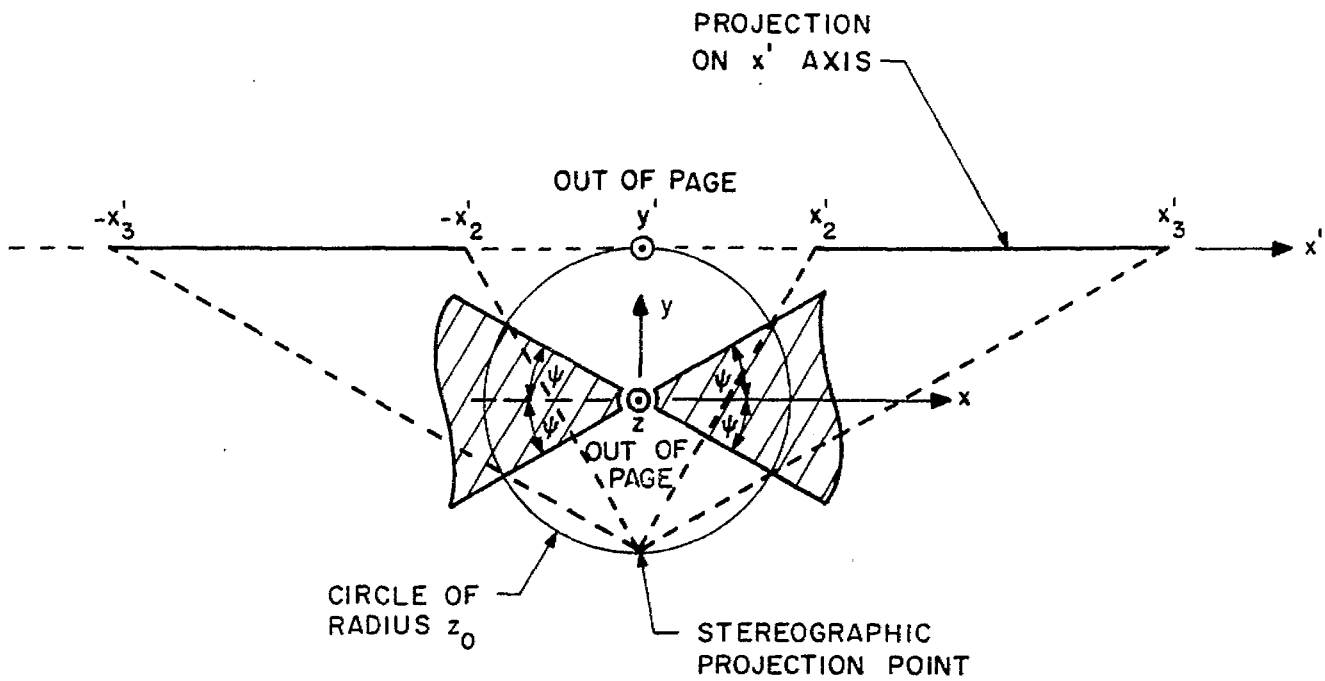


FIGURE 6. TRANSFORMATION FROM PLANAR BICONE TO EQUIVALENT TWO STRIPS

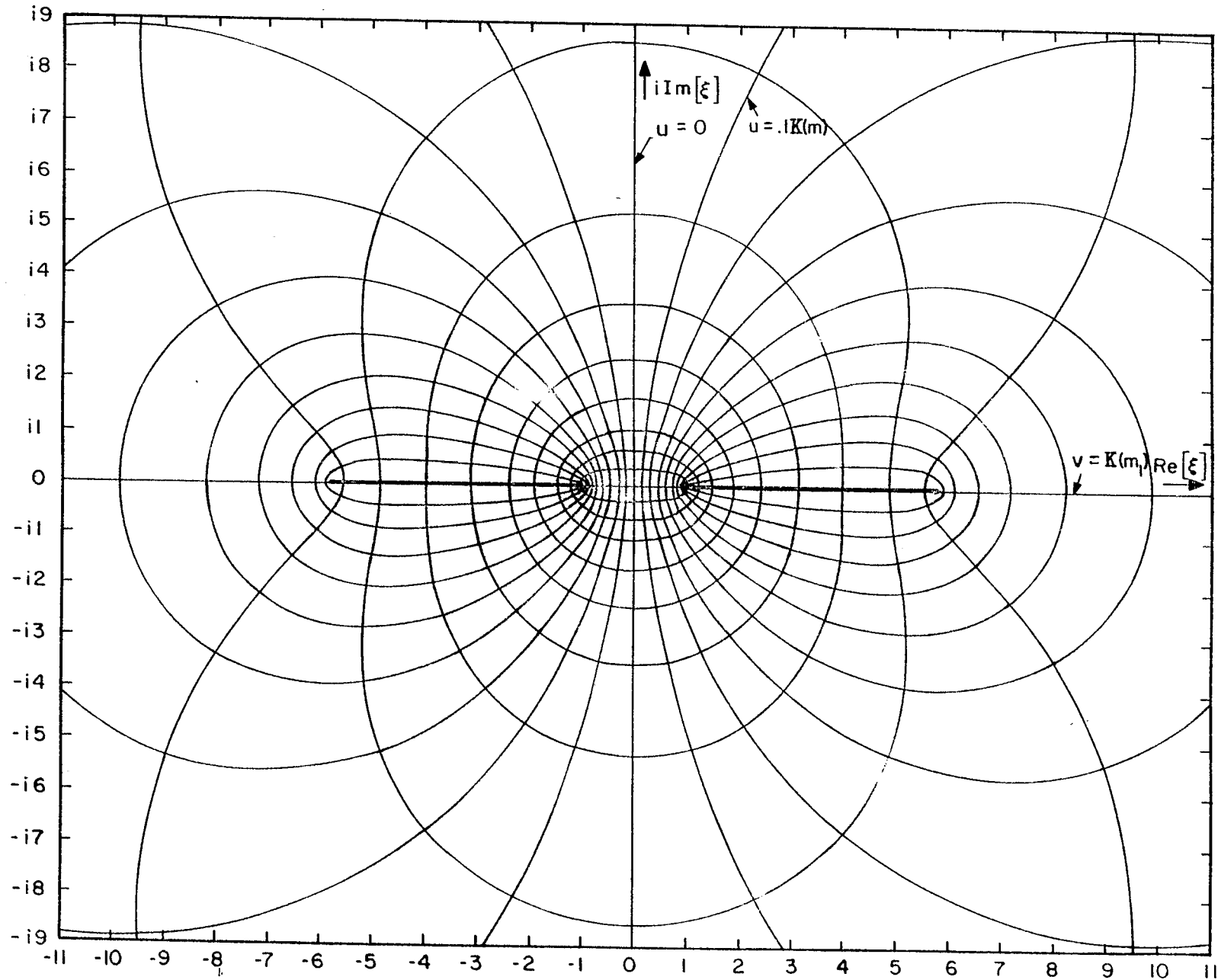


FIGURE 7. COMPLEX POTENTIAL FUNCTION FOR TWO SYMMETRICAL COPLANAR STRIPS FOR THE CASE OF $f_n = 0.5$

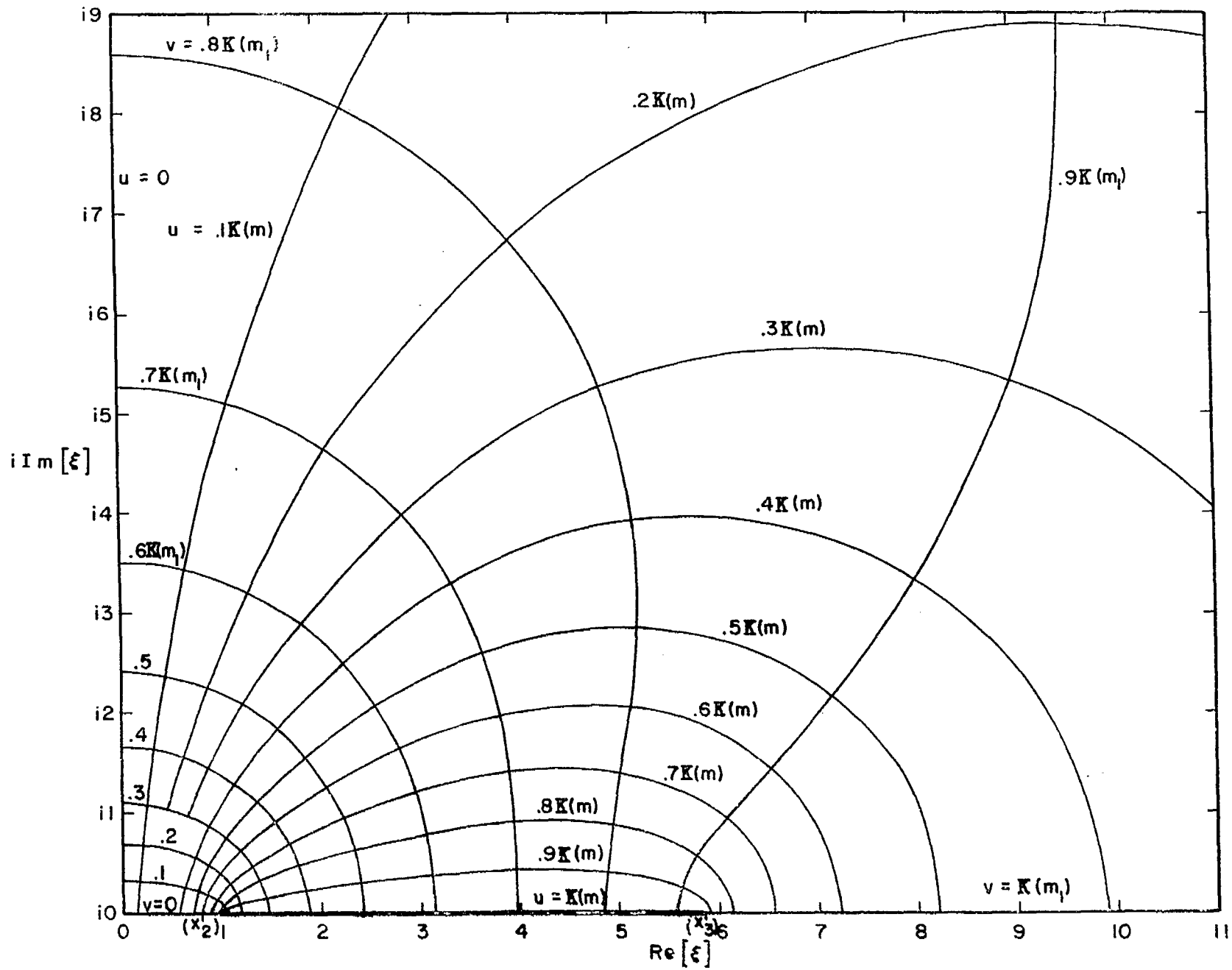


FIGURE 8. COMPLEX POTENTIAL FUNCTION FOR TWO SYMMETRICAL COPLANAR STRIPS: EXPANDED VIEW OF FIRST QUADRANT FOR THE CASE OF $f_g = 0.5$

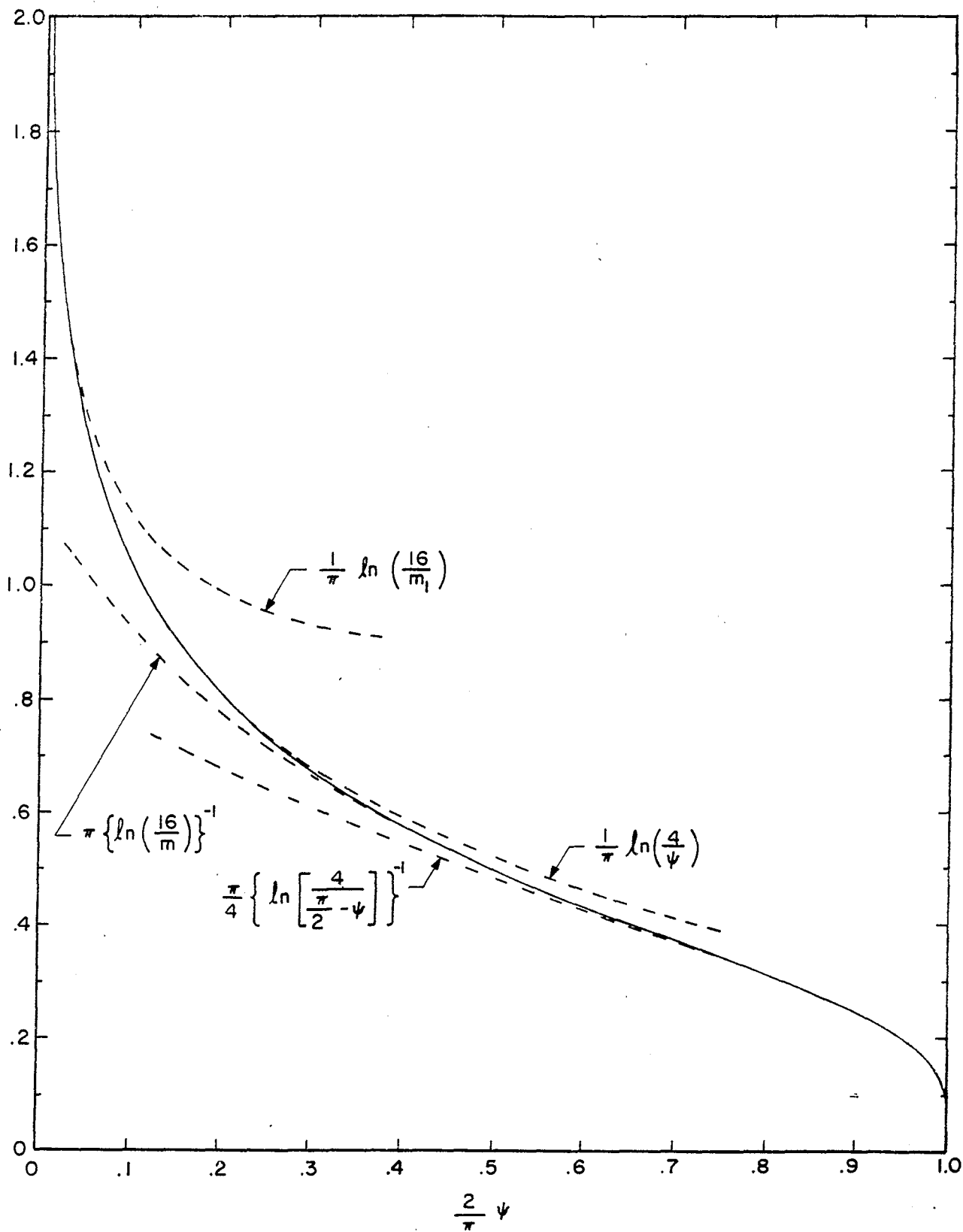


FIGURE 9. GEOMETRICAL IMPEDANCE FACTOR FOR SYMMETRICAL PLANAR BICONES

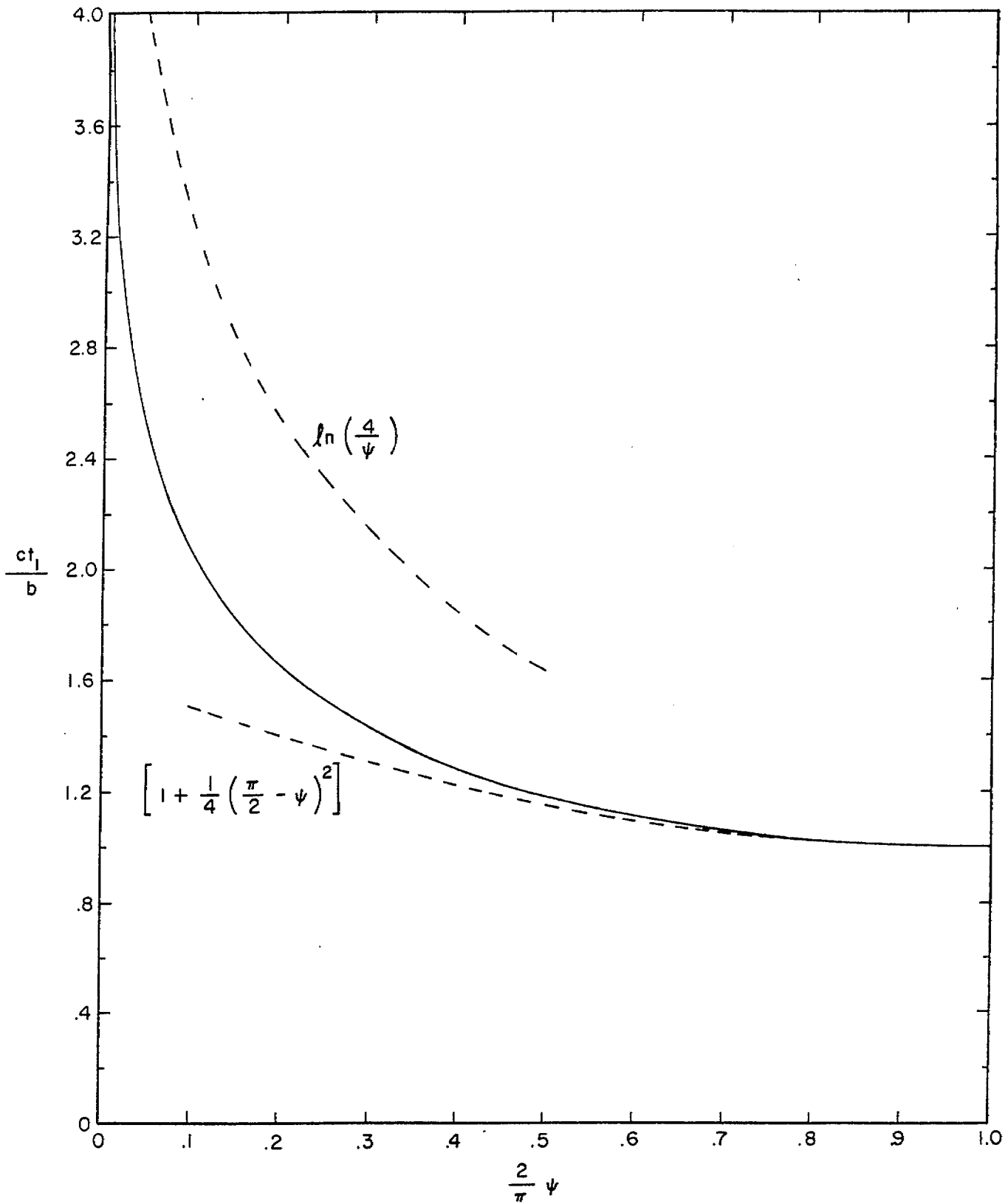


FIGURE 10. ct_1/b AND ASYMPTOTIC FORMS FOR $\theta_1 = 0$

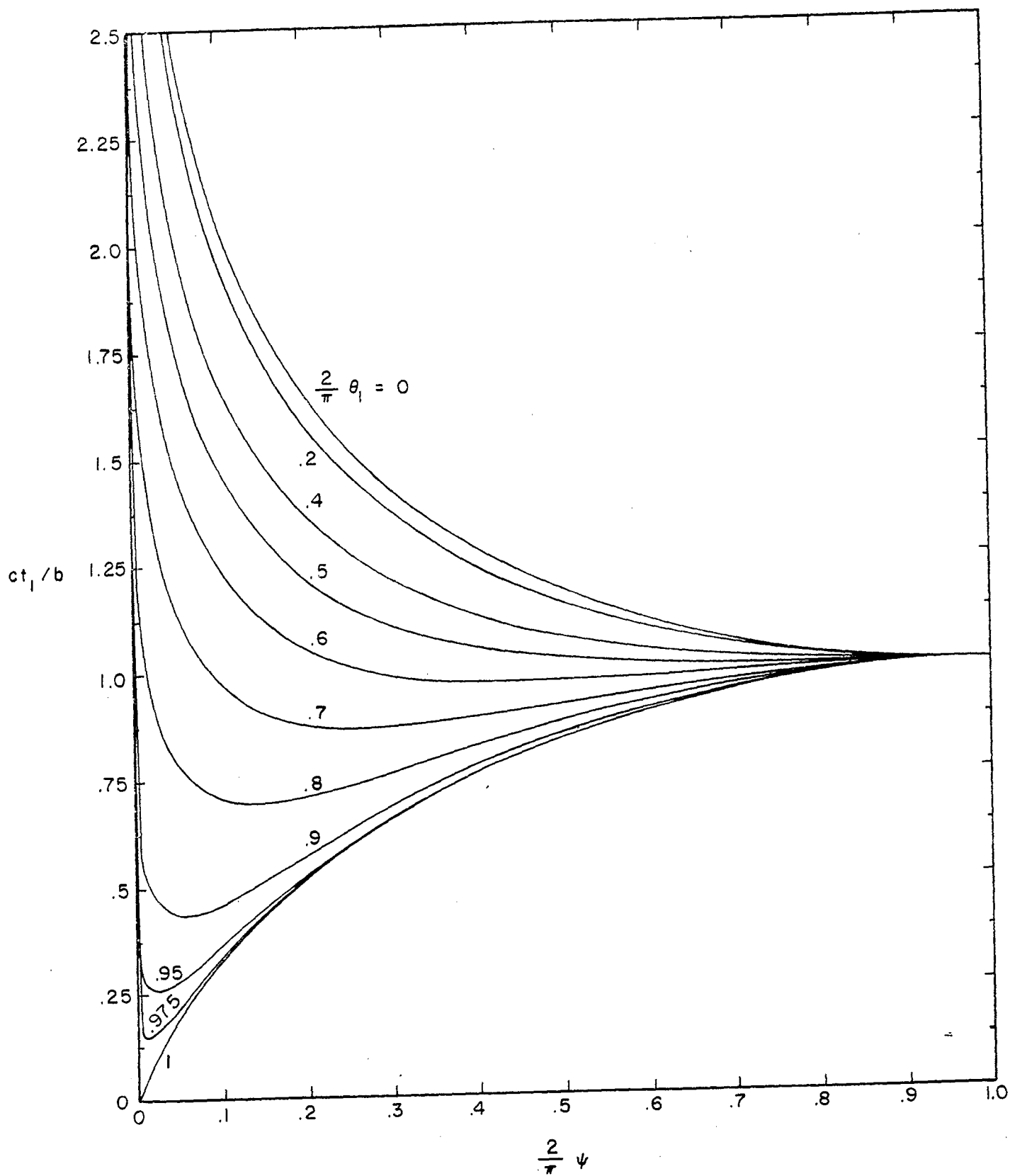


FIGURE 11. ct_1/b FOR $\phi_1 = 0, \pm \pi$ WITH θ_1 AS A PARAMETER

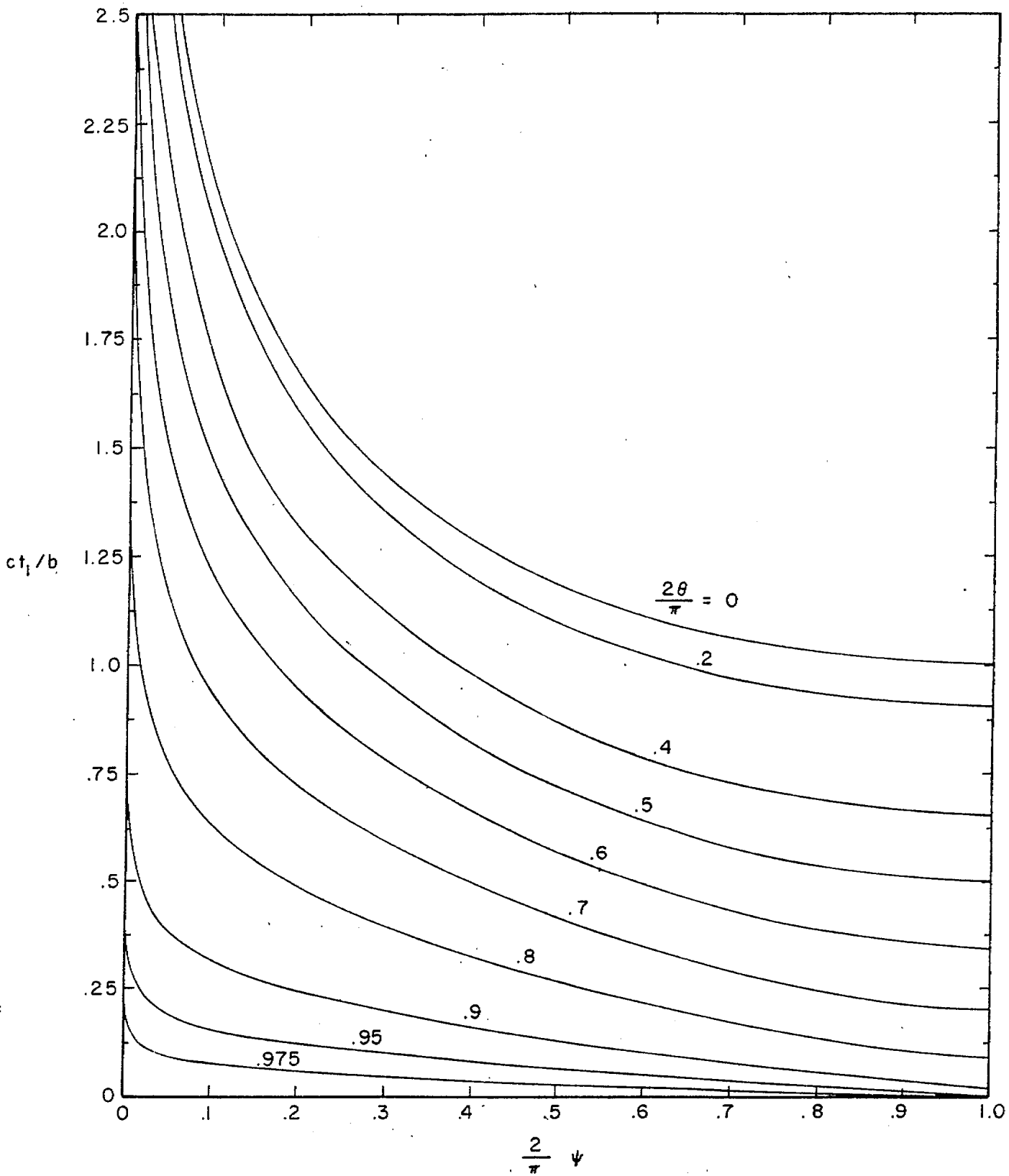


FIGURE 12. ct_1/b FOR $\phi_1 = \pm \frac{\pi}{2}$ WITH θ_1 AS A PARAMETER

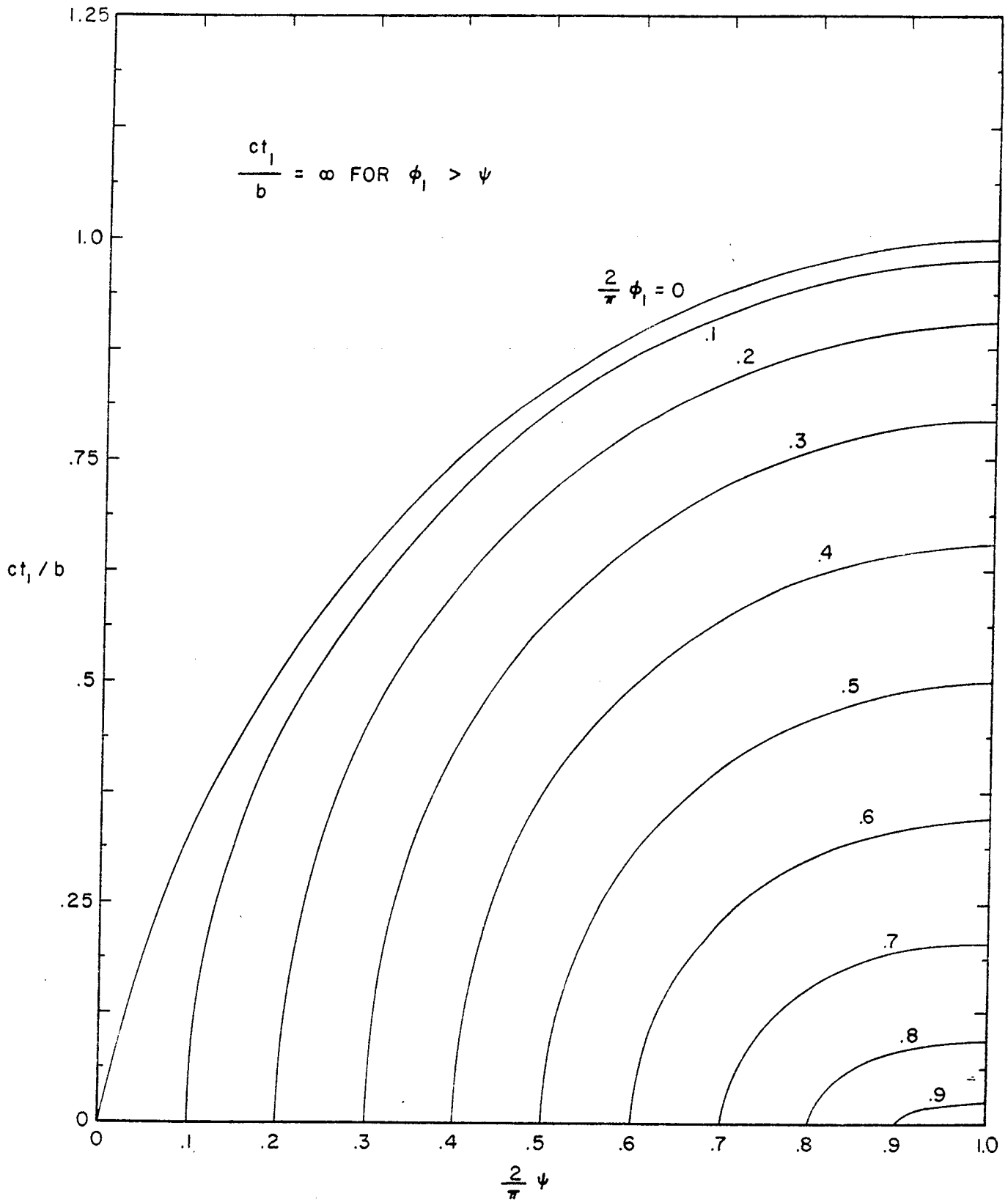


FIGURE 13. ct_1/b FOR $\theta_1 = \frac{\pi}{2}$ WITH ϕ_1 AS A PARAMETER

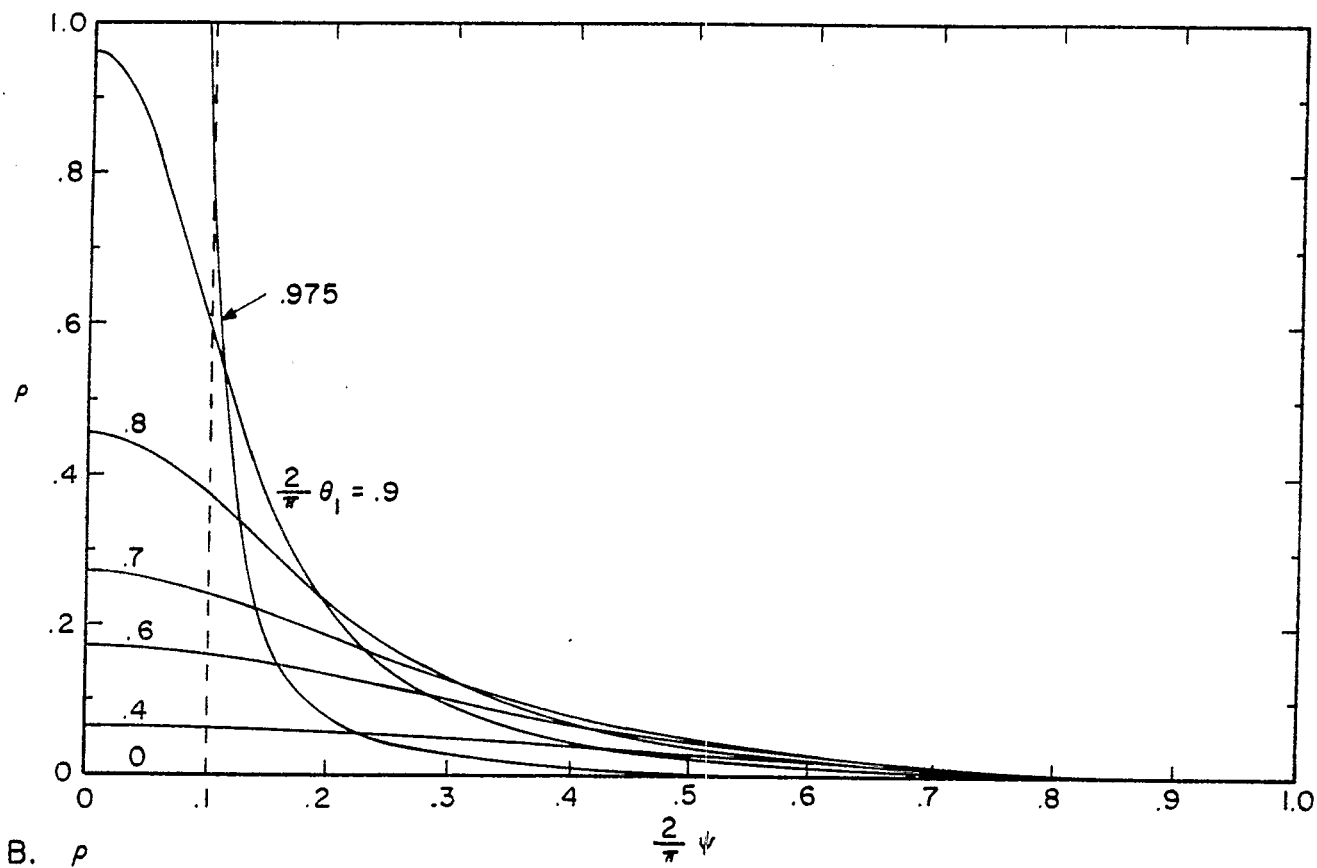
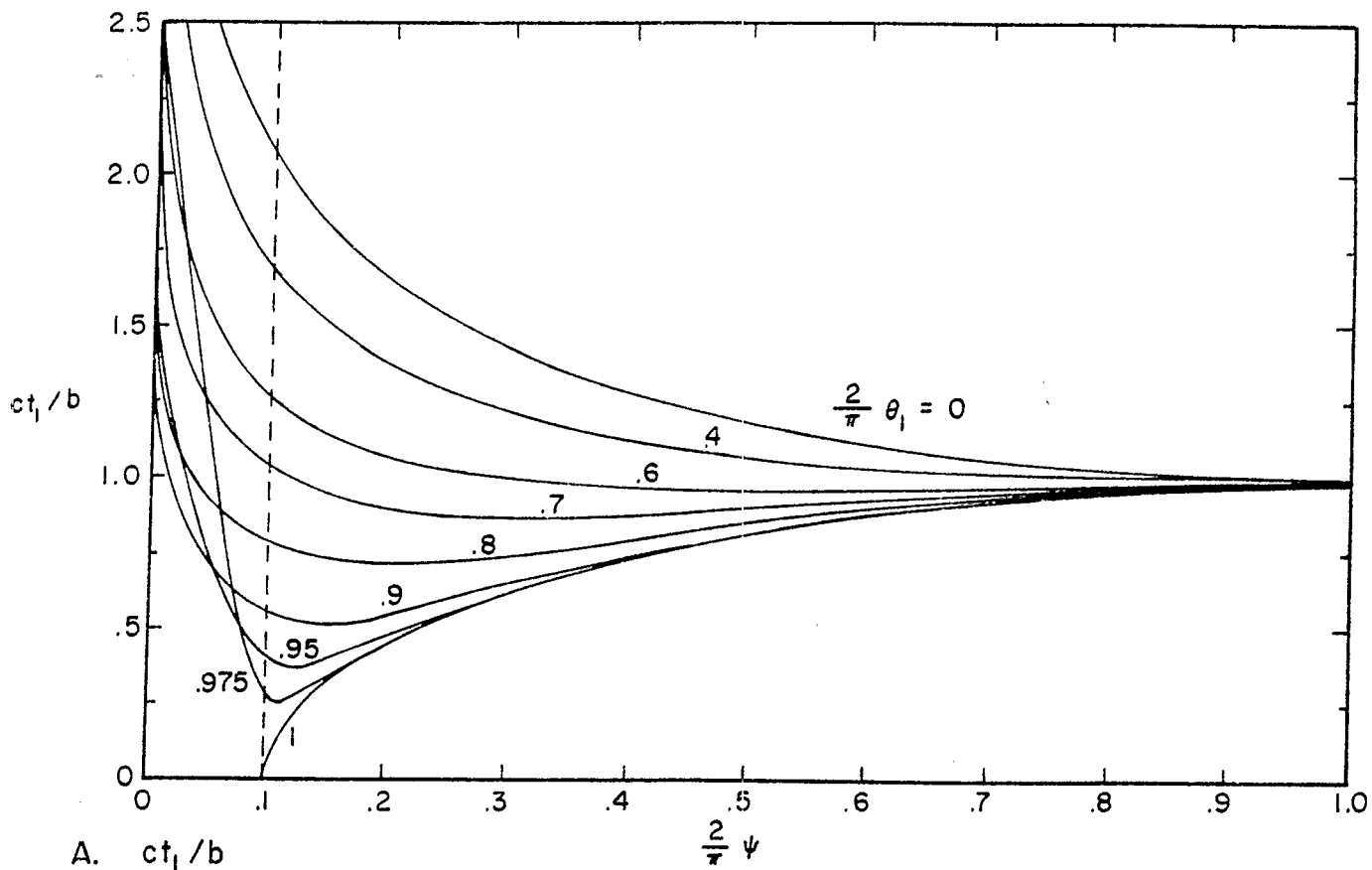


FIGURE 14. ct_1/b AND ρ FOR $\frac{2}{\pi} \phi_1 = .1$ WITH θ_1 AS A PARAMETER

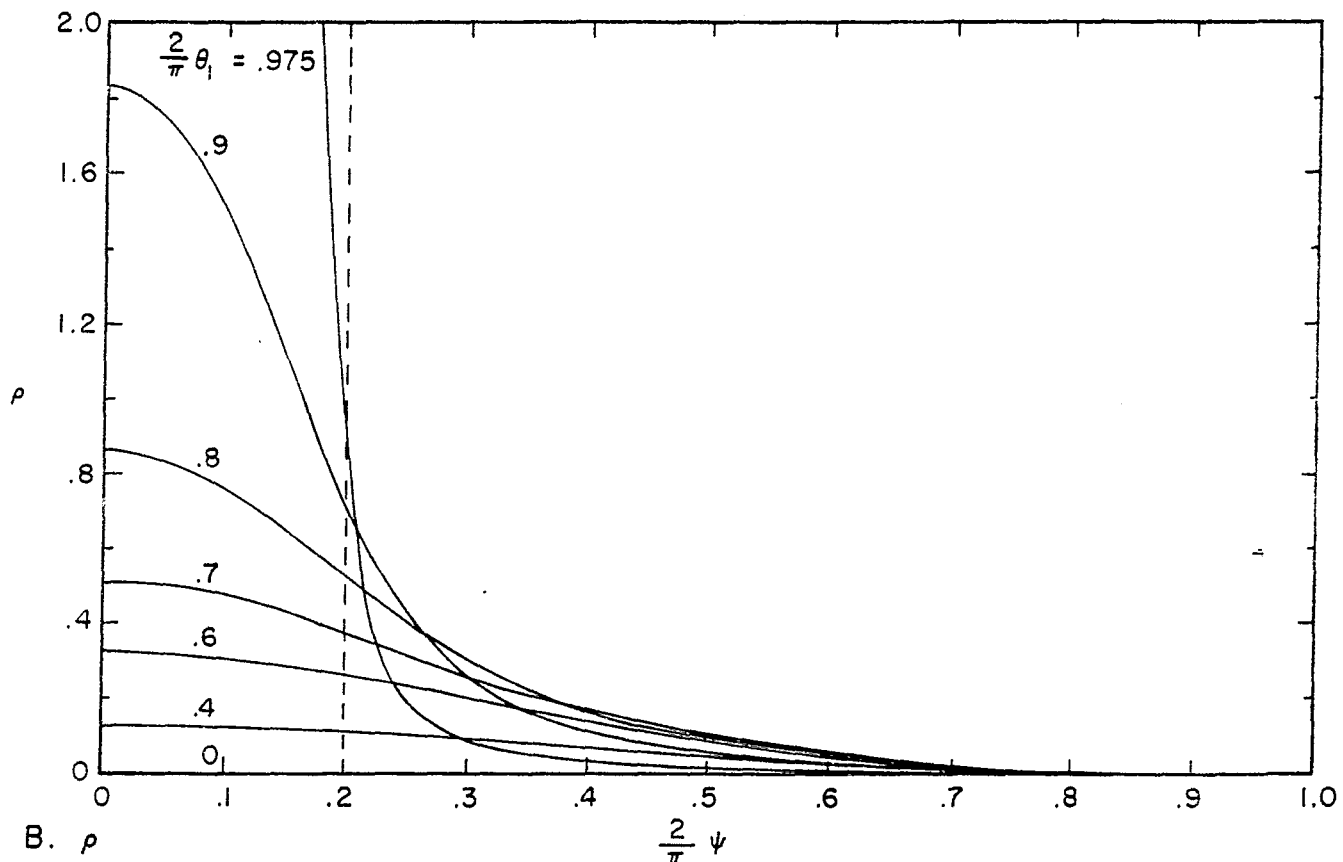
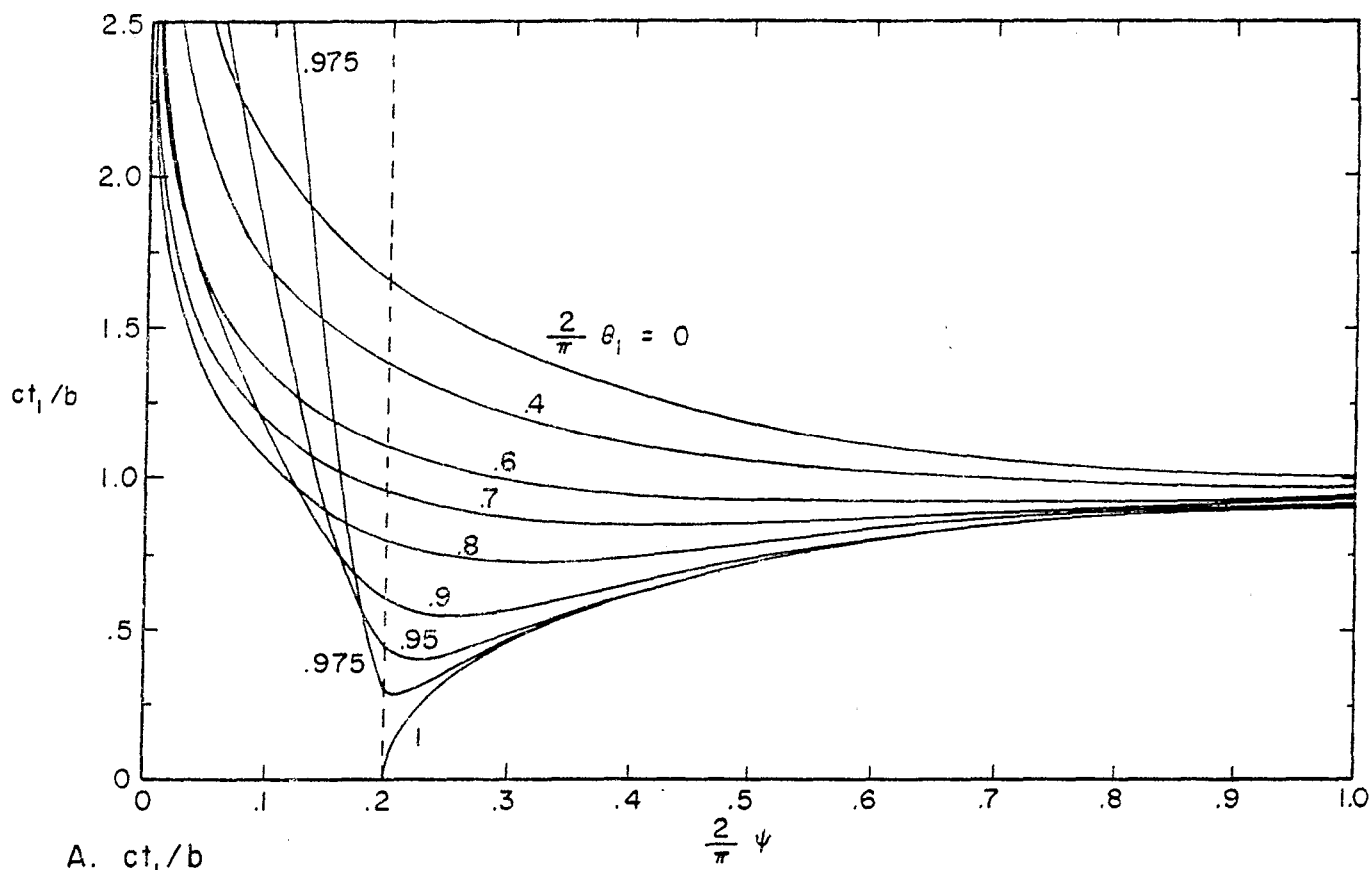


FIGURE 15. ct_1/b AND ρ FOR $\frac{2}{\pi} \phi_1 = .2$ WITH θ_1 AS A PARAMETER

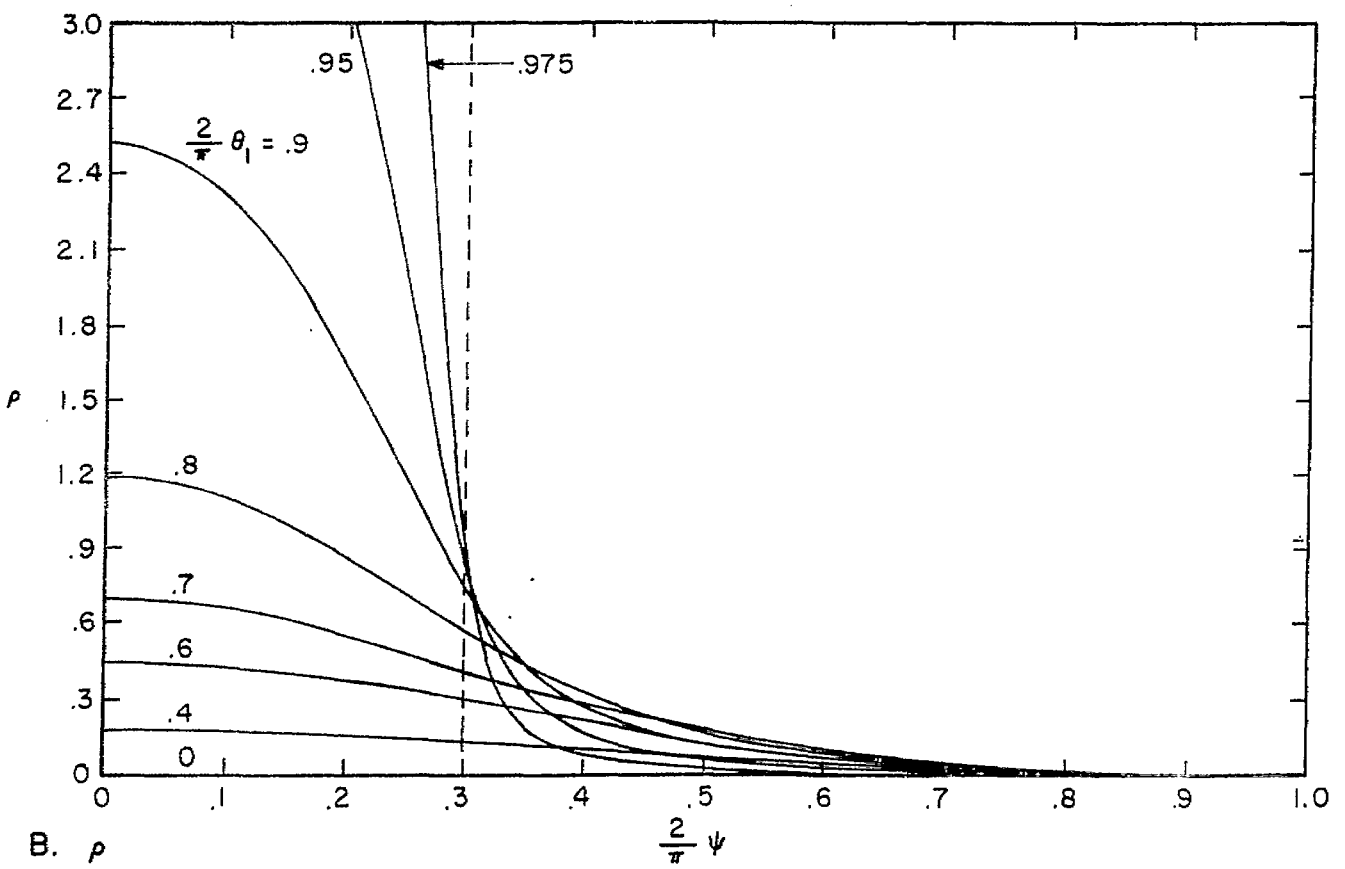
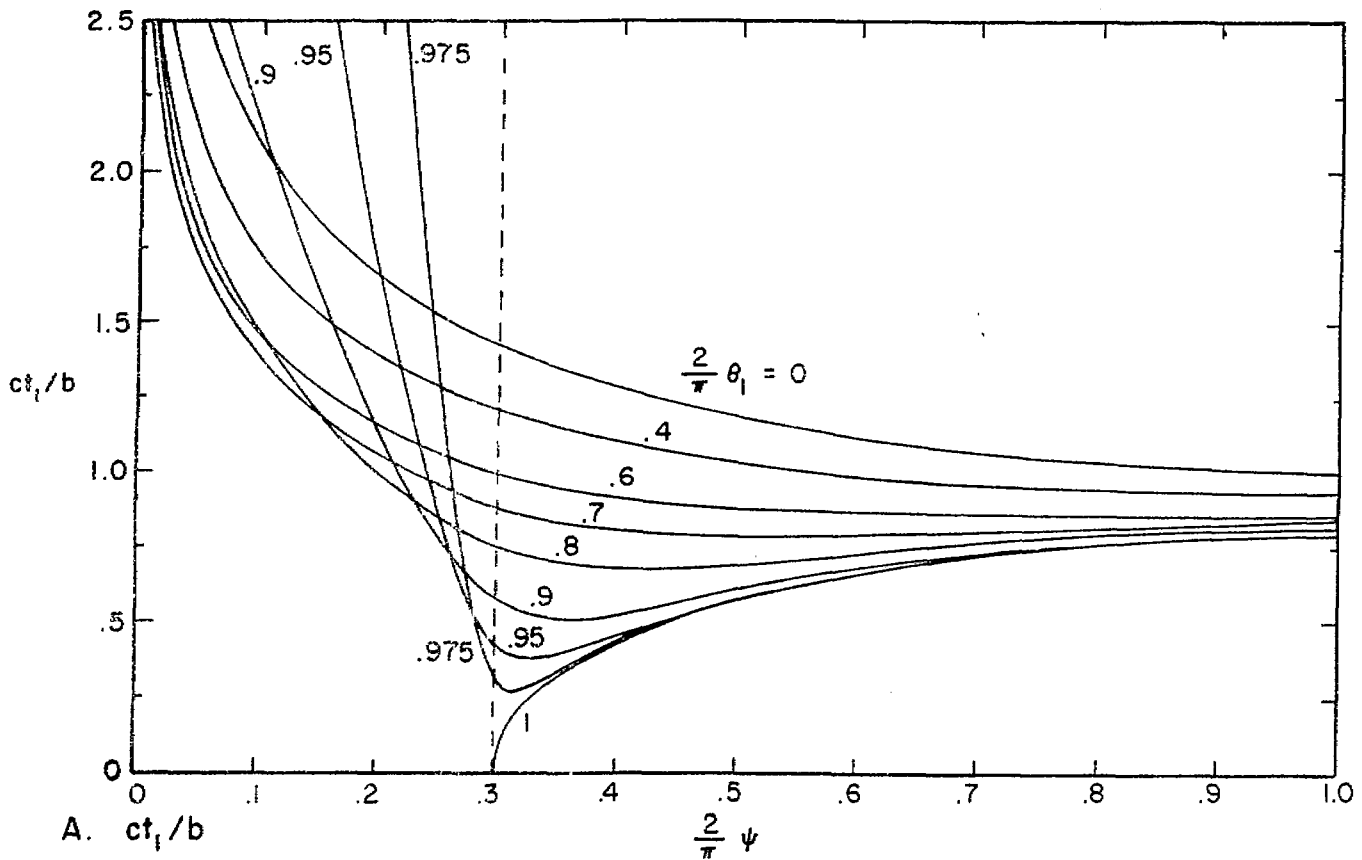


FIGURE 16. ct_1/b AND ρ FOR $\frac{2}{\pi} \phi_1 = .3$ WITH θ_1 AS A PARAMETER

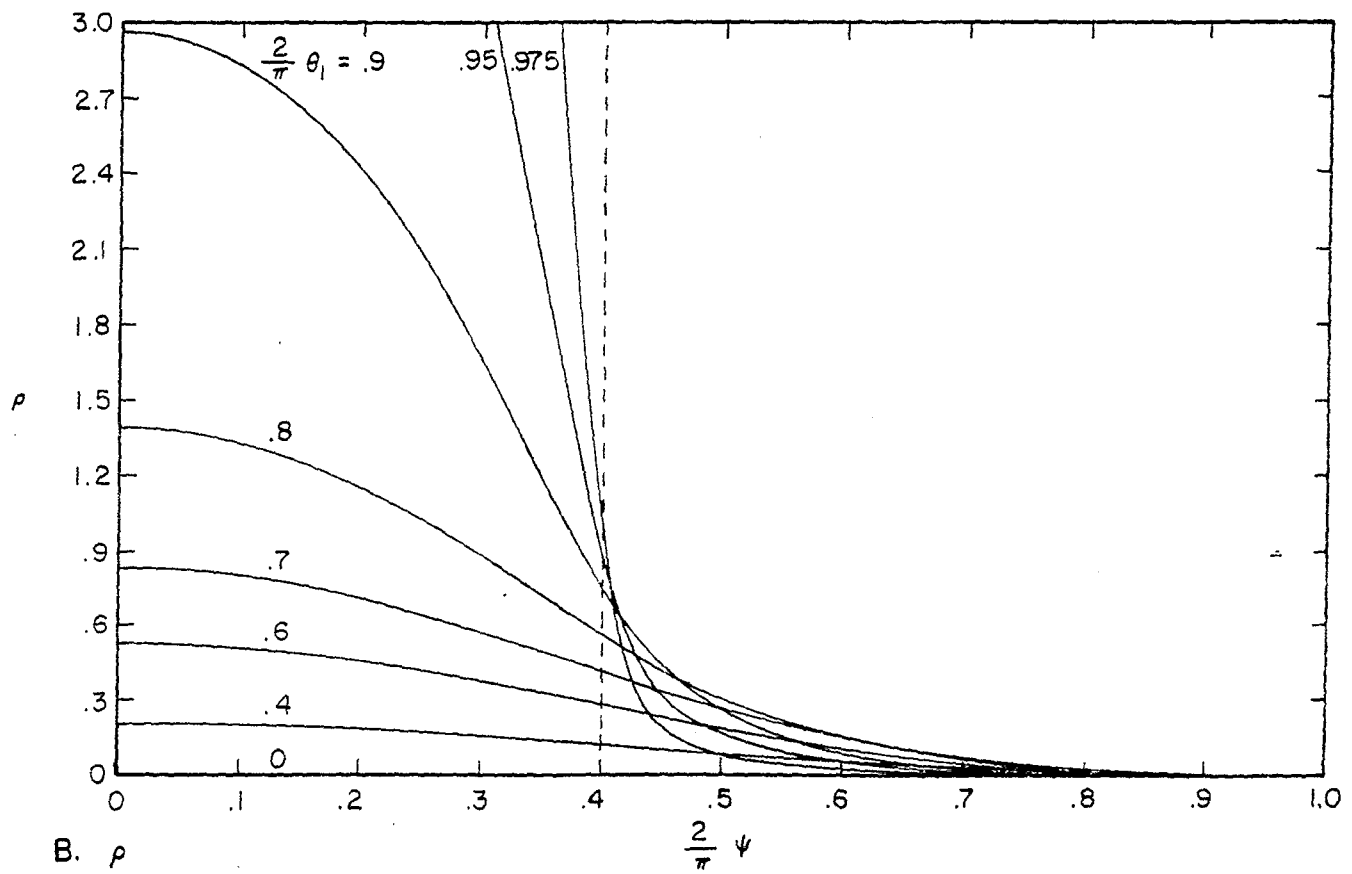
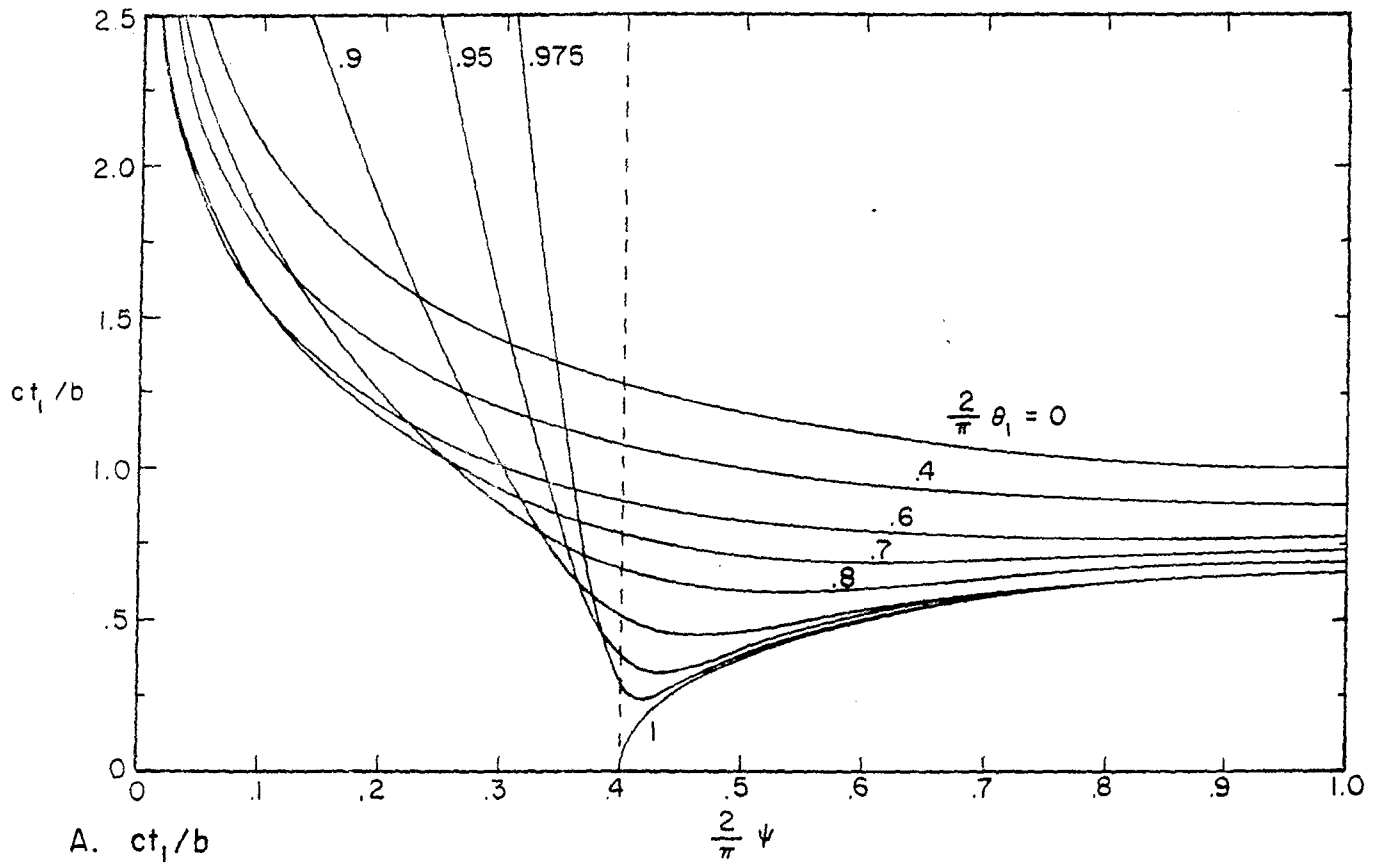


FIGURE 17. ct_1/b AND ρ FOR $\frac{2}{\pi} \phi_1 = .4$ WITH θ_1 AS A PARAMETER

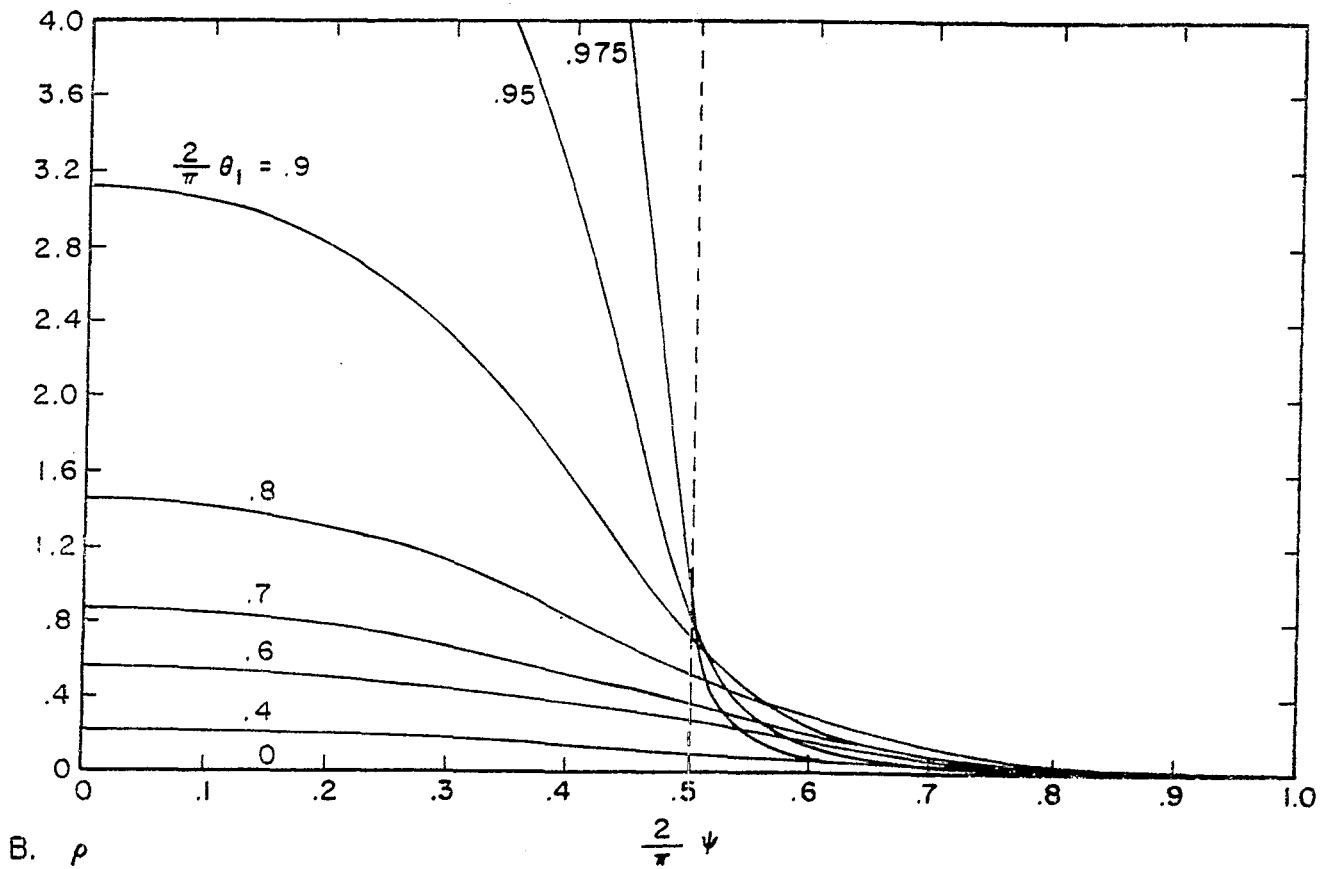
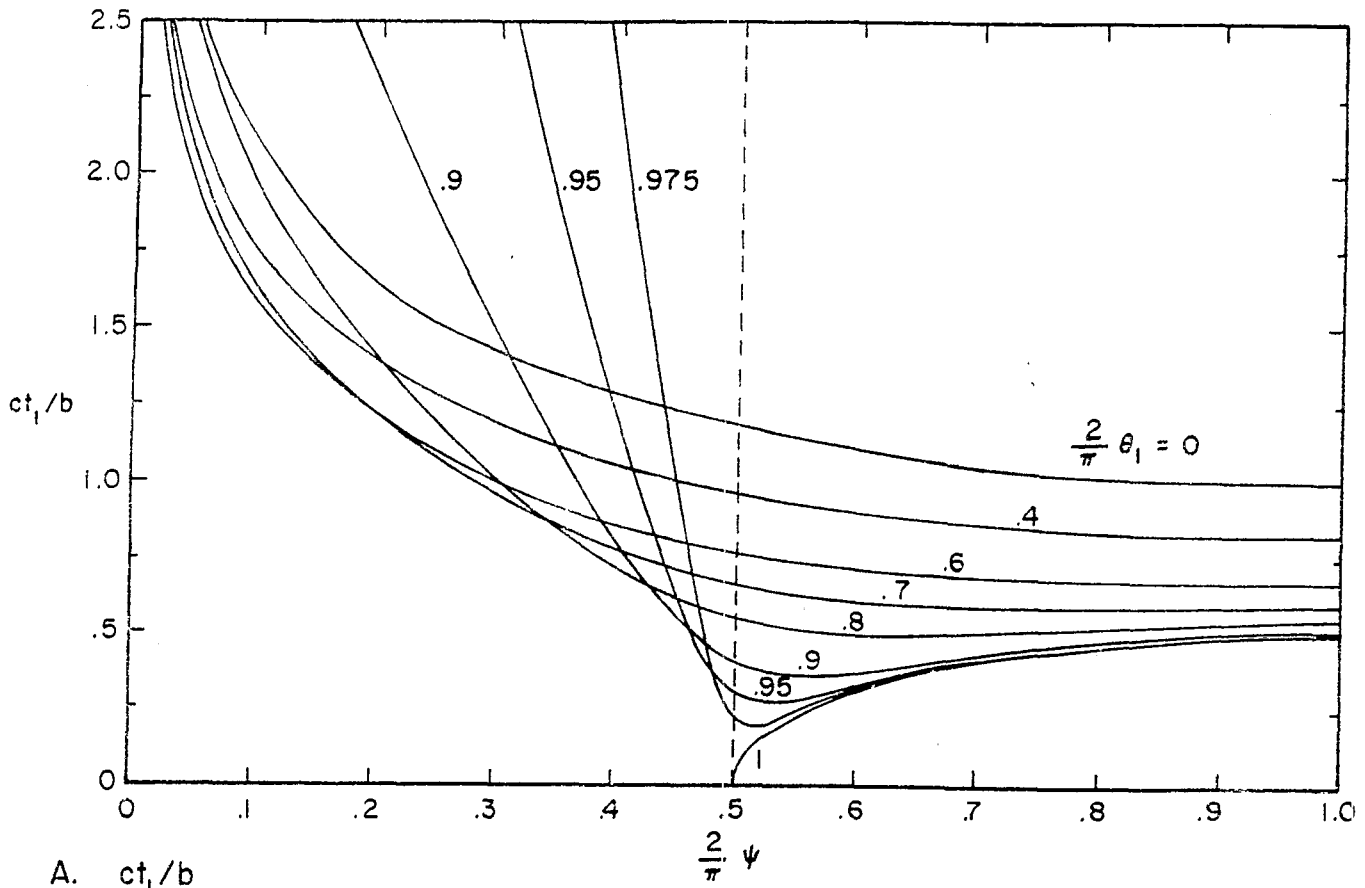


FIGURE 18. ct_1/b AND ρ FOR $\frac{2}{\pi} \phi_1 = .5$ WITH θ_1 AS A PARAMETER

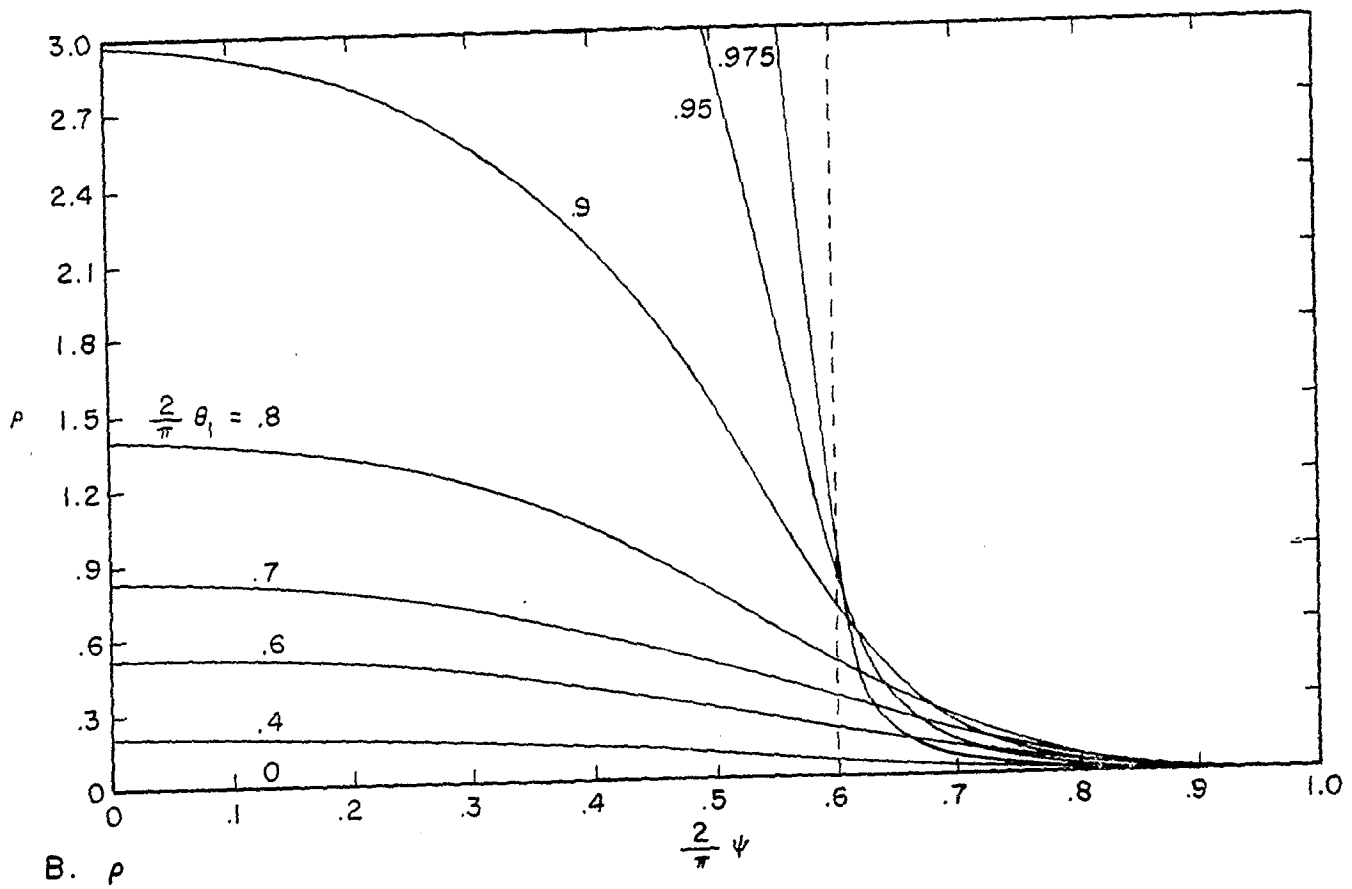
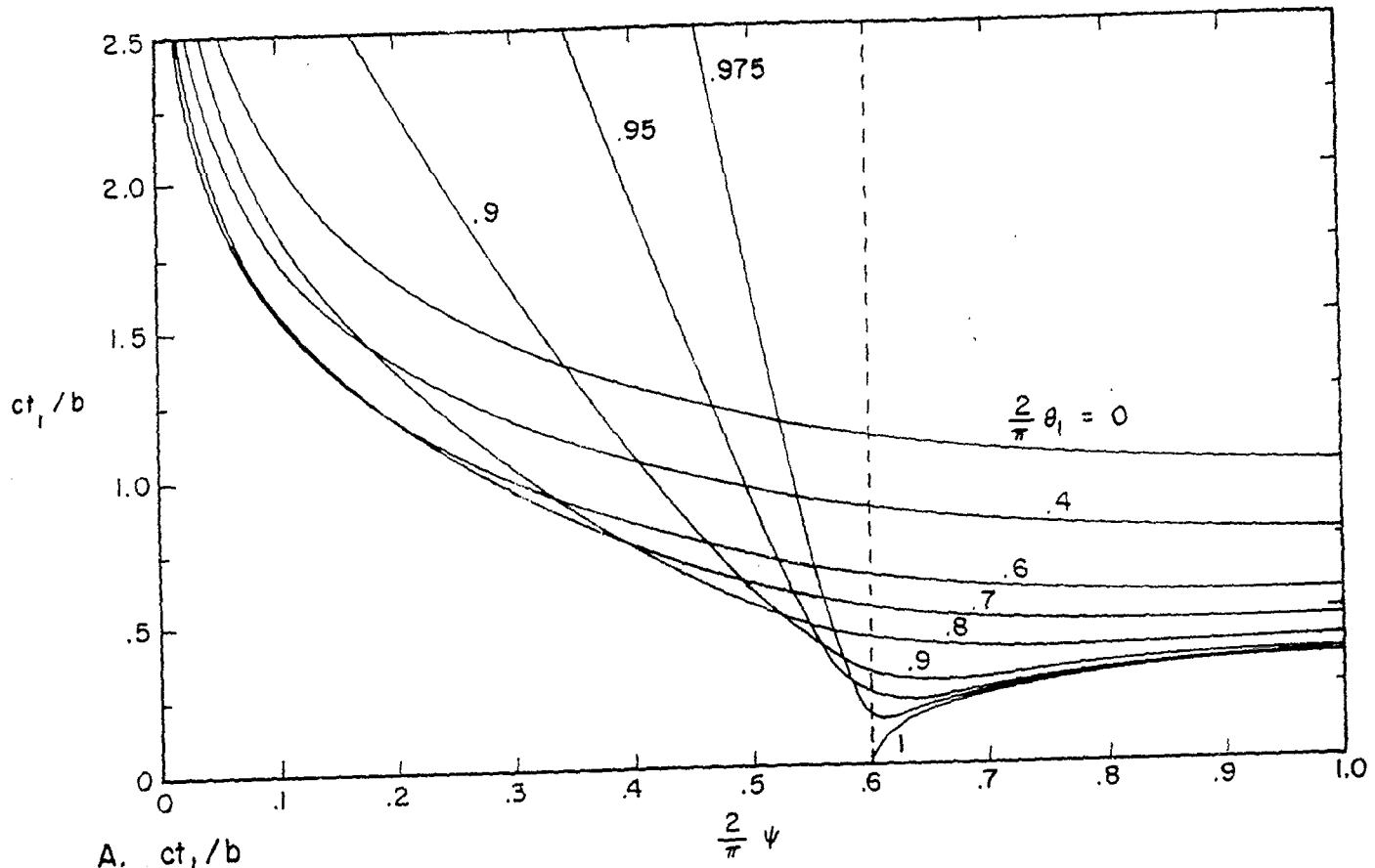


FIGURE 19. ct_1/b AND ρ FOR $\frac{2}{\pi} \phi_1 = .6$ WITH θ_1 AS A PARAMETER.

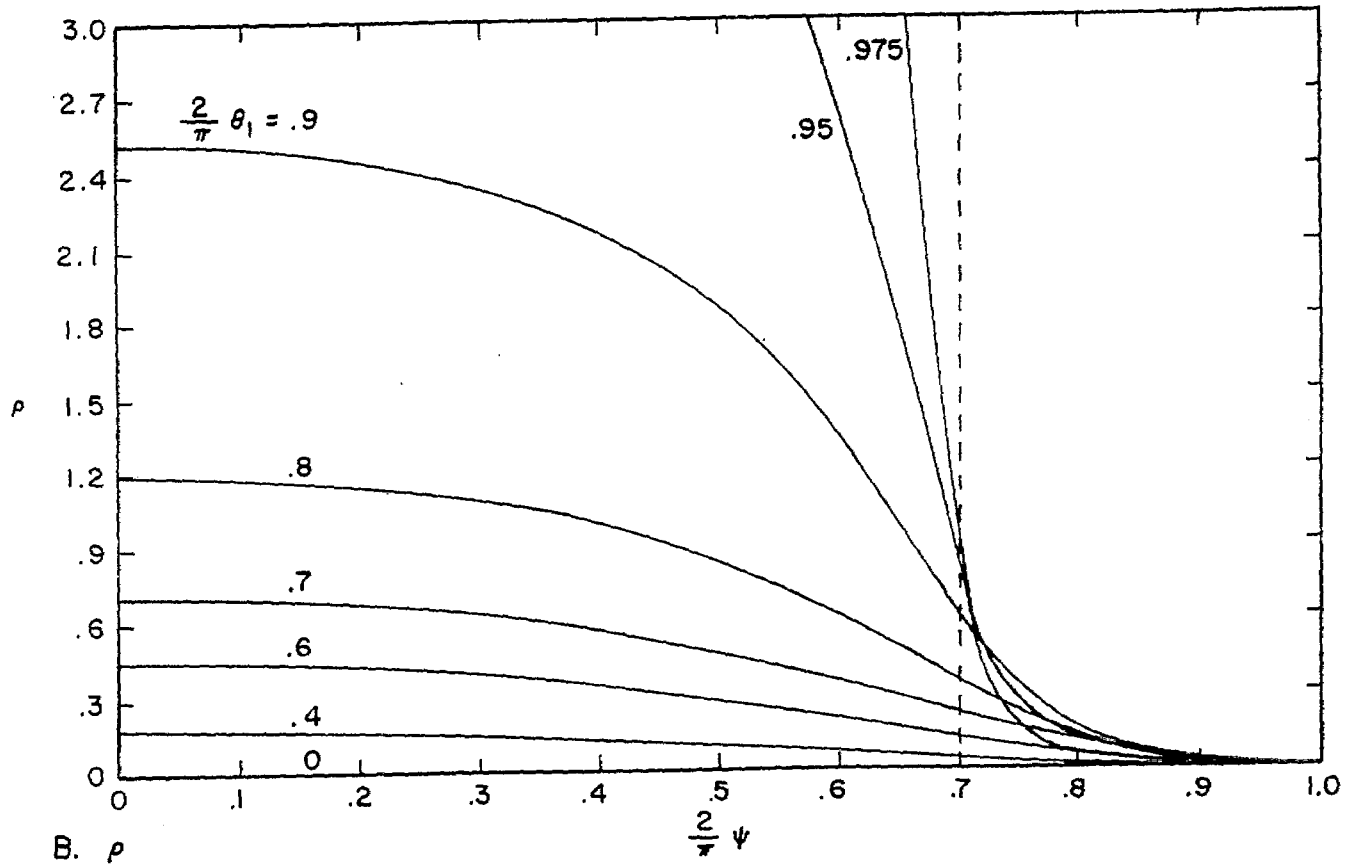
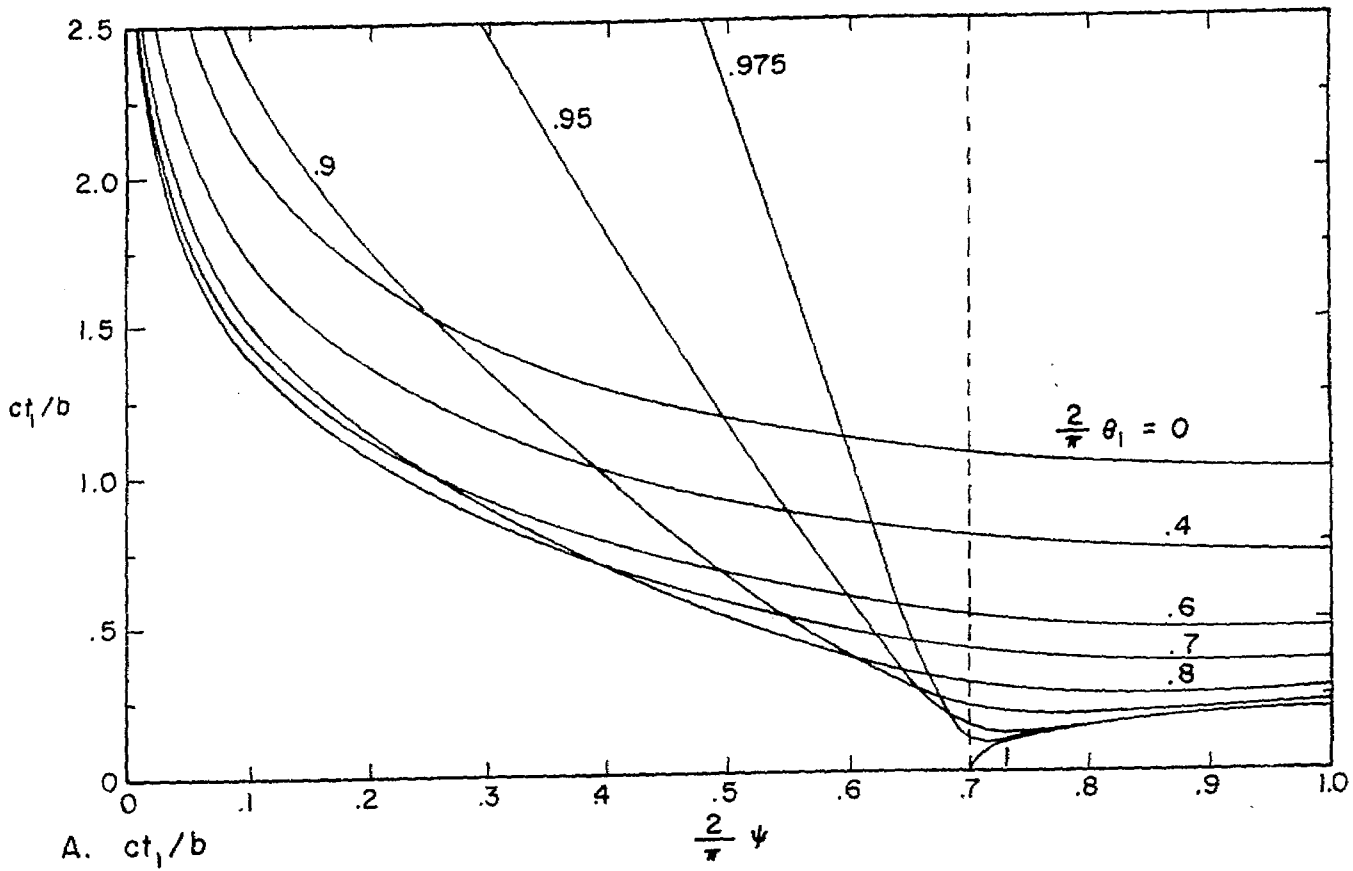
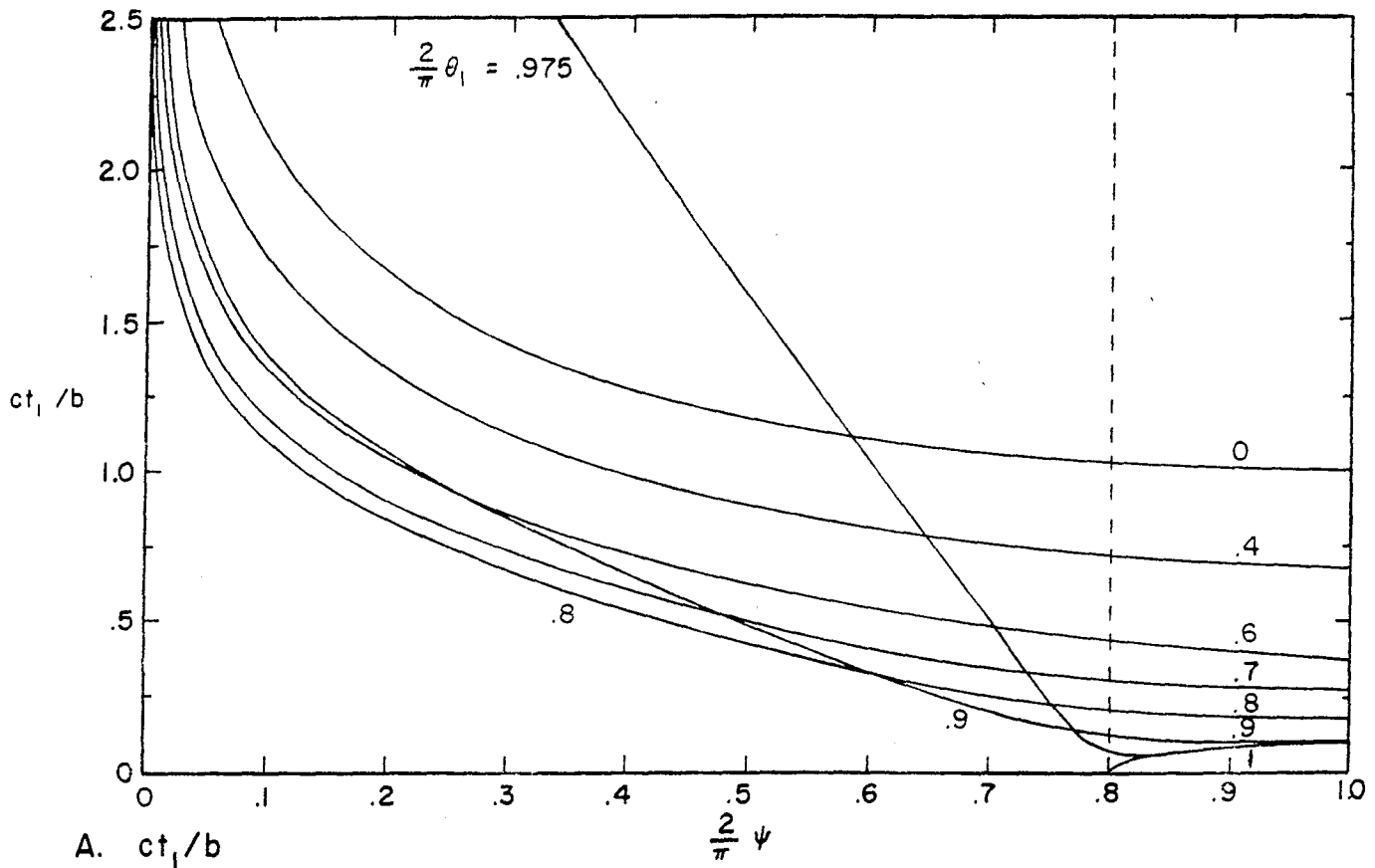
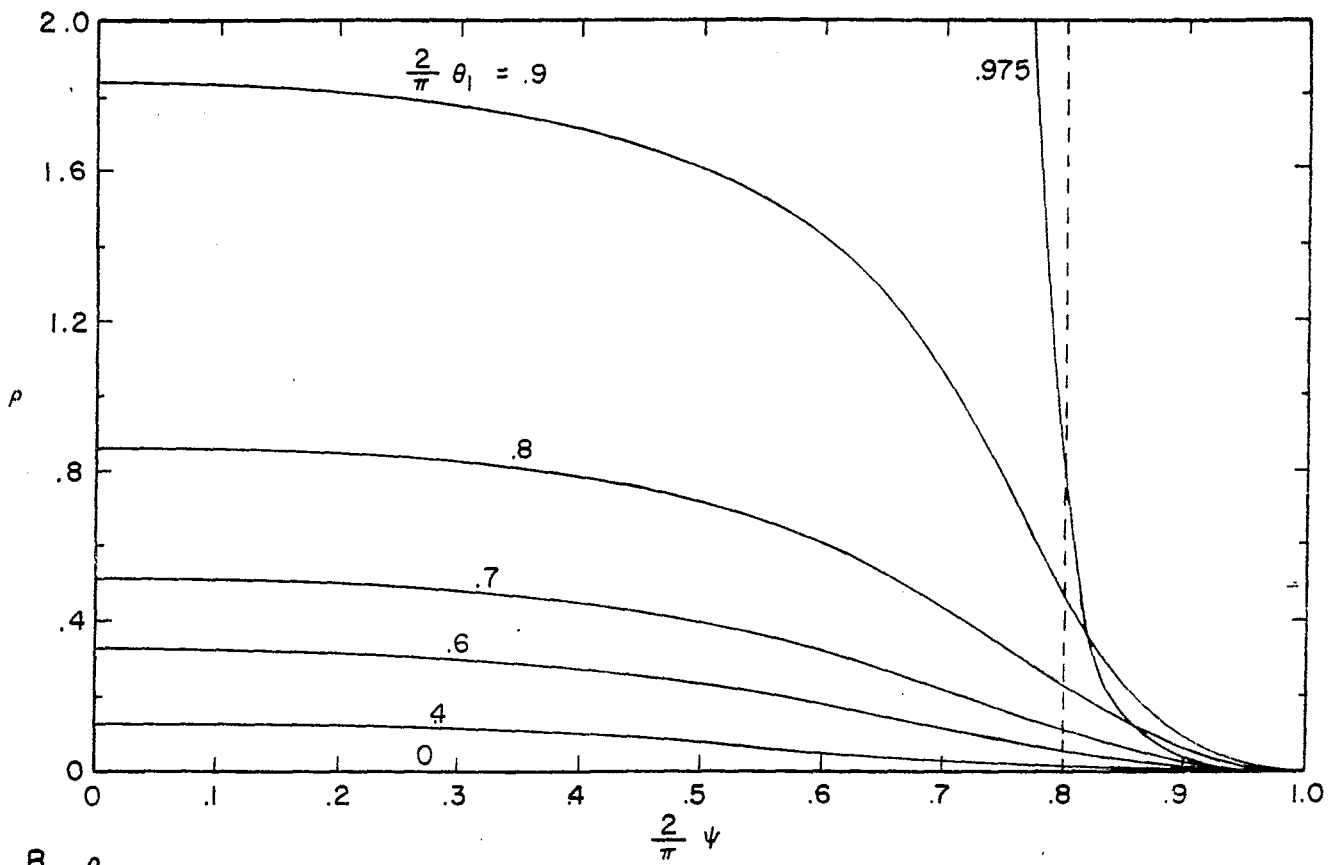


FIGURE 20. ct_1/b AND ρ FOR $\frac{2}{\pi} \phi_1 = .7$ WITH θ_1 AS A PARAMETER



A. ct_1/b



B. ρ

FIGURE 21. ct_1/b AND ρ FOR $\frac{2}{\pi} \phi_1 = .8$ WITH θ_1 AS A PARAMETER

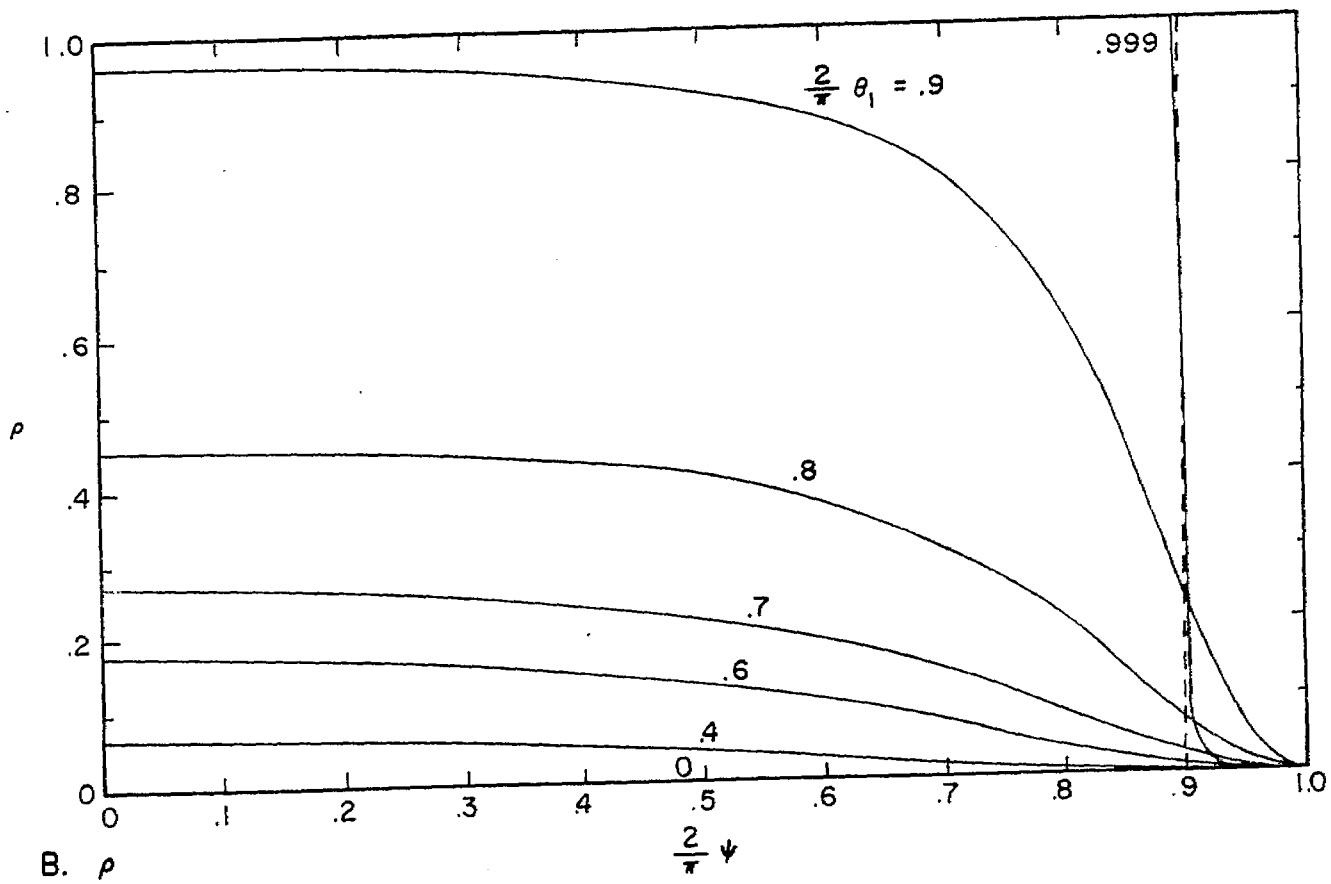
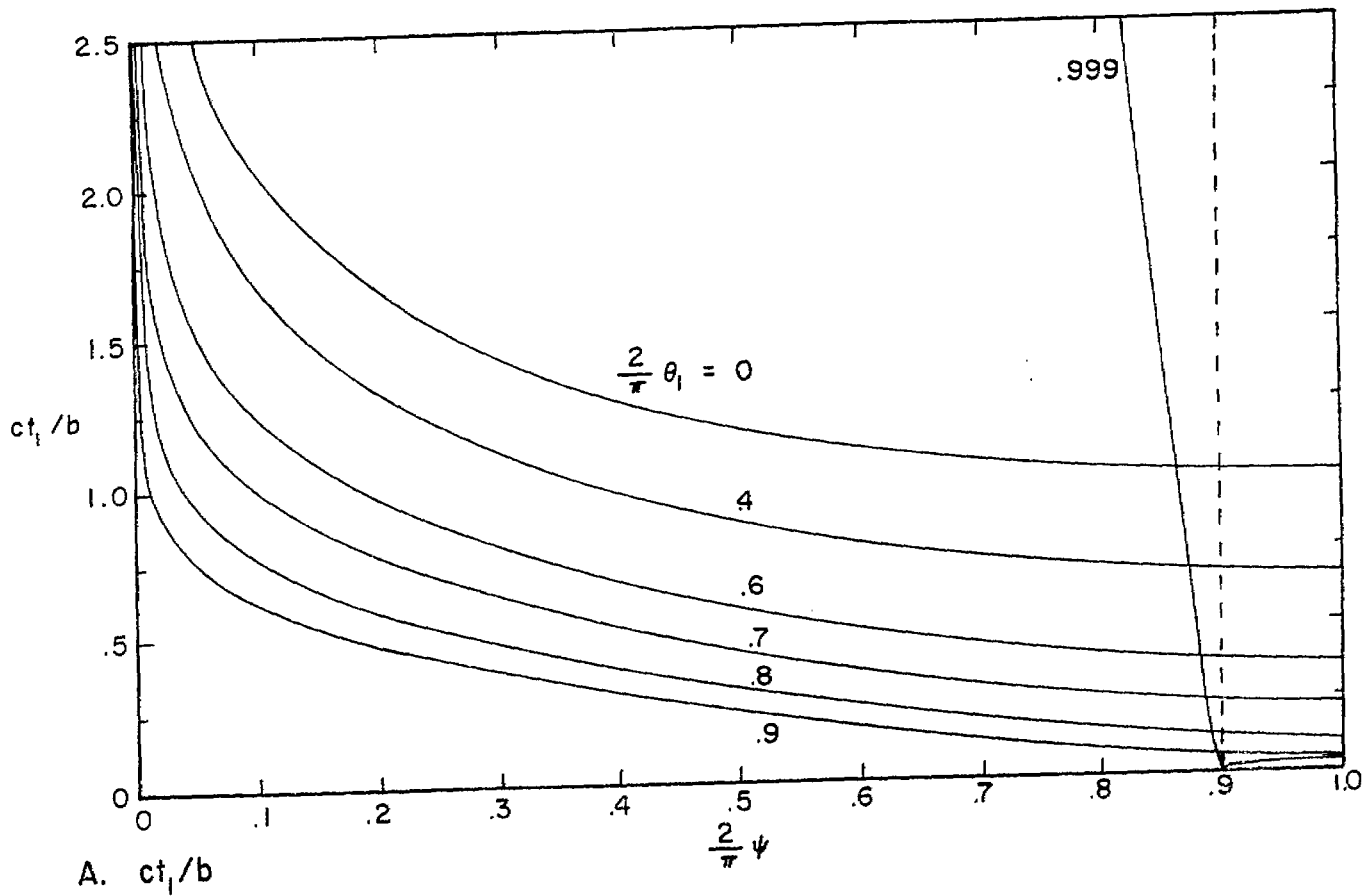


FIGURE 22. ct_1/b AND ρ FOR $\frac{2}{\pi} \phi_1 = .9$ WITH θ_1 AS A PARAMETER

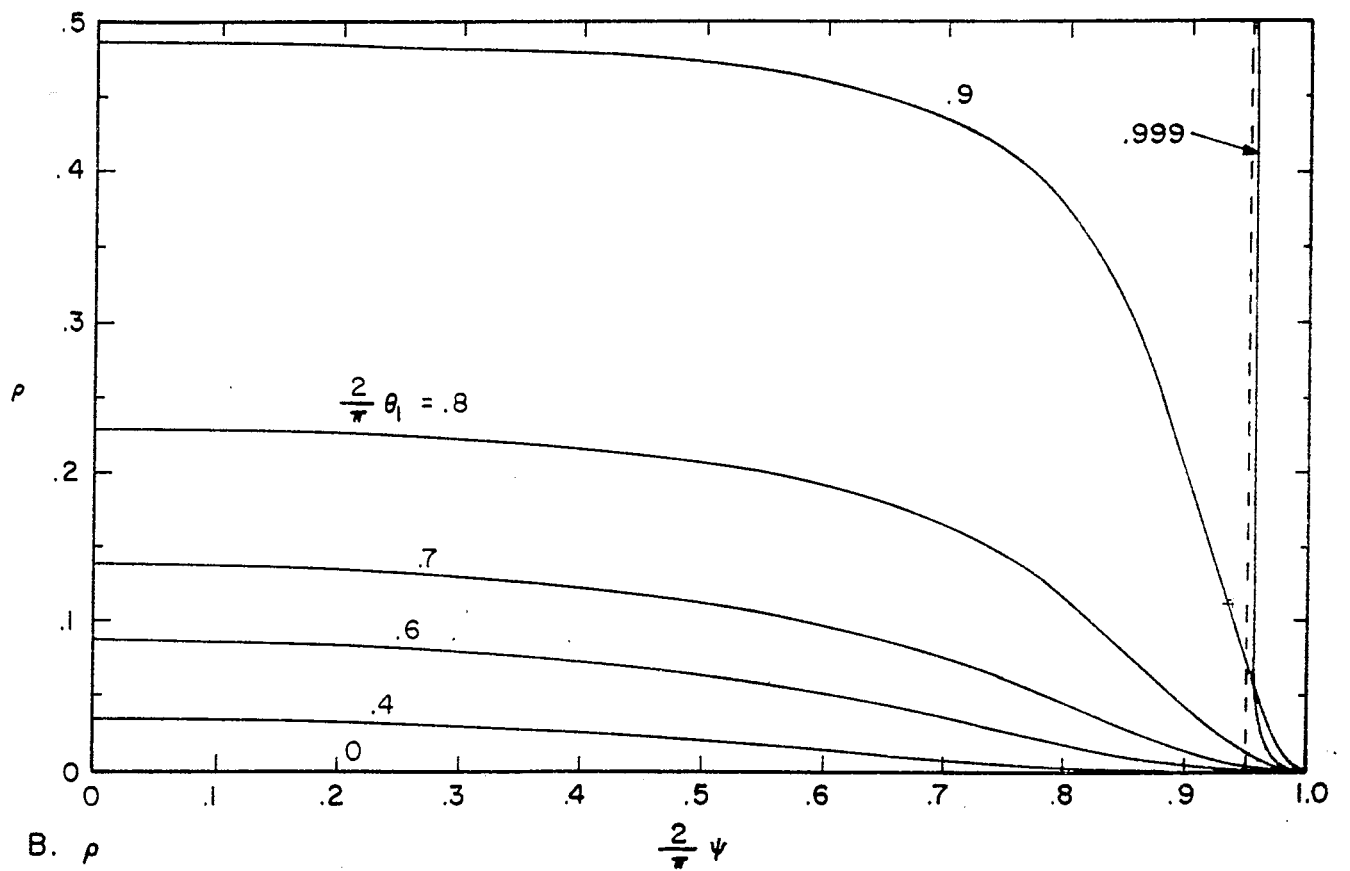
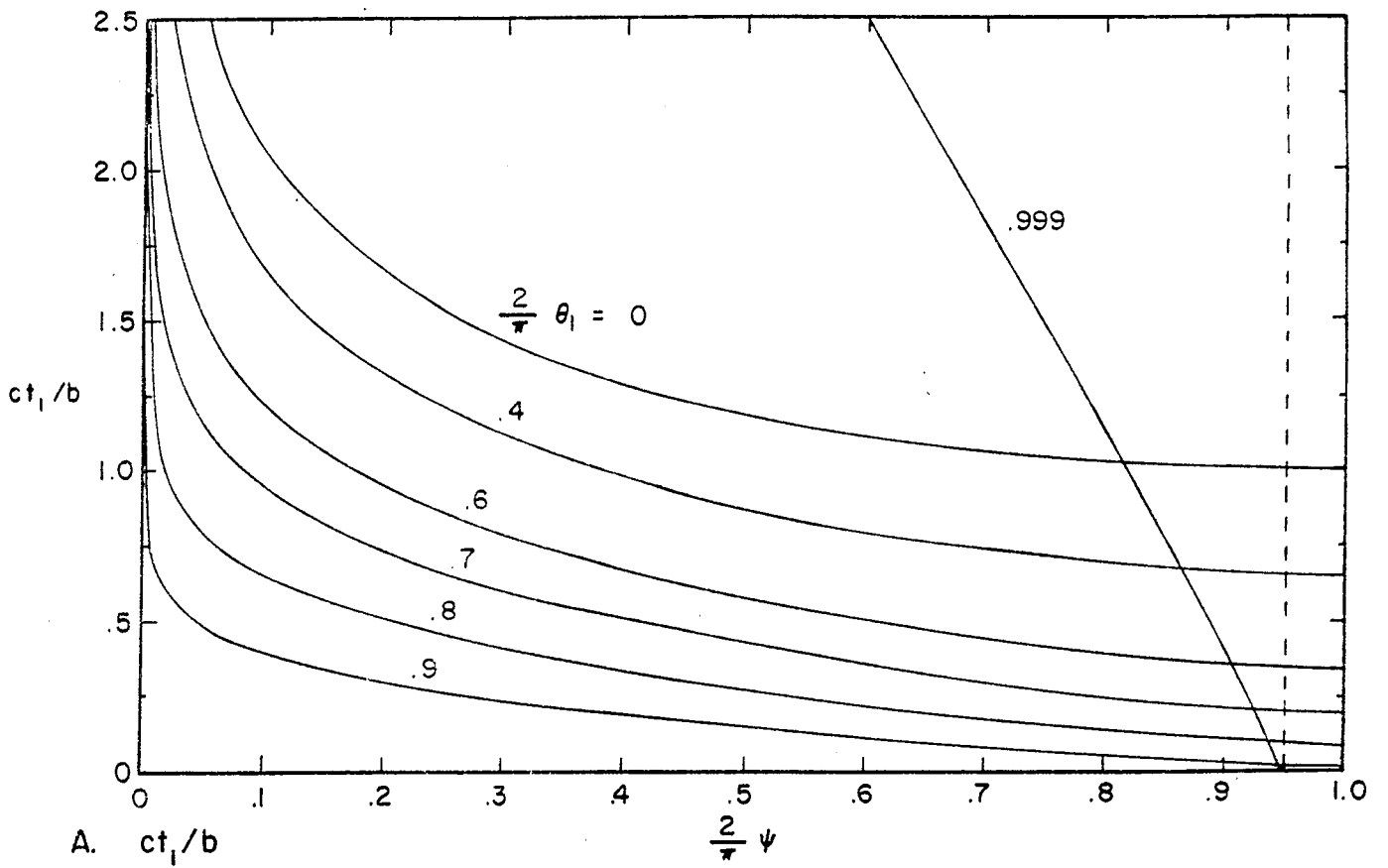


FIGURE 23. ct_1/b AND ρ FOR $\frac{2}{\pi} \phi_1 = .95$ WITH θ_1 AS A PARAMETER